ILLINOIS

UNIVERSITY OF ILLINOIS AT URBANA-CHAMPAIGN

-

PRODUCTION NOTE

University of Illinois at
Urbana-Champaign Library
Large-scale Digitization Project, 2007.

UNIVERSITY OF ILLINOIS
COLLEGE OF ENGINEERING

ENGINEERING EXPERIMENT STATION
BULLETIN 493

INVESTIGATION OF PRESTRESSED REINFORCED CONCRETE FOR HIGHWAY BRIDGES, PART IV: STRENGTH IN SHEAR OF BEAMS WITH WEB REINFORCEMENT

by

S. Ø. Olesen
M. A. Sozen
C. P. Siess

ENGINEERING EXPERIMENT STATION
BULLETIN 493

INVESTIGATION OF PRESTRESSED REINFORCED CONCRETE FOR HIGHWAY BRIDGES, PART IV: STRENGTH IN SHEAR OF BEAMS WITH WEB REINFORCEMENT

by

S. Ø. Olesen
Associate Professor of Civil Engineering,
Danmarks Ingeniørakademi,
Copenhagen, Denmark

M. A. Sozen
Professor of Civil Engineering,
University of Illinois

C. P. Siess
Professor of Civil Engineering,
University of Illinois

Price: $3.00

Prepared as a part of an investigation
conducted by
The Engineering Experiment Station
University of Illinois
in cooperation with

The State of Illinois
Division of Highways
and
The U.S. Department of Transportation
Federal Highway Administration
Bureau of Public Roads
Project IHR-10
The Investigation of Prestressed Reinforced
Concrete for Highway Bridges

Illinois Cooperative Highway Research Program
Series No. 70

Edited by
Ann C. Riggins

REQUESTS FOR THIS PUBLICATION should be addressed to Engineering Publications Office, 112 Engineering Hall, University of Illinois, Urbana 61801. On your order refer to the Bulletin number on the front cover.

UNIVERSITY OF ILLINOIS BULLETIN

Volume 64, Number 134; July 5, 1967. Published twelve times each month by the University of Illinois. Entered as second-class matter December 11, 1912, at the post office at Urbana, Illinois, under the Act of August 24, 1912. Office of Publication, 114 Altgeld Hall, Urbana, Illinois 61801.

ABSTRACT

THIS REPORT SUMMARIZES THE INFORMATION ON SHEAR STRENGTH OF PRESTRESSED CONCRETE BEAMS WITH WEB REINFORCEMENT OBTAINED IN THE COURSE OF AN EXTENSIVE EXPERIMENTAL RESEARCH PROGRAM CARRIED OUT DURING THE PERIOD 1957 THROUGH 1965.

CHAPTERS 1 AND 2 CONTAIN AN OUTLINE OF THE EXPERIMENTAL PROGRAM AND A DESCRIPTION OF TESTING PROCEDURES.

CHAPTER 3 DESCRIBES QUALITATIVELY THE BEHAVIOR OF PRESTRESSED CONCRETE BEAMS BRINGING OUT THE EFFECTS OF THE MAJOR VARIABLES.

CHAPTERS 4 AND 5 DEVELOP METHODS OF ANALYSIS, AND THEIR EXPERIMENTAL CONFIRMATIONS, FOR THE SHEAR STRENGTH OF BEAMS WITH AND WITHOUT WEB REINFORCEMENT.

CHAPTER 6 PRESENTS A DESIGN METHOD FOR WEB REINFORCEMENT IN PRESTRESSED CONCRETE BEAMS AND DISCUSSES RELATED DESIGN PROBLEMS. THE INFORMATION IN THIS CHAPTER CAN BE USED WITHOUT A STUDY OF CHAPTERS 1 THROUGH 5.

ACKNOWLEDGMENTS

This study was carried out as a part of the research under the Illinois Cooperative Highway Research Program Project IHR-10, "Investigation of Prestressed Reinforced Concrete for Highway Bridges." The work on the project was conducted by the Department of Civil Engineering of the University of Illinois in cooperation with the Division of Highways, State of Illinois, and the U.S. Department of Transportation, Federal Highway Administration, Bureau of Public Roads.

At the University, the work covered by this report was conducted under the general administrative supervision of W. L. Everitt, Dean of the College of Engineering; Ross J. Martin, Director of the Engineering Experiment Station; N. M. Newmark, Head of the Department of Civil Engineering; and Ellis Danner, Director of the Illinois Cooperative Highway Research Program and Professor of Highway Engineering.

At the Division of Highways of the State of Illinois, the work was under the administrative direction of Virden E. Staff, Chief Highway Engineer; Theodore F. Morf, Deputy Chief Highway Engineer; and John E. Burke, Engineer of Research and Development.

The program of investigation has been guided by a Project Advisory Committee on which the following persons have served:

Representing the Illinois Division of Highways:

W. E. Chastain, Sr., Engineer of Physical Research, (deceased)

W. J. Mackay, Engineer of Research Coordination
C. E. Thunman, Jr., Bridge Section, Bureau of Design
F. Jacobsen, Bridge Section, Bureau of Design

Representing the U.S. Bureau of Public Roads:

Harold Allen, Chief, Division of Physical Research
E. L. Erickson, Chief, Bridge Division

Representing the University of Illinois:

C. E. Kesler, Professor of Theoretical and Applied Mechanics
Narbey Khachaturian, Professor of Civil Engineering

Fred Kellam, R. E. Lloyd, K. Scheffey, G. S. Vincent, and E. G. Wiles, Bureau of Public Roads, and D. D. Fowler, Illinois Division of Highways also participated in the meetings of the Advisory Committee and contributed materially to the guidance of the program.

The investigation was directed by Dr. C. P. Siess, Professor of Civil Engineering, as Project Supervisor and as ex-officio chairman of the Project Advisory Committee. Immediate Supervision of the investigation was provided by Dr. M. A. Sozen, Professor of Civil Engineering, as Project Investigator.

Acknowledgment is also extended to the reviewers of this Bulletin: John E. Burke, Engineer of Research and Development, Illinois Division of Highways; William L. Gamble, Assistant Professor of Civil Engineering, University of Illinois; and N. M. Hawkins, Portland Cement Association.

This page is intentionally blank.

CONTENTS

This page is intentionally blank.

FIGURES

TABLES

This page is intentionally blank.

I. INTRODUCTION

1.1 OBJECT AND SCOPE

The experimental study described in this report is a continuation of an earlier investigation which was concerned primarily with the shear strength of beams without web reinforcement [1]*. Since most prestressed concrete beams need web reinforcement in order to develop the full flexural capacity, the second phase of the investigation was mainly concerned with the effect of web reinforcement on the strength and behavior of prestressed concrete beams.

The primary variables included in the test program were: shape of cross section, prestress level, amount of longitudinal reinforcement, length of shear span, moving loads, concrete strength, and the amount and properties of the web reinforcement. Beams with both straight and draped longitudinal reinforcement were tested.

The majority of the beams were tested and analyzed by G. Hernandez [2] and J. G. MacGregor [3,4,5] during the years 1957 through 1960. Hernandez related, for the first time, the effect of web reinforcement on the load capacity of a beam to its inclined cracking load. MacGregor examined the effects of draped reinforcement and moving loads. These two basic series of tests also led to a better understanding of the mechanism of inclined cracking in prestressed concrete beams.

Most of the composite beams and the beams with unbonded stirrups were tested by R. N. Bruce [6]. The final series of tests, carried out by S. Ø. Olesen, included beams without prestress designed expressly for the purpose of studying the mechanism of the action of web reinforcement.

The results from all beams tested since 1957 in the course of this investigation are presented and discussed in this report. The various observed patterns of behavior are classified and procedures are developed to predict the inclined cracking load and the amount of web reinforcement required to develop a flexural failure.

1.2 OUTLINE OF TESTS

This report is based on the results of 129 tests on simply-supported prestressed concrete beams. A total of 119 beams had overall cross-sectional dimensions of 6 by 12 inches. The remaining 10 beams were of composite construction consisting of a precast and prestressed section with overall dimensions of 6 by 12 inches and a nonprestressed cast-in-place slab with 2-inch thickness and a width of 24 inches. All beams were tested over 9-foot spans.

Straight as well as draped longitudinal tension reinforcement was used. The drape profiles consisted of straight segments with

*Numbers in parentheses refer to corresponding entries in the References, Chapter VIII.

the tendons deflected under the load points.

Five beams were rectangular in section, 61 were I-beams with 3-inch thick webs and 53 were I-beams with 1 3/4-inch thick webs. The composite beams all had 1 3/4-inch web thickness.

The properties of all specimens are listed in Tables 1 and 2. The ranges of the variables are given below:

Rectangular Beams

- Shear span:
  - Less than 40 inches — 5 beams
- Prestress:
  - Less than 90 ksi — 2 beams
  - More than 90 ksi — 3 beams
- Draped tendons — 1 beam
- Straight tendons — 4 beams
- Longitudinal reinforcement ratio: 0.398 to 0.713 per cent
- Concrete strength: 2,500 to 5,400 psi
- Web reinforcement:
  - Ratio $(\frac{A_v}{bs})$: 0 to 0.25 per cent
  - Spacing: 6.5 inches
  - Yield stress: 53.7 ksi

I-Beams with 3-Inch Thick Webs

- Shear span:
  - Less than 40 inches — 41 beams
  - More than 40 inches — 17 beams
  - Moving Loads — 3 beams
- Prestress:
  - Less than 90 ksi — 21 beams
  - More than 90 ksi — 40 beams
- Draped tendons — 15 beams
- Straight tendons — 46 beams
- Longitudinal reinforcement ratio: 0.192 to 0.611 per cent
- Concrete strength: 2,600 to 7,200 psi
- Web reinforcement:
  - Ratio $(\frac{A_v}{bs})$: 0 to 0.67 per cent
  - Spacing: 2.0 to 10.5 inches
  - Yield stress: 34.0 to 79.5 ksi

I-Beams with 1 3/4-Inch Thick Webs

- Shear span:
  - Less than 40 inches — 46 beams
  - More than 40 inches — 3 beams
  - Moving loads — 4 beams
- Prestress:
  - Less than 90 ksi — 4 beams
  - More than 90 ksi — 49 beams
- Draped tendons — 3 beams
- Straight tendons — 50 beams
- Longitudinal reinforcement ratio: 0.191 to 0.595 per cent
- Concrete strength: 2,500 to 7,600 psi
- Web reinforcement:
  - Ratio $(\frac{A_v}{bs})$: 0 to 0.46 per cent
  - Spacing: 2.5 to 9.0 inches
  - Yield stress: 30.0 to 79.5 ksi

Composite Beams

- Shear span:
  - 36 inches — 10 beams
- Prestress:
  - More than 90 ksi — 10 beams
- Draped tendons — 4 beams
- Straight tendons — 6 beams
- Longitudinal reinforcement ratio: 0.0467 to 0.0970 per cent
- Concrete strength: 2,600 to 4,200 psi
- Web reinforcement:
  - Ratio: $(\frac{A_v}{bs})$: 0.26 to 0.60 per cent
  - Spacing: 1 7/8 to 3 1/8 inches
  - Yield stress: 30.0 to 41.2 ksi

1.3 NOTATION

1.3.1 Designation of Test Specimens

Although the specimens were originally numbered according to the order of testing, they have for easier reference been regrouped and redesignated according to the major variables. Each beam is designated by one or two letters and two pairs of numerals, e.g.,

BW.14.58. The code for the first four symbols in the designation is as follows:

First Letter (BW.14.58)

- A - Rectangular beam
- B - I-beam, 3-inch web
- C - I-beam, 1 3/4-inch web
- F - Composite beam

Second Letter (BW.14.58)

- W - Bonded web reinforcement included
- D - Draped reinforcement
- V - Draped reinforcement and bonded web reinforcement
- I - Inclined bonded web reinforcement
- U - Unbonded web reinforcement

First Numeral (BW.14.58)

- 1 - Prestress greater than 90 ksi
- 2 - Prestress less than 90 ksi

Second Numeral (BW.14.58)

- 0 - Beams tested under moving loads
- 3 - 28- or 30-inch shear span
- 4 - 36-inch shear span
- 5 - 45- or 48-inch shear span
- 6 - 54- or 60-inch shear span
- 8 - 70-inch shear span
- 9 - 75- or 78-inch shear span

The second pair of numerals (BW.14.58) represents the value the dimensionless parameter pE_s/f'_c to two significant figures. Three numerals are used for the composite beams. The beams with 54-inch shear span were loaded at midspan by a single load. Beams with a reported shear span shorter than 54 inches were loaded with two loads located symmetrically about midspan. Beams with shear spans longer than 54 inches were loaded with a single load. All beams had a span of 9 feet.

1.3.2 Symbols

Beam Properties:

- A_c = gross area of cross section
- A_s = area of longitudinal tensile reinforcement
- a = length of shear span
- b = width of flange
- b' = web thickness
- c = distance from centroid of precast section to bottom fiber
- c_t = distance from centroid of composite section to bottom fiber
- d = effective depth of the reinforcement
- e = eccentricity of prestressing force with respect to centroid of prestressed section
- I = moment of inertia of prestressed section
- I_t = moment of inertia of composite section
- L = length of span
- Q = first moment of area below centroid of composite section with respect to centroid of prestressed section. If centroid of composite section is in the flange, first moment of area below the flange is used.
- Q_t = first moment of area below centroid of composite section (below the flange, if centroid is in the flange) with respect to centroid of composite section
- s = stirrup spacing
- y = distance from centroid of prestressed section to point considered (positive towards the tension reinforcement)
- y_t = distance from centroid of composite section to point considered (positive towards the tension reinforcement)
- α = inclination of stirrups with respect to axis of beam
- φ = drape angle, angle between axis of beam and resultant prestressing force

Loads:

- F_{se} = effective prestressing force after losses
- M = moment at a section

M_{cr} = flexural cracking moment

M_d = dead load moment

M_u = ultimate moment

P = applied load

P_c = applied load at inclined cracking

V = shear at a section

V_c = calculated inclined cracking shear

V_{cf} = calculated shear at flexure-shear cracking

V_{cm} = measured shear at inclined cracking

V_{cs} = calculated shear at shear cracking

V_D = dead load shear

V_f = calculated shear at flexural failure

V_{um} = measured shear at failure

V_{us} = calculated shear at shear failure

w = dead weight of precast section

w_t = dead weight of composite section

Stresses:

General

σ_θ = principal stress (tension positive)

σ_x = normal stress parallel to axis of beam

σ_y = normal stress perpendicular to axis of beam

τ = shearing stress

Concrete

f'_c = compressive strength of concrete determined from 6- by 12-inch cylinders

f_{cu} = average concrete stress in compression zone at failure

f_r = tensile strength of concrete determined as the modulus of rupture

f_t = tensile strength of concrete determined as the splitting strength of 6- by 12-inch cylinders

Steel

E_s = modulus of elasticity of steel

f_{se} = effective longitudinal prestress after losses

f_{sev} = effective prestress in stirrups

f_{su} = stress in longitudinal reinforcement at failure of beam

f'_s = ultimate steel stress

Strains:

Concrete

ϵ_{cc} = concrete strain at top of beam at inclined cracking

ϵ_{ce} = concrete strain at level of longitudinal reinforcement caused by effective prestress

ϵ_u = limiting strain at which concrete crushes in a beam

Steel

ϵ_{sc} = steel strain at inclined cracking

ϵ_{se} = steel strain corresponding to effective prestress

ϵ_{su} = steel strain at failure of beam

Dimensionless Factors:

a/d = ratio of shear span to effective depth of beam

F_1 = strain compatibility factor before inclined cracking

F_2 = strain compatibility factor after inclined cracking

k_c = ratio of depth of neutral axis at inclined cracking to effective depth

k_u = ratio of depth of neutral axis at ultimate to effective depth

k_2 = ratio of depth of the resultant compressive force to depth of neutral axis

p = A_s/bd = longitudinal reinforcement ratio

r = web reinforcement ratio based on width of precast flange

II. MATERIALS, FABRICATION, AND TESTING

2.1 MATERIALS

2.1.1 Cement

Marquette brand Type III Portland cement or Atlas brand Type III Portland cement was used for all the specimens. The cement was purchased from local dealers in lots of 20 or 40 bags.

2.1.2 Aggregates

Wabash River sand and pea gravel were used in all the beams. Both aggregates have been used in this laboratory for many previous investigations and have passed the usual specification tests. The maximum size of the gravel was 3/8 inches.

The origin of these aggregates is an outwash of the Wisconsin glaciation. The major constituents of the gravel were limestone and dolomite; the sand consisted mainly of quartz. The absorption of both the fine and the coarse aggregate was about 1 per cent by weight of surface dry aggregate.

2.1.3 Concrete Mixes

Mixes were designed by the trial batch method. Two batches were used in each beam, batch one being in the lower half to two-thirds of the beam. The slabs of the composite beams were usually cast from one batch each although two batches were used in a few cases. Table 3 lists the proportions of the concrete batches used in each beam along with the slump, compressive strength, tensile strength determined as modulus of rupture and/or splitting strength, and age at the time of beam test. Proportions are in terms of oven-dry weights.

In Figures 1 and 2, the modulus of rupture and the splitting strength are compared to the compressive strength of the concrete. The modulus of rupture was obtained from control beams with 6- by 6-inch cross sections. The beams were loaded at the third-points of an 18-inch span. The splitting strength was found from tests on 6- by 6-inch or 6- by 12-inch cylinders. A compressive force was applied along opposite generators of the cylinder. Strips of stiff fiber board with 1/8-inch thickness and 1/2-inch width were placed between the cylinder and the heads of the testing machine to distribute the load evenly along the length of the specimen.

Since a measure of the tensile strength of the concrete in each beam was necessary for the interpretation of the test results, and since the scatter in the data did not warrant use of the results of individual control specimens, two expressions were selected to represent the accumulated data:

For the modulus of rupture:

$$f_r = 6\sqrt{f'_c} \qquad (1)$$

For the tensile strength determined from the splitting test:

$$f_t = 5\sqrt{f'_c} \qquad (2)$$

The strength values are all in pounds per square inch.

2.1.4 Longitudinal Reinforcement

Single wire reinforcement and seven-wire strand were used. The properties of each lot are given in Table 4. The single wire reinforcement had properties in accordance with the requirements of ASTM-A-421-59T. The wire contained in lots 8, 10, 11, 12, and 13 was designated as "Hard-Drawn Stress-Relieved Super-Tens Wire," while the wire in lot 14 was classified as "0.196-inch Tufwire." The seven-wire strand conformed with the specifications in ASTM-A-416-59T.

The stress-strain relationships for the different lots were determined from tests of samples cut from different portions of each coil. All samples were tested in a 120,000-pound capacity Baldwin-Southwark-Tate-Emery hydraulic testing machine. The strains were measured with an 8-inch extensometer employing a Baldwin "microformer" coil and recorded with an automatic device.

To improve the bond characteristics, both the single wire and the seven-wire strand were first wiped with a rag dipped in a weak solution of hydrocloric acid and then rusted by storing in a moist room for several days.

2.1.5 Web Reinforcement

The stirrups in most of the beams with web reinforcement were made from black annealed wire of different nominal diameters. In the remaining beams, the stirrups were made from 0.129-inch square cold-finished bars of AISI C-1018 steel. All stirrup steel was rusted and samples were tested in the same manner as described for the prestressing steel. The properties of the stirrup steel used in each particular beam are listed in Table 2.

In the analysis of the test results, the yield point stress for the stirrup steel has been defined as the stress corresponding to 1 per cent strain. The actual strain distribution in the stirrups was not measured. However, measurements of crack openings and in some cases measurements of the average strain along a stirrup indicated that the maximum strain in a stirrup at ultimate usually was 1 per cent or more.

2.1.6 Slab Reinforcement

The slab reinforcement in beams FW.14.064 and FW.14.070 consisted of intermediate grade No. 3 deformed bars with a stress at 1 per cent of 65.0 ksi. The remaining eight composite beams had slab reinforcement of high strength 1/4-inch diameter plain bars with a stress at 0.2 per cent offset of 70.1 ksi and ultimate stress of 71.0 ksi.

2.2 DESCRIPTION OF SPECIMENS

All the beams were modifications of a basic member 6 inches by 12 inches in cross section and 10 feet 2 inches to 10 feet 10 inches in overall length. The I-beams were formed by metal inserts placed in rectangular forms. Rectangular end blocks 12 to 18 inches in length were provided at each end of the beams. Ten of the beams had slabs, with nominal cross-sectional dimensions of 2 by 24 inches, cast on top of them. The nominal dimensions of the beams are shown in Figure 3 and the measured dimensions are listed in Table 1.

The longitudinal reinforcement consisted of four to twelve single wires or four to eight seven-wire strands, pretensioned, and anchored by bond. The tendons were placed in one, two, or three horizontal layers. The single wires were spaced at 0.70 inches center to center in

the horizontal direction and 0.75 inches in the vertical direction. The vertical and horizontal spacing between seven-wire strands was one inch.

In the beams with draped tendons, the reinforcement profiles consisted entirely of straight line segments, the tendons being draped from the load points in every case. The tendons were either all draped parallel to one another or some of the tendons were draped and the rest were straight. The vertical and horizontal spacing of the tendons was the same as in beams with straight reinforcement. The amount of reinforcement, which was draped, is given in Table 1 in proportion of the total amount of longitudinal steel together with the drape angle Φ. This angle is given as the angle between the axis of the beam and the resultant prestressing force.

Stirrups having one, two, or three legs were used in all beams which had web reinforcement. The nominal dimensions of these stirrups are given in Figure 4. The amount of stirrups and their spacing as well as the properties of the stirrup steel are summarized in Table 2. In the majority of the beams, a uniform stirrup spacing was used throughout the length of the beam. In seven beams, however, the spacing was varied along the length of the beam. The web reinforcement ratios for these beams reported in Table 2 are those at midspan or adjacent to the load point.

2.3 PRESTRESSING

2.3.1 End Details of Tendons

Threaded connections were used to grip the single wire in the tensioning process until transfer. Threads were cut on the end-3 inches of the wires to fit a specially made nut with a No. 12 thread. The nuts were 5/8 inch long. This was sufficient to develop at least 160,000 psi in the wires for several days.

In beams using seven-wire strand as reinforcement, the anchorage prior to transfer was provided by 1/4-inch steelcase Strandvise grips (Figure 5).

2.3.2 Tensioning Apparatus

The reaction for the tensioning force was provided by a prestressing frame. It was made from two 11-foot 6-inch lengths of standard 3-inch pipe, and two bearing plates, 2 by 6 by 20 inches. For beams with draped reinforcement, the bearing plates were 2 by 10 by 20 inches. The frame was built to fit around the form for the beam. The bearing plates were provided with holes to accommodate the spacing between tendons, described in Section 2.2.

A 30-ton Simplex center-hole hydraulic ram operated by a Blackhawk pump was used to tension all tendons. The prestressing force was transferred from the ram through a rod to the tendon and through a jacking frame to the prestressing frame as shown in Figure 6. The rod was threaded directly onto the threads in the end of the single wire. Connection between the rod and a seven-wire strand was provided by a special device which gripped the strand and onto which the rod could be threaded.

The tendons which were to be draped were tensioned in their uppermost position and then pulled down to their final position by two draping saddles, one at each load point. The draping saddles consisted of two long threaded 3/8-inch diameter rods with two 2 1/2-inch lengths of 1/2-inch diameter rod welded across them at one end. The lower ends of the threaded rods passed through holes in the bottom of the form and the saddles were held in position by nuts bearing on the bottom of the form.

The form rested on a stiffening beam built up from plates and two 15-inch channels. This beam prevented the form from warping when the tendons were draped.

In beams with a small drape angle it was possible to do all the draping by screwing nuts onto the threaded rods of the saddles. Where this was not possible, a hydraulic ram was used to pull down the saddles.

2.3.3 Tensioning Procedure

The reinforcement was tensioned in the prestressing frame prior to casting the beam. The tendons were stressed one at a time and anchored as described in Section 2.3.1. Since the prestressing frame underwent an elastic shortening with the tensioning of the tendons, the first tendons to be stressed were overstressed a certain amount, dictated by the experience with previous beams. Minor adjustments in the prestress were usually necessary after tensioning of all the tendons.

In beams with draped reinforcement, the tendons were stressed in their uppermost position. The initial prestress in the tendons was chosen so that the additional increment added by draping brought the total prestress up to the desired level. After initial tensioning the prestressing frame with the tendons was transported to the form and the tendons to be draped were pulled down to their final position by welded steel saddles at each load point.

The prestress was transferred to the beam, when the concrete in the beam was strong enough. The transfer in beams with single wire reinforcement was accomplished by loosening the nuts slowly so that the tension in each of the wires was approximately equal at all times. In beams with seven-wire strand reinforcement, the transfer was effectuated by burning through the strands with an oxy-acetylene torch. The torch was adjusted to a low heat, and the strands heated as uniformly as possible over a length of eight to ten inches between the prestressing frame and the end of the beam. With increase in temperature, the strand elongates and its yield point decreases. If the operation is performed correctly, the strands break gently with marked ductility and necking at the failure point. In the beams with draped reinforcement, the longitudinal prestress was released first so that the beam would be prestressed before the vertical reaction of the draping saddles was transferred to the beams.

2.3.4 Measurement of Prestress

The tensioning force in each tendon was determined by measuring the compressive strain in small aluminum dynamometers placed on the tendons between the end plate of the prestressing frame and the anchorage nut or the Strandvise grip. The dynamometers were placed at the end of the beam opposite that to which the tension was applied. They were made of 2-inch lengths aluminum rods with holes drilled through their centers. The diameter of the rods was 1/2 inch or 5/8 inch and the holes were 0.2 inch and 0.275 inch for dynamometers used in connection with single wires and seven-wire strands, respectively. Strains were measured by means of type A7 SR-4 electric strain gages, attached to the outside of each dynamometer. The dynamometers used with single wires had two strain gages mounted longitudinally on opposite sides. The gages were wired in series, thus giving a strain reading which was the average of the strains in the two gages. Four strain gages were used on the second type of dynamometers. Two of these gages were mounted longitudinally and two circumferentially on opposite ends of two diameters, the diameters being at right

angles. All four gages were wired to form a four-arm bridge, so that the measured strain, for a given load, was the sum of the various gage outputs. Both gage configurations cancel the effect of a reasonable amount of nonaxial loading. The four-arm bridge, in addition, compensates for temperature changes.

All the dynamometers were calibrated using a Baldwin hydraulic testing machine. The calibration constants for each of the two groups of dynamometers were nearly the same. The strain output from the dynamometers was about 2000 and 4300 millionths at a prestress of 120 ksi in the single wires and the seven-wire strands, respectively. The sensitivity of the strain indicator used was two or three millionths.

2.4 PLACING AND PRESTRESSING OF WEB REINFORCEMENT

Most of the beams had bonded, vertical stirrups. These were tied to the longitudinal reinforcement using baling wire. In addition, a reinforcing bar was tied to the top of the stirrups to keep them vertical and at the proper spacing. After the first batch of concrete had been placed and vibrated, this bar was removed.

In the beams with unbonded stirrups, vertical holes on 4-inch centers were formed in the beam by 0.275-inch diameter drill rods which were properly positioned by means of a steel template prior to casting. About 12 hours after casting, the template and drill rods were removed, leaving the holes into which the 1/4-inch stirrups were later placed.

The unbonded stirrups were anchored in both ends by visegrips. The stirrups were prestressed by means of a bolt and nut placed between the visegrip and the top surface of the beam. The bolt had a 0.275-inch diameter hole drilled through its centerline, which permitted the stirrup to pass through the bolt. By turning the nut, a prestress could be applied to the stirrup. The prestressing force was measured at the bottom end of the stirrup by a dynamometer of the four-arm type previously described. Steel bearing plates 1/4 by 2 by 1 inch were placed between the bottom surface of the beam and the dynamometer and between the top surface and the bolt and nut.

2.5 CASTING AND CURING

All concrete was mixed in a nontilting drum-type mixer of 6 cubic feet capacity. A butter mix of 1 cubic foot preceded two batches of about 4 cubic feet each, which were used in the specimens. The mixing time for each batch was from three to six minutes. Before batching, samples of the aggregates were taken for free moisture tests. Slump was determined immediately after mixing.

Metal forms were used to cast all the beams, although wooden forms were used to cast the slab of the composite beams. Removable metal inserts were used to shape the I-beams.

Two batches of concrete were required in each beam. The first batch was placed in a layer of uniform height through the beam, filling half to three-quarters of the depth. At least three and usually six 6- by 12-inch cylinders were cast from each batch to determine the compressive strength of the concrete. In addition, one 6- by 6- by 20-inch modulus of rupture beam and/or an additional number of 6- by 12-inch or 6- by 6-inch cylinders were cast for determination of the splitting strength.

The freshly cast concrete in the test beam as well as in the control beams and cylinders was vibrated with a high frequency internal vibrator. The tops of the test beam and control beams were troweled smooth and the

cylinders were capped with a paste of neat cement four or five hours after casting. The forms were removed after one day and the beam and control specimens were wrapped in wet burlap for several days. The burlap was removed two to three days before testing to allow the concrete surface to dry before electric strain gages were applied.

The beams which were to have a slab cast on top were manufactured in the same way as indicated above, except for the following difference. Three hours after casting the beam, Rugasol-C was applied on the top surface of the beam and on the protruding ends of the stirrups. This retarded the set of the cement paste for a depth of 1/8 to 1/4 inch and permitted the loose paste to be removed after about sixteen hours, thus exposing the aggregate and providing shear connection between the beam and the slab.

After the prestress was transferred to the concrete, the beam was supported at two points, the span being the same as during the test, and a wooden form was built around and supported on the beam. The slab reinforcement was placed at midheight of the slab with 6-inch spacing in both directions. The top surface of the beam was wetted before casting the slab. Usually one batch was used for the entire slab. In the few slabs where two batches were used, the second batch was placed outside the supports.

2.6 STRAIN GAGES

2.6.1 Electric Strain Gages on Reinforcement

Two tendons in each beam were instrumented with electric strain gages placed at a section of maximum moment. In beams subjected to moving loads, the gages were placed at midspan. The gages used on single wire reinforcement were Type A7 SR-4 electric strain gages with a nominal gage length of 1/4 inch and a minimum trim width of 3/16 inch. The seven-wire strands were instrumented with Type A12-2 SR-4 or C6-111 Budd electric strain gages. The former consisted of a single wire grid, approximately 1 5/8 inches long, which could be trimmed to less than 1/8 inch in width. The latter had a nominal gage length of 1/16 inch and a width of 1/16 inch. Gages on the seven-wire strands were mounted along a single outside wire.

The surface of the tendons was prepared for gage application by using fine emery cloth and acetone. The gages were mounted using Eastman 910 or Duco cement as the bonding agent. Heat lamps were used to accelerate the drying of the Duco cement. After several hours of air drying, and after the lead wires were soldered to the gages and insulated with tape, the gages were waterproofed with a coating of Petrolastic or Epoxoid.

2.6.2 Electric Strain Gages on Concrete

In most of the beams, strains on the top surface of the concrete were measured with Type A3 SR-4 electric strain gages which have a nominal gage length of 3/4 inch and a width of 3/8 inch. A portable grinder was used to smooth the top surface of the beam at the desired locations. A thin layer of Duco cement was applied to the concrete surface and allowed to dry for several minutes. Then the gage was mounted with Duco cement. Steel weights of one pound were left on the gages for a period of one hour with a sponge rubber cushion under each weight. The gages were placed along the longitudinal centerline of the beam except for those placed immediately around the load points. Wherever strain distributions are presented in the text, the location of the gages is indicated.

2.6.3 Mechanical Strain Gages

In the two series of beams with 30-inch and 45-inch shear spans, the vertical deformation between the flanges was measured at sections with 2-inch spacing. This was done to obtain an estimate of the strain in the stirrups. The deformation was measured by means of a 10-inch Whittemore strain gage. Gage lines were established by mounting 1/2-inch by 1/2-inch steel plates to the sides of the specimens. Each plate had a gage hole drilled to a depth of about 1/8 inch. A typical layout of the gage lines is shown in Figure 21.

2.7 LOADING APPARATUS

All the specimens tested under stationary loads were loaded in specially constructed frames employing a 30-ton capacity Simplex hydraulic jack operated by a Blackhawk pump. Details of one of the two frames used are shown in Figure 7. The distributing beam was omitted for specimens subjected to a single concentrated load. The loading blocks were in most cases 8- by 6- by 2-inch steel plates resting on 4- by 4- by 1/4-inch leather plates. In the remaining cases, 3- by 3- by 1-inch steel plates were mounted to the beam with hydrocal plaster. The bearing blocks at the reactions were always 8- by 6- by 2-inch steel plates. The block at one end was supported on a "half-round" and that at the other end on a roller.

The frame shown in Figure 7 was also used in tests of beams subjected to simulated moving loads. Loads were applied by 20-ton Blackhawk rams held below the longitudinal beam in the testing frame by a supporting device. This device was composed of a 6-inch by 3/16-inch plate 7 feet 5 inches long which was held 7/8 inch below the bottom of the longitudinal beam by 7/8-inch square bars running across the plate at 8 inches on centers. Slots into which the rams fitted, were cut in the plate at 8-inch centers. The ends of the slots were circular to position the rams accurately. The hydraulic rams had 6- by 6- by 3/4-inch shoes which fitted loosely into the space between the supporting plate and the longitudinal beam in the test frame. In this way the rams could be placed accurately in eleven successive positions, each 8 inches apart. The center load position was at midspan. Thus, the "moving load" consisted of a series of concentrated loads applied one after the other at positions 8 inches apart along the beam. Two hydraulic rams were used, each operated by a separate pump.

2.8 MEASUREMENTS

The load was measured by means of a 50,000-pound elastic-ring dynamometer or, in the case of moving loads or a single concentrated load, by means of a specially designed load cell. The elastic-ring dynamometer was equipped with a 0.0001-inch dial indicator and had a sensitivity of 110.8 pounds per division. The load cells consisted of cold-drawn seamless steel tubes machined to a wall thickness of 0.10 inch in the zone where measurements were made. Each load cell had eight type A7 SR-4 electric strain gages mounted at midheight and wired to form a four-arm bridge with a strain magnification factor of about 2.6. This gave the load cell a sensitivity of 134 pounds per dial division on the strain indicator.

Deflections were measured at midspan, and usually also at the third points, with 0.001-inch dial indicators.

Strains in the longitudinal reinforcement and on the top surface of the beam were measured by electric strain gages.

In some of the beams, vertical deformations between the flanges were measured with a 10-inch mechanical Whittemore gage.

The cracks were marked on the sides of the beams after each increment of load and the number of the increments at which the crack was observed was marked on the beam beside the pertinent crack. Photographs were taken at different stages of the test to be kept as a permanent record of the development of the crack pattern.

After completion of each test, the width of the flange, the depth of the beam and the reinforcement, and the thickness of the web were measured at the section of failure.

2.9 TEST PROCEDURE

2.9.1 Beams Tested with Stationary Loads

The failure load was usually reached in about ten increments. Load and deflection readings were taken at frequent intervals during the application of each increment of load. After a load increment, all deflection, load, and strain measurements were taken and the cracks were marked. Load and midspan deflection were measured again immediately before the resumption of loading. The flexural cracking load was reached in two or three increments. After flexural cracking, the magnitude of the load increments depended on the development of the crack pattern. The beams were loaded until complete failure. Each test took four to eight hours. Control specimens were tested immediately after the beam test.

2.9.2 Beams Tested with Moving Loads

Beams under moving loads were tested in two stages. In the first stage, the beam was loaded with a concentrated load at midspan until flexural cracking developed or until some predetermined load level was reached. Usually, this took three load increments. The second stage of loading consisted of a number of increments of "moving load." In this stage, one "load increment" consisted of applying the same load successively at each of the eleven loading positions along the beam. Two rams were used so that, when the load was transferred from one position to the next, the load could be decreased gradually in the first ram as it was increased in the second. The total load acting on the beam during a transfer rarely fell below 70 per cent of the nominal "moving load" for that increment.

At each loading position, a complete set of readings was taken and the cracks were marked. One load increment consisting of eleven separate loadings and sets of readings took approximately two and a half hours to complete. Beams without web reinforcement were tested in one day, but the beams with web reinforcement were tested over a two-day period, since up to twenty hours were required for such a test.

• • •

III. BEHAVIOR

3.1 CRACK PATTERNS

The macrocracks observed in prestressed concrete beams may be arbitrarily divided into three categories according to the dominant influences on their formation: flexure cracks, shear cracks, and flexure-shear cracks.

When a beam is loaded, the first cracks to be observed are usually short flexure cracks perpendicular to the beam axis at or close to the maximum moment region (Figure 8a). An increase in load will increase the number and extent of these flexure cracks (Figure 8b).

As the load is increased further, cracks may appear in a direction inclined to the longitudinal axis of the beam. These inclined cracks may develop in two different ways as follows.

In some cases a crack forms in the web close to the centroid of the beam while the tension zone in the vicinity of this section is still uncracked. Since this inclined crack develops with shear as the dominant cause, it will be called a shear crack (Figure 8c).

In other cases a flexure crack is formed first and the inclined crack may then develop rather suddenly on top of the flexure crack or more gradually as the propagation of the flexure crack forms a smaller and smaller angle with the beam axis. Since this type of crack develops in conjunction with a flexure crack and is affected by both the moment and the shear at the section, it will be referred to as a flexure-shear crack (Figure 8d).

Because of the nature of a shear crack, the development of such a crack is easily detected. The same is not always true for a flexure-shear crack. Here it often becomes a matter of definition when a flexure crack is "inclined enough" to be characterized as an inclined crack or rather when the behavior of the beam changes as a result of inclined cracking.

3.2 EFFECTS OF CRACK PATTERN ON BEHAVIOR

The effect of cracking on the behavior of a prestressed concrete beam can be illustrated in terms of

(1) distribution along the axis of the strains in the top of the compression zone,

(2) relation between strains in the reinforcement and strains in the concrete.

(3) change in the distance between the flanges,

(4) load-deflection curve.

Figure 9 shows the strains in the top fiber of the concrete in a simply supported beam. The strains at different sections are plotted along the span for three values of the load on the beam. Strains were measured electrically over a series of 3/4-inch gage lengths. For small loads the strains were distributed as the moment. As the load was increased, the strains tended to concentrate at or close to the top of an inclined crack.

The same trend can be observed in Figure 10 where the strain in the top fiber of the concrete at different points along the axis is plotted against the strain in the longitudinal reinforcement at midspan. Before flexural cracking, the ratio between concrete strain and steel strain is rather high corresponding to a large depth to the neutral axis. After flexural cracking, this depth is decreased and the steel strain increases faster. One further drastic change may occur when the inclined crack develops. The concrete strain at the top of the inclined crack increases faster than the steel strain (Curves A and C) while the concrete strain at points in the shear span away from the top of the inclined crack may start decreasing (Curve D). Strains at midspan (Curve B) are unaffected by the inclined crack.

A very useful way to present the response of a beam to load is a plot of the relationship between the load and the change in vertical distance between top and bottom flanges of the beam. Of interest is also the distribution along the span of this change in distance. Curves of this type are shown in Figure 11. The distance change was negligible until cracking took place in the shear span. From then on not only the distance but also the rate of change was increasing.

It is important to note that the change in distance which is necessary to obtain failure is quite large. In fact, if this change is assumed uniformly distributed over the 10-inch gage length which is also approximately the total height of the stirrup, the corresponding strain is much larger than the yield strain for the stirrup steel. Furthermore, this large strain is developed over a large part of the shear span.

Load-deflection curves need little introduction. Such curves illustrate the features in which the designer is most interested -- the load capacity and the ductility.

It may be pertinent at this stage to point out that all these means of registering the behavior of the beam are subject to limitations. For example, concrete strains are not easy to measure and in regions with high strain gradients it is certainly unrealistic to be looking for "true" values of strain. However, all the measurements can give certain qualitative information. The aim of this chapter is, therefore, to report trends rather than specific numbers. In Chapters IV and V, these trends will be used to develop analytical procedures.

3.3 INFLUENCE OF DIFFERENT VARIABLES ON THE CRACK PATTERN

3.3.1 Effect of Prestress and Amount of Reinforcement

Figures 12 and 13 show load-deflection curves for eleven beams reported in Reference 1. The three beams in Figure 12a were similar except for the variation of prestress from 34 to 131 ksi. As the prestress level is increased, both the flexural and inclined cracking loads increase. The ultimate loads also increase, but it is worth noting that the load carried beyond inclined cracking becomes smaller as the prestress level is raised. The same is true for the I-beams (Figure 12b). The increase in prestress results in a substantial increase in the inclined cracking load. However, for the beams with high prestress, the formation of the inclined crack leads to an immediate failure, while the ultimate load for the beams with no prestress is about twice the inclined cracking load. This suggests that the failure mechanisms are different.

A similar increase in the inclined cracking load can be observed in Figure 13a which

contains load-deflection curves for two beams with the same prestress but with different amounts of longitudinal reinforcement.

Figure 13b shows the effect of an increase in reinforcement ratio combined with a decrease in prestress to give the same total prestressing force. The inclined cracking loads are almost equal, demonstrating that the effect on inclined cracking of both the prestress level and the reinforcement ratio can be expressed in terms of the total prestressing force.

3.3.2 Effect of Shape of Section

Figure 12b also shows the effect of web thickness. The inclined cracking load appears to be independent of the web thickness as long as the prestress level is low, while an increase in web thickness at a high prestress level seems to delay inclined cracking.

It was observed that the beams with no prestress developed flexure-shear cracks while beam C.12.50 developed a shear crack. In beam B.12.50, the thicker web apparently increased the load corresponding to the formation of a shear crack. Before this load could be reached a flexure-shear crack had formed. From this it may be hypothesized that the web thickness has an effect only on shear cracking.

3.3.3 Effect of Concrete Strength

Figure 14 shows load-deflection curves for four beams reported in Reference 1. Reinforcement ratio, web thickness, and loading arrangement were almost identical for these beams but concrete strength and prestress level were different. Although the change in concrete strength was somewhat larger for the beams without prestress, it is apparent from Figure 14 that the relative increase in the inclined cracking load compared with the increase in concrete strength is much smaller for beams with prestress than for the beams without prestress.

This is not surprising in view of the way in which the inclined crack develops. In the case of a shear crack, the inclined cracking load should be related to the principal tensile stresses in the web. The contribution from the prestress to the principal tensile stress at the centroid is usually opposed to the contribution from the shear force; hence, the prestress may be thought of as an increase in the concrete strength. The flexure-shear crack is expected to be related to a combination of flexural cracking and principal tensile stresses. Therefore, the effect of the prestress should also be the same as an increase in the concrete strength in this case. This explains the trends with respect to inclined cracking observed in Figures 12-14.

3.3.4 Effect of Draped Reinforcement and Vertical Prestress

In this connection it is of interest to observe the behavior of a series of beams with vertical, unbonded, and prestressed stirrups. The load-deflection curves for four beams with vertical prestress are shown in Figure 15. The only variable in this set of beams was the level of prestress in the stirrups. The vertical prestress increased the load at shear cracking. This should be expected since the effect of the vertical prestress on the principal tensile stress is almost the same as the effect of a horizontal prestress. However, the flexural cracking is unaffected by the vertical prestress and since a flexure-shear crack apparently is related closely to flexural cracking, a vertical prestress should have only a small effect on flexure-shear cracking. Consequently, it was possible to increase the vertical prestress to a level at which a flexure-shear crack formed prior to a shear crack. A further increase in the stirrup

prestress had only a small effect on the inclined cracking load.

Similar considerations can be used in interpreting the results from a series of beams with draped longitudinal reinforcement. Load-deflection curves for two of these beams and a similar beam with straight reinforcement are shown in Figure 16. All three beams developed flexure-shear cracks. The load at inclined cracking appears to be decreasing with an increase in drape angle. This may be explained by the fact that the flexural cracking moment is reduced because of the draping of the reinforcement at the section where the inclined crack initiates (as a flexure crack).

In a few beams with draped reinforcement, the inclined crack developed as a shear crack. Directly comparable beams were not tested but it appears that the shear cracking load increases with an increase in the angle of drape. Since the draping of the reinforcement introduces a vertical component of prestress, this result agrees with the result from the beams with prestressed stirrups.

3.3.5 Effect of the Length of Shear Span

If the flexure-shear cracking load is affected by flexural cracking as it was concluded in the preceding discussion, it should be expected that the length of the shear span compared to the depth of the beam is an important factor in evaluating the flexure-shear cracking load. That this is correct is demonstrated in Figure 17 where load-deflection curves are shown for three comparable beams reported in Reference 1. The three beams had shear spans varying in length from 24 inches to 54 inches, and all the beams developed flexure-shear cracks. The reduction in the inclined cracking load is marked.

Load-deflection curves for two beams developing shear cracks are shown in Figure 18. Although the change in length of the shear span is only 25 per cent, Figure 18 indicates that the length of the shear span has little if any bearing on the shear cracking load. Considering that the shear crack seems to be governed by the principal tensile stress in the web where bending stresses are small, this result is reasonable.

An interesting demonstration of the effect of shear-span length on flexure-shear cracking is provided by the test results from a beam subjected to a moving load. The inclined cracking loads for various positions of the moving load are plotted in Figure 19. The trend of the plotted data shows the reduction in inclined cracking load with increasing distance from the nearer reaction.

3.3.6 Effect of Cast-in-Place Slab

Figure 20 shows load-deflection curves for six simply-supported beams. Three of these beams had cast-in-place slabs while the other three did not. The prestressing force was varied by changing the longitudinal reinforcement ratio. In all six beams inclined cracking developed as shear cracks. For the I-beams the inclined cracking was increased with increase in the prestressing force. For the composite beams this effect seems to be somewhat smaller. Furthermore, the inclined cracking load appears to be consistently smaller for the composite beam than for the I-beam, which may be explained as follows.

For beams without web reinforcement the propagation of a shear crack is very rapid. If a reasonably large amount of web reinforcement is provided, it is often possible to delay the crack propagation so much that an idea about the point of initiation can be obtained. This revealed that in the I-beams the inclined crack usually formed close to the centroid or in the lower part of the web,

while the point of initiation in the composite beams usually was in the upper part of the web, close to the intersection between the web and the compression flange. An analytical study of the principal tensile stresses in the web showed that the maximum tensile stress for the I-beam existed a little below the middle of the web. With the particular geometry and prestressing force chosen for the composite beams, the point of maximum tensile stress was found at the junction between compression flange and web. However, at this point the longitudinal stress from the prestress was smaller than at the centroid of the web. Consequently, the load at the formation of a shear crack decreased as the result of the presence of a slab.

It may be pointed out that the six beams referred to in Figure 20 all had thin webs and high prestress levels. It is entirely possible that a similar set of beams with a larger web thickness and a smaller prestress would develop flexure-shear cracks. Since the flexural cracking load is increased by the slab, the inclined cracking load for this set of beams should be increased as a result of both an increase in prestress and the addition of a cast-in-place slab.

3.3.7 Effect of Web Reinforcement

The crack patterns up to the first inclined cracking observed in beams with web reinforcement were in general similar to the pattern in corresponding beams without web reinforcement. Flexural and inclined cracking loads were not significantly changed by the presence of stirrups. However, in a few cases a marked difference was observed in the crack propagation after inclined cracking depending on the amount of web reinforcement. Figures 21 and 22 show crack patterns for two series of beams recorded just before failure occurred. All eleven beams had similar properties except for varying amounts of web reinforcement. The shear spans were 30 inches and 45 inches for the beams in Figures 21 and 22, respectively.

The photographs in Figure 21 show a significant change in slope of the cracks with increased amount of web reinforcement. This change may be explained by the manner in which the beam carries the total shear force. After the inclined crack has formed, a certain shear force has to be transmitted across the inclined crack in order to maintain beam action. In a beam without web reinforcement, this shear can be carried by the so-called doweling force in the longitudinal reinforcement. The doweling force may be large enough to introduce a succession of inclined cracks near the bottom end of the first inclined crack as seen in Figure 21a. If the beam has web reinforcement, part of the shear transfer across the inclined crack will be provided by the stirrups and the doweling force would decrease accordingly. With a sufficient amount of web reinforcement it is then possible to avoid cracks caused by the doweling action and the resulting crack pattern may be as shown in Figure 21g.

The photographs in Figure 22 illustrate a case for which the influence from the web reinforcement on the cracks is practically negligible. In these beams with a larger shear span, the total shear at the formation of the first inclined crack was smaller than the inclined cracking shear in a beam with a shorter shear span. The doweling force at this stage of the loading was, therefore, not large enough to affect the crack pattern. As the load on the beam was increased, new inclined cracks were formed parallel to the first one until the shear became large enough for doweling forces to cause additional cracking at the bottom of the inclined cracks.

The change in distance between the

flanges of the beam is primarily a measure of the vertical projection of the crack width. Since the stirrups were firmly anchored in both top and bottom flanges, the total elongation of a stirrup must be equal to the change in vertical distance between the flanges. Before yielding, the stirrup is usually crossed by at least two cracks. Considering the bond characteristics of the stirrup steel, it seems reasonable to assume that the stirrup strains at this stage were almost uniformly distributed over the entire length of the stirrup. Measured total deformations between flanges larger than, say, 0.01 inch may therefore give a reasonably good estimate of the strain in the stirrup. Yielding should be definitely expected at a deformation of about 0.015 inch.

Figure 23 illustrates how the deformation between the flanges was distributed along the shear span for three of the beams shown in Figure 21. The deformation is seen to have a peak value close to the center of the shear span. It should also be noted that the deformation required to produce yielding in the stirrups was reached over a large portion of the shear span.

Figure 24 shows plots of load versus deformation between flanges for the same three beams. The curves shown refer to maximum and minimum deformation measured in a 10-inch zone along the shear span starting 6 inches from the load point. No significant deformation was measured until a crack crossed a gage line. This crack was not necessarily the inclined crack. The load at which the first deformation was measured was independent of the amount of web reinforcement. The curves relating to beam B.23.17 exhibited a very large decrease in slope as the load was increased until a deformation of about 0.005 inch was reached. This corresponds to the formation of the inclined crack. Since this beam had no web reinforcement, a further increase in load resulted in rapidly increasing deformations. The slope of the lower part of the curves relating to beams BW.23.20 and BW.23.22 depended on the amount of web reinforcement. In fact, the load corresponding to a deformation of 0.015 inch increased linearly with rf_y. After yielding of the stirrups had taken place -- at a deformation of 0.010 to 0.015 inch -- the slope of the curves remained almost constant up to failure. It is important to note that both beams BW.23.20 and BW.23.22 failed at loads considerably higher than the load at which the stirrups yielded.

The three beams discussed in connection with Figures 23 and 24 were part of a series of eight beams in which only the amount of web reinforcement was varied. In Figure 25 is shown the deformation between the flanges at ultimate for these beams plotted against the amount of web reinforcement. The ultimate deformation was obtained by extrapolation of load-deformation curves of the type shown in Figure 24. It is seen that an increase in rf_y from 0 to about 175 resulted in a drastic reduction in ultimate deformation, while larger amounts of web reinforcement seemed to have little or no effect. This does not imply that an $rf_y = 175$ is the most efficient amount of web reinforcement in this beam since it required $rf_y = 250$ to develop the flexural capacity. It may be noted that an $rf_y = 175$ was approximately the amount of web reinforcement which was needed to change the crack pattern as indicated in Figures 21a through 21g.

The effect on the concrete strains in the top flange from inclined cracks and the restraint of these cracks caused by the stirrups may be seen from Figure 26. The figure shows strain distributions at ultimate along the top surface of three beams in which only the amount of web reinforcement was varied. Inclined

SUPPORTING DATA

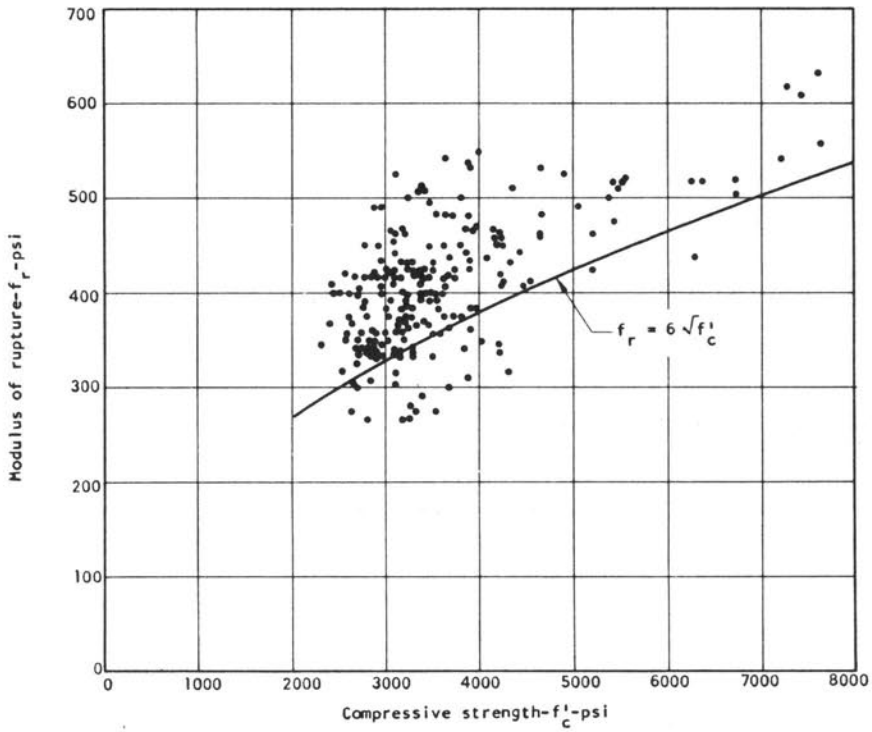

FIGURE 1. VARIATION OF MODULUS OF RUPTURE WITH CONCRETE COMPRESSIVE STRENGTH

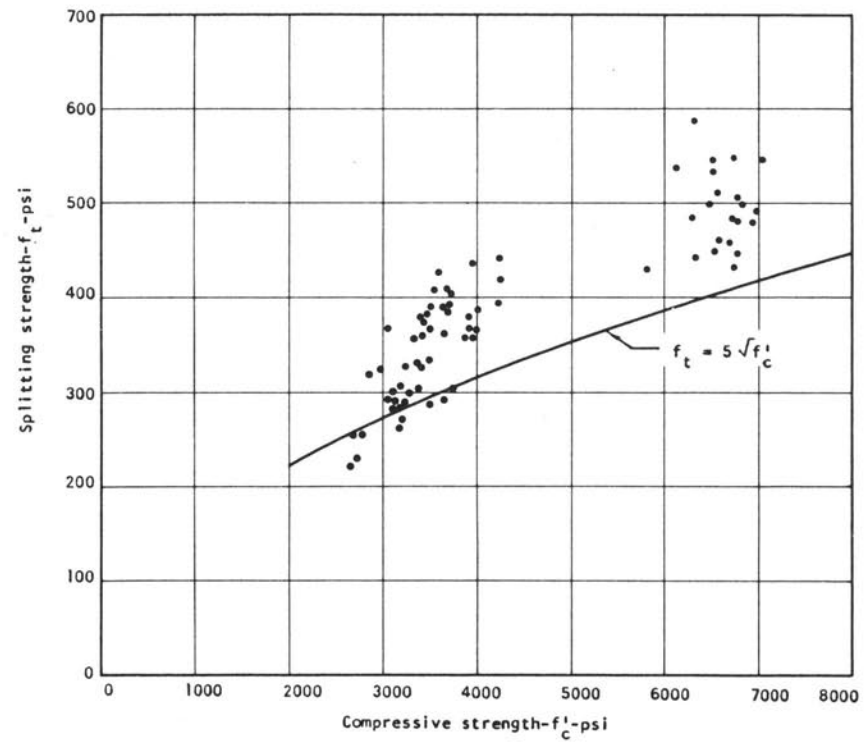

FIGURE 2. VARIATION OF SPLITTING STRENGTH WITH CONCRETE COMPRESSIVE STRENGTH

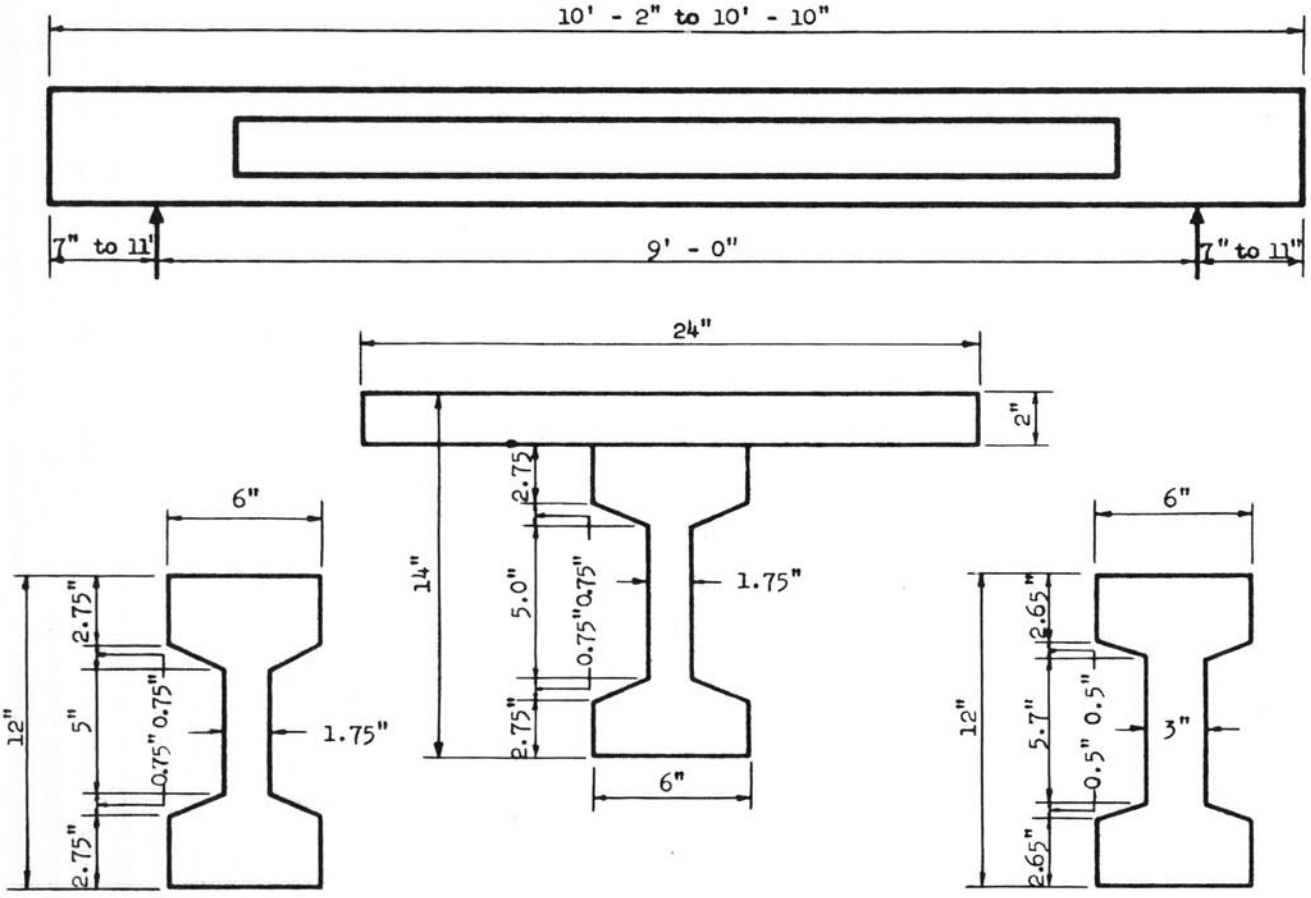

FIGURE 3. NOMINAL DIMENSIONS OF TEST BEAMS

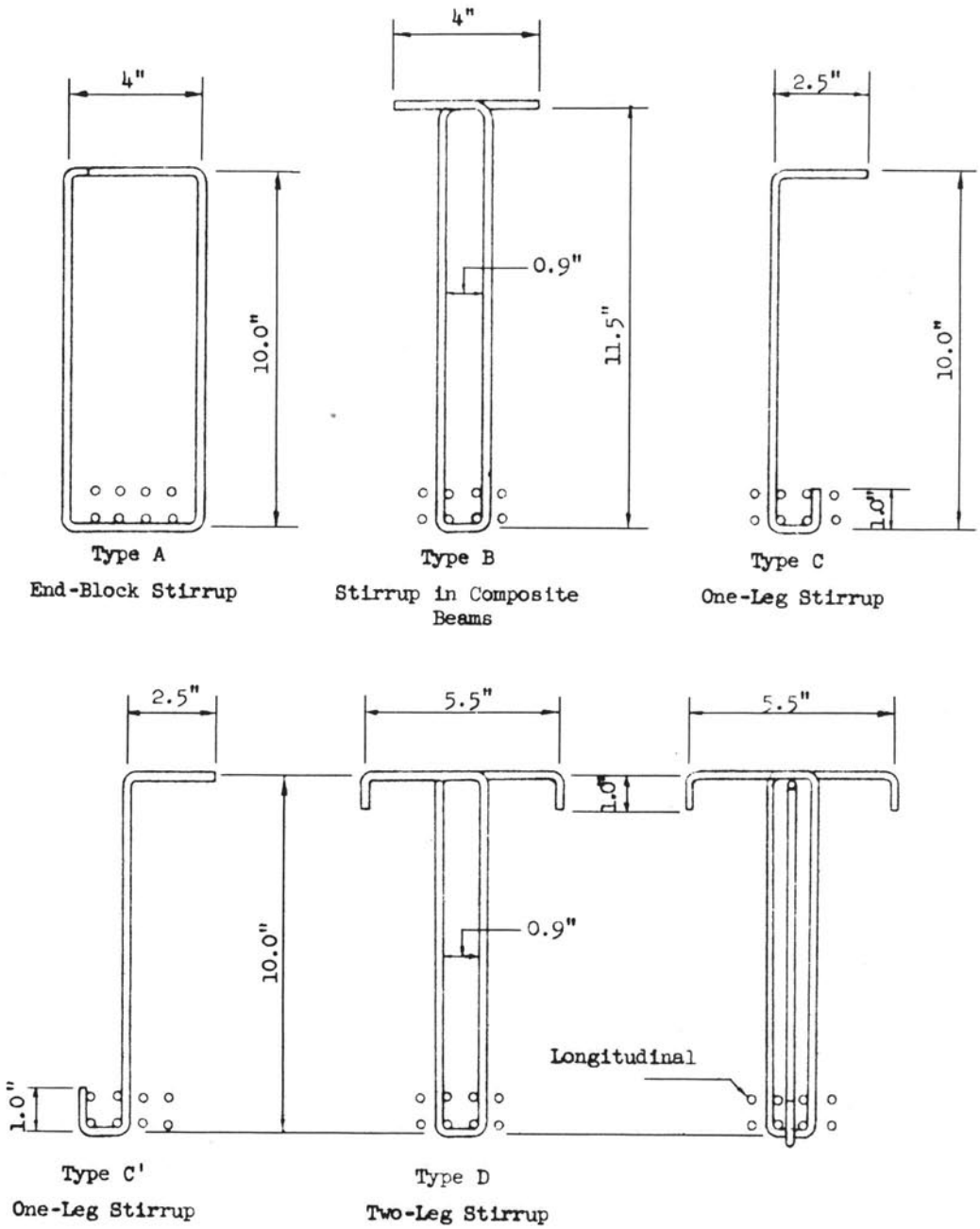

FIGURE 4. NOMINAL DIMENSIONS OF STIRRUPS

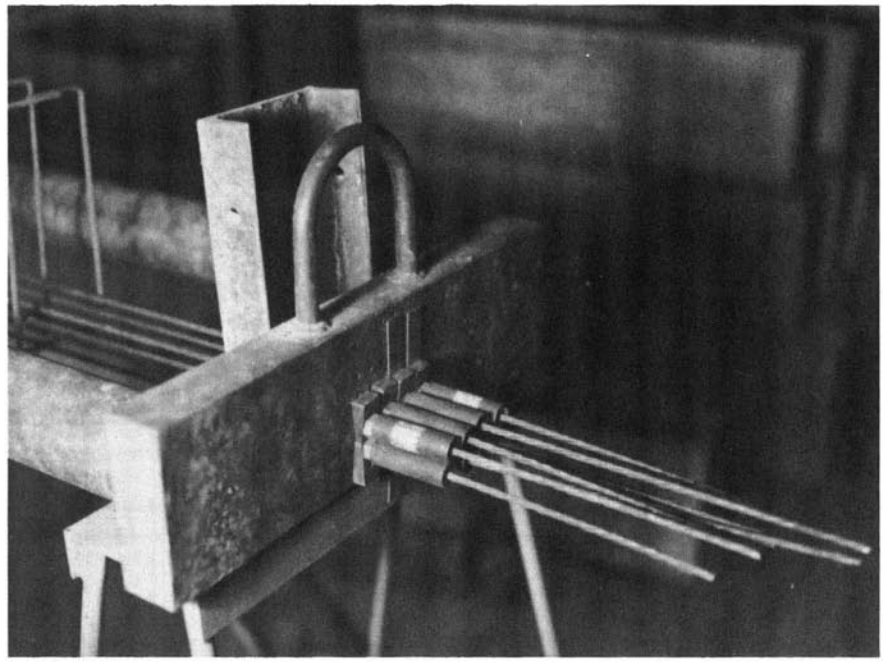

FIGURE 5. DETAILS OF ANCHORAGE FOR SEVEN-WIRE STRAND

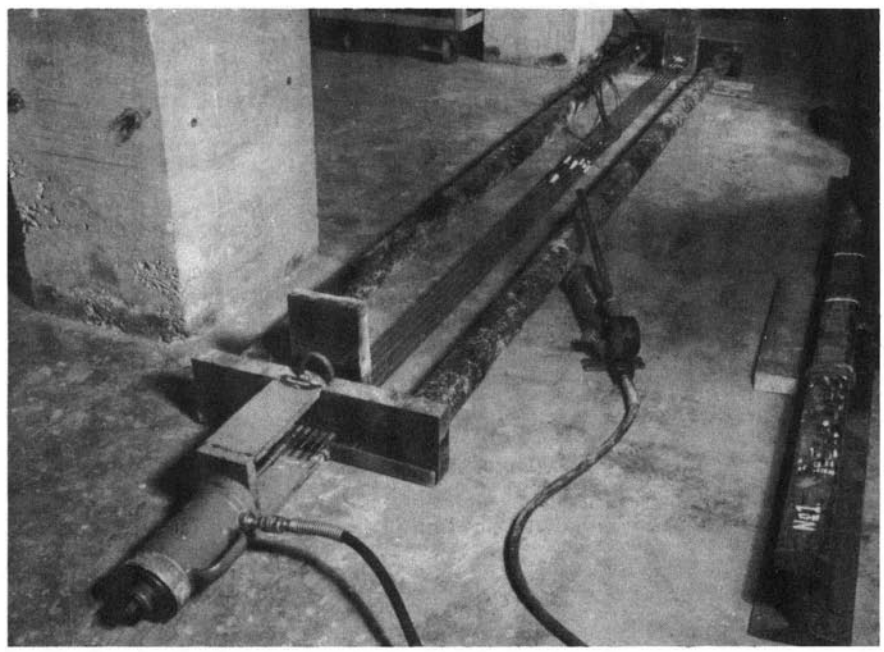

FIGURE 6. PRETENSIONING APPARATUS

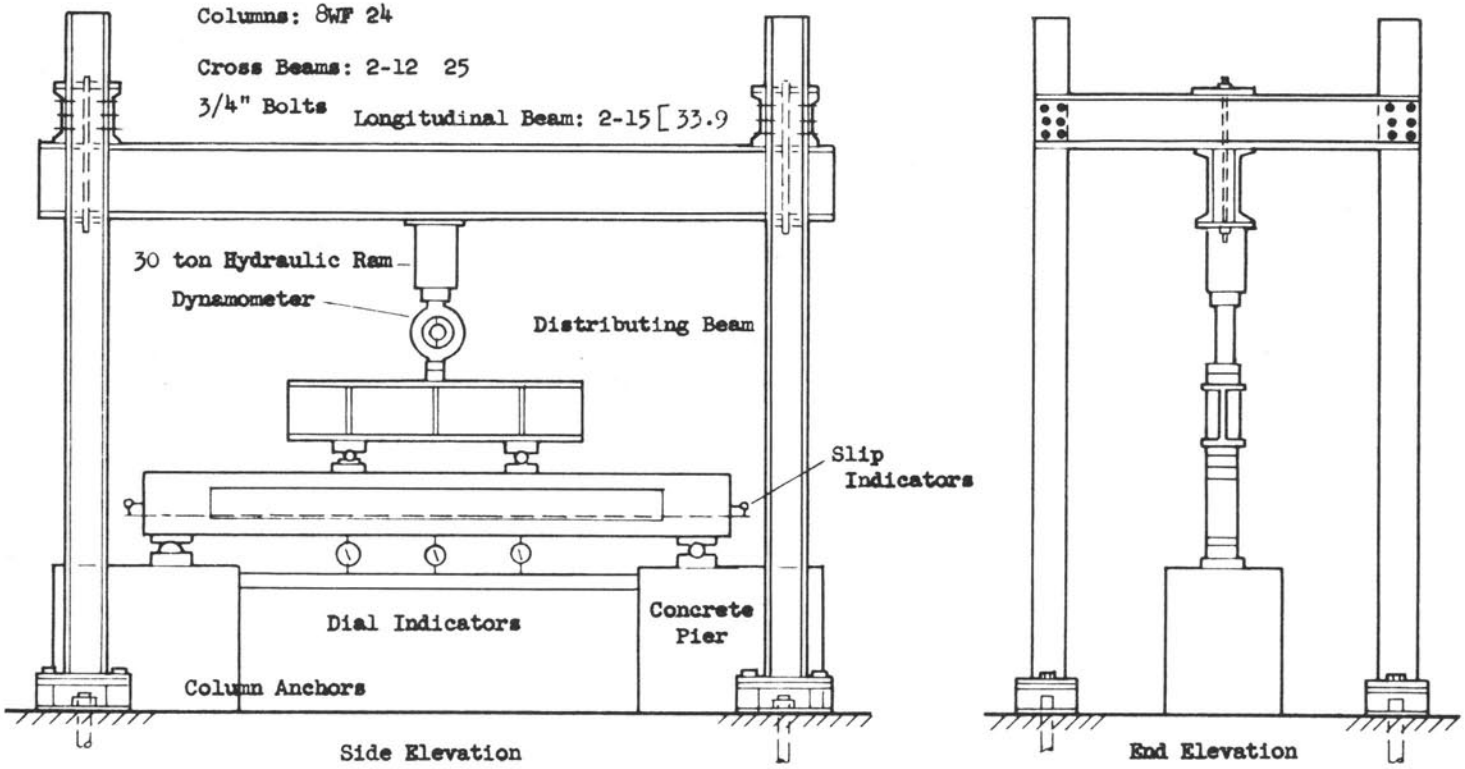

FIGURE 7. DETAILS OF TESTING APPARATUS

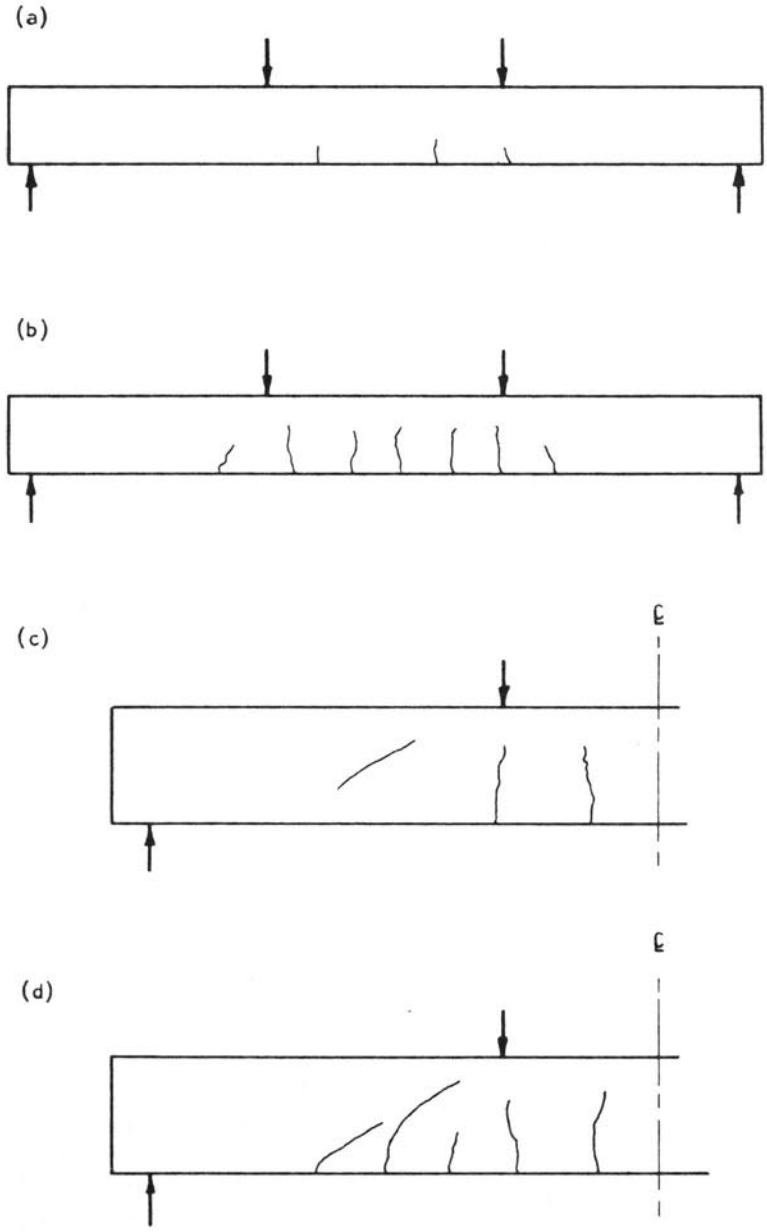

FIGURE 8. CRACK DEVELOPMENT IN PRESTRESSED BEAM

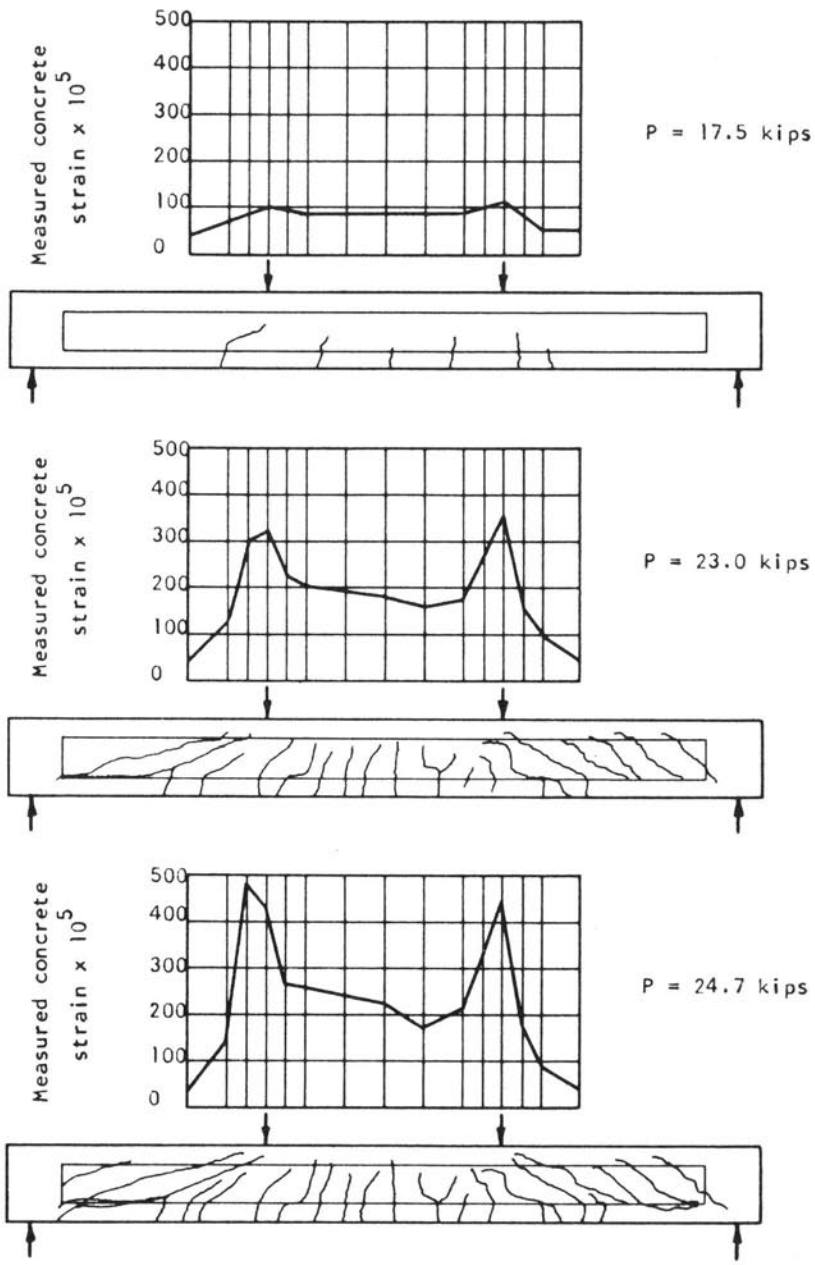

FIGURE 9. CRACK PATTERN AND ITS EFFECT ON THE DISTRIBUTION OF STRAIN ON TOP SURFACE OF BEAM CW.14.37

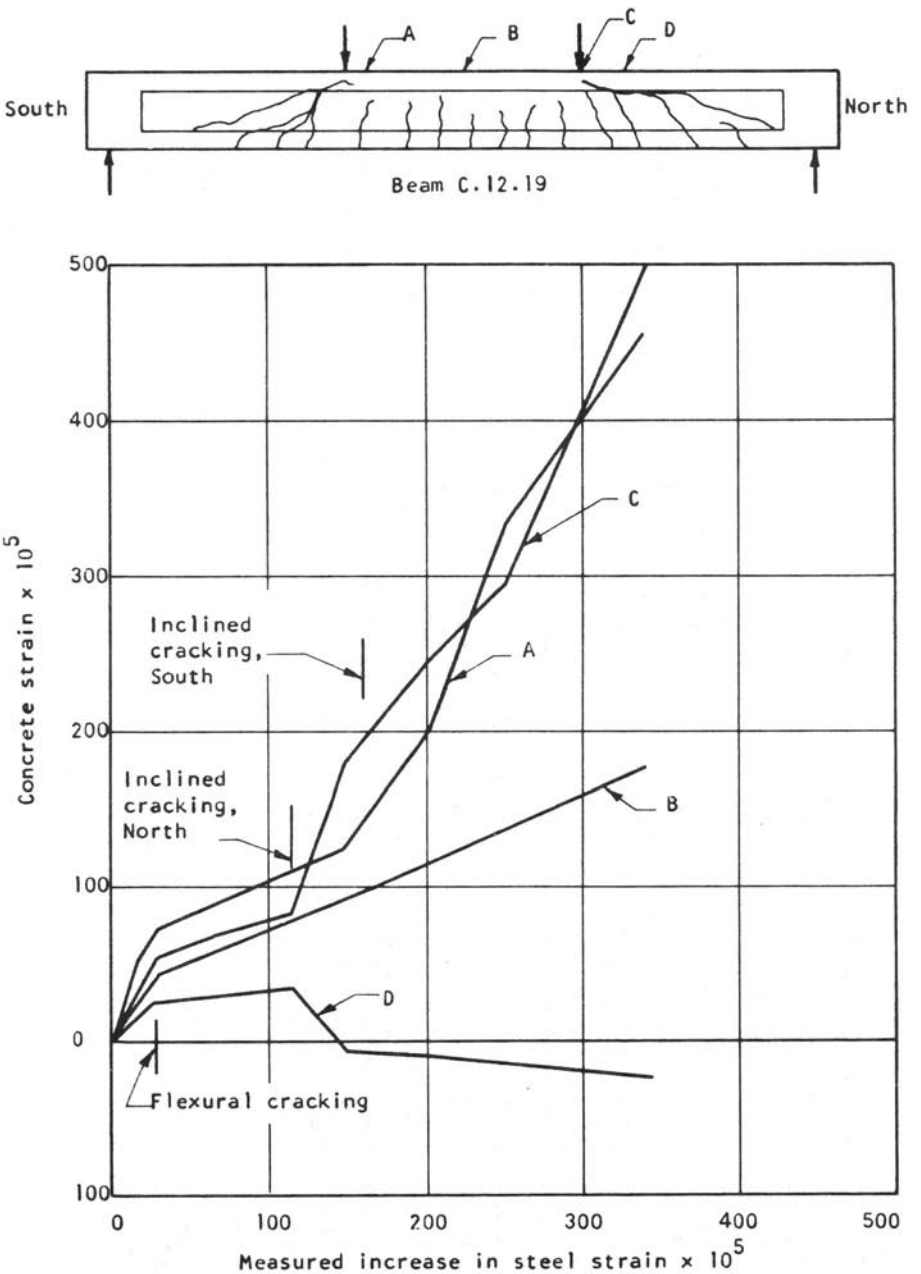

FIGURE 10. RELATION BETWEEN CONCRETE AND STEEL STRAINS

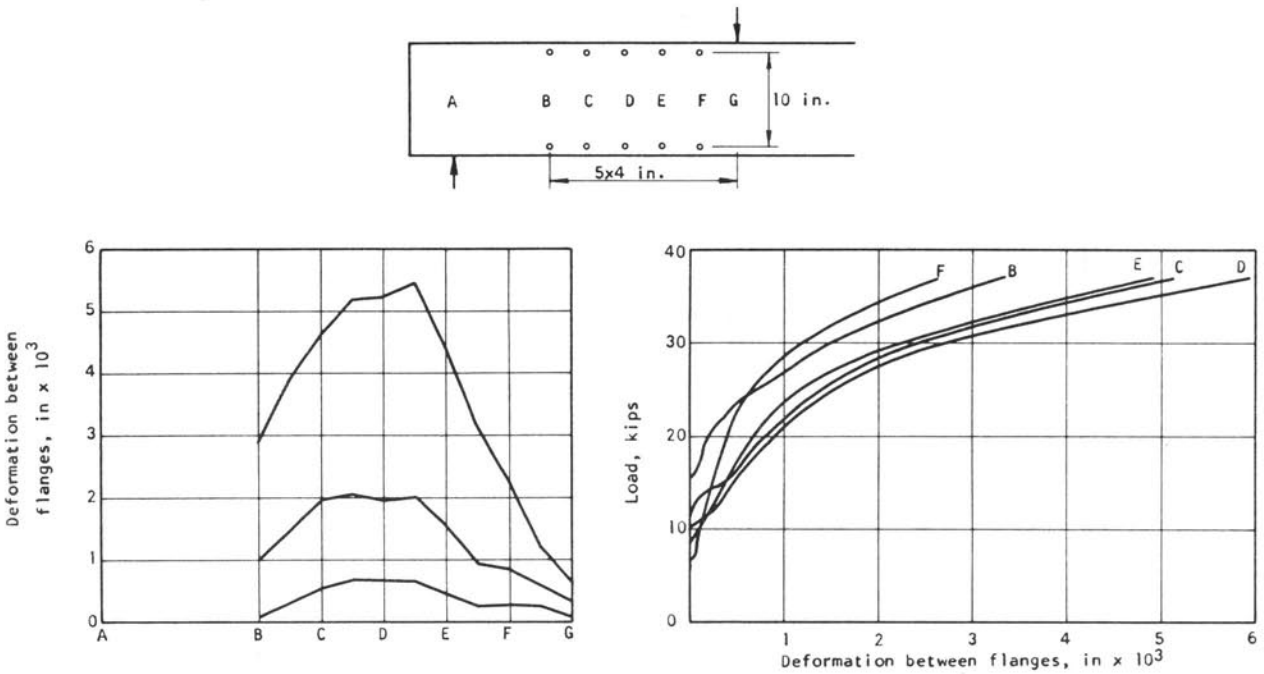

FIGURE 11. DEFORMATION BETWEEN FLANGES IN BEAM BW.23.22

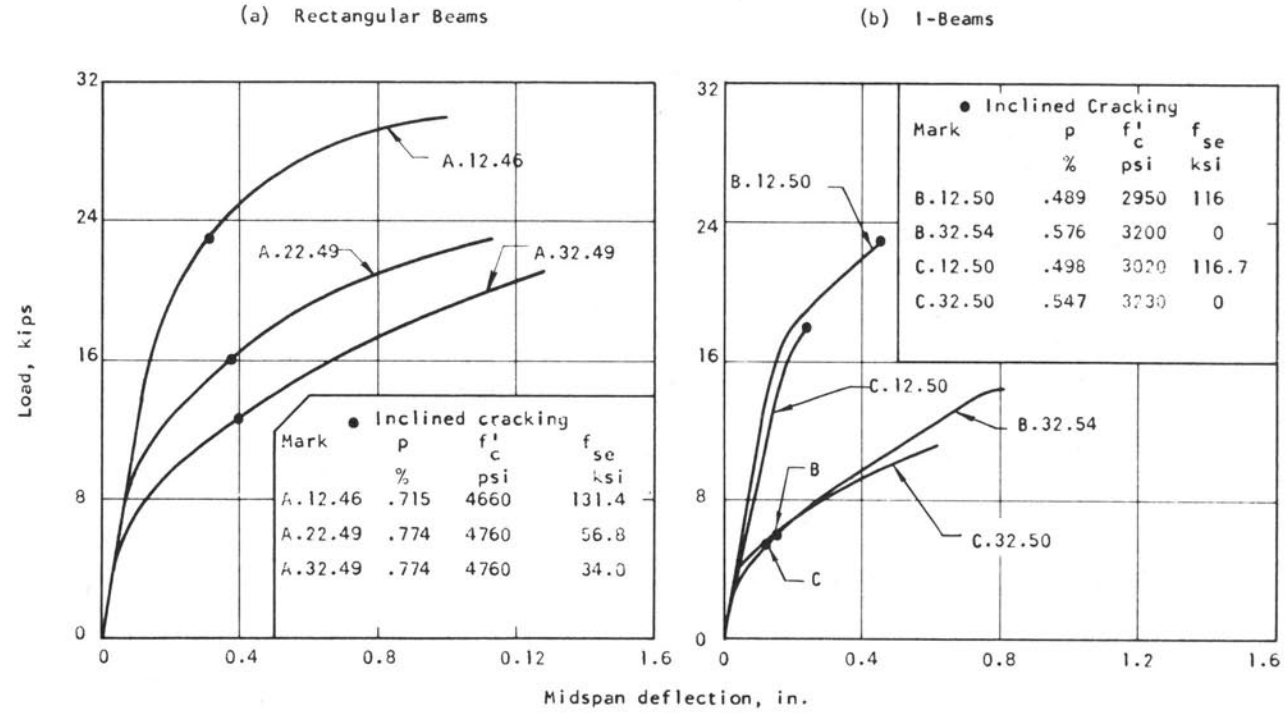

FIGURE 12. EFFECT OF PRESTRESS LEVEL AND WEB THICKNESS ON INCLINED CRACKING

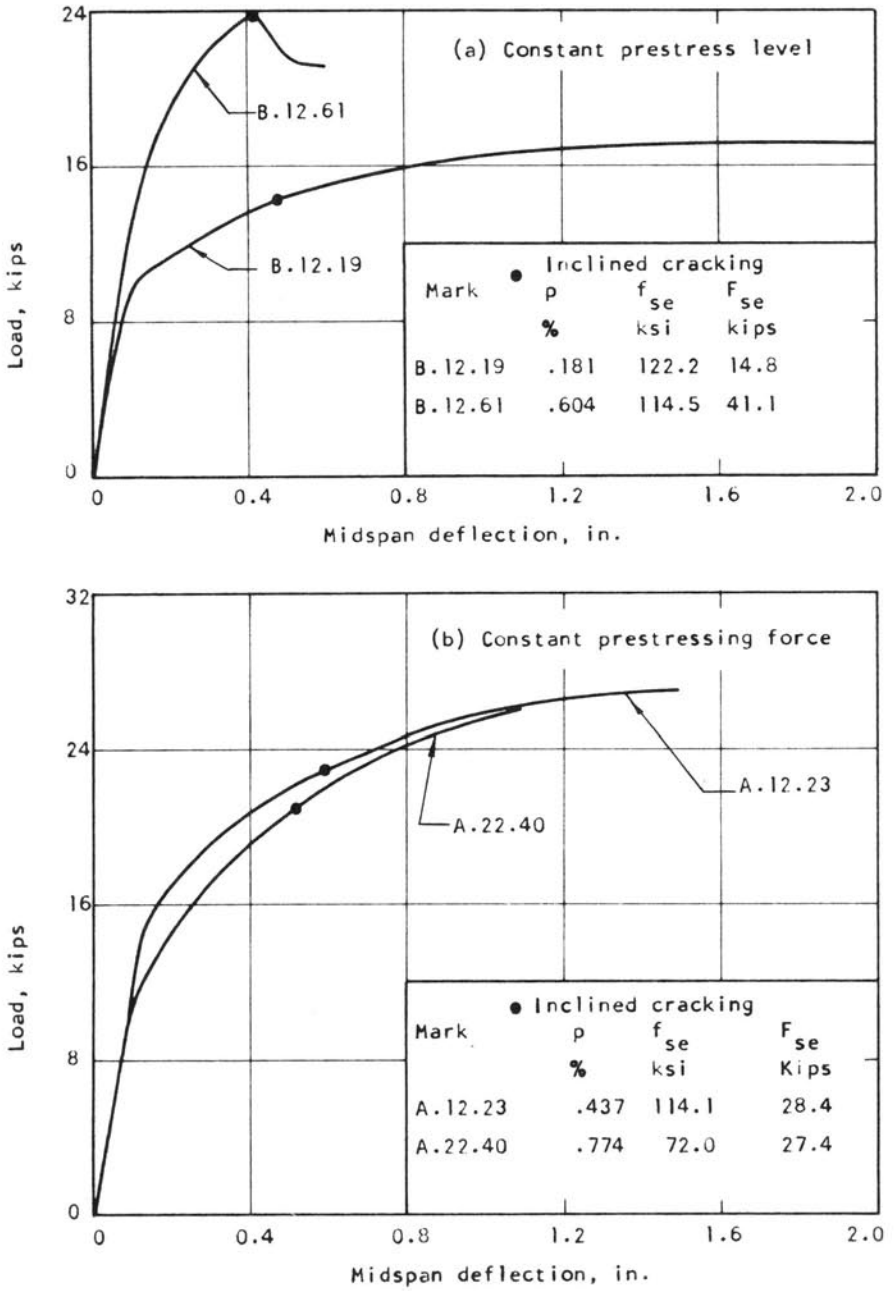

FIGURE 13. EFFECT OF PRESTRESSING FORCE ON INCLINED CRACKING

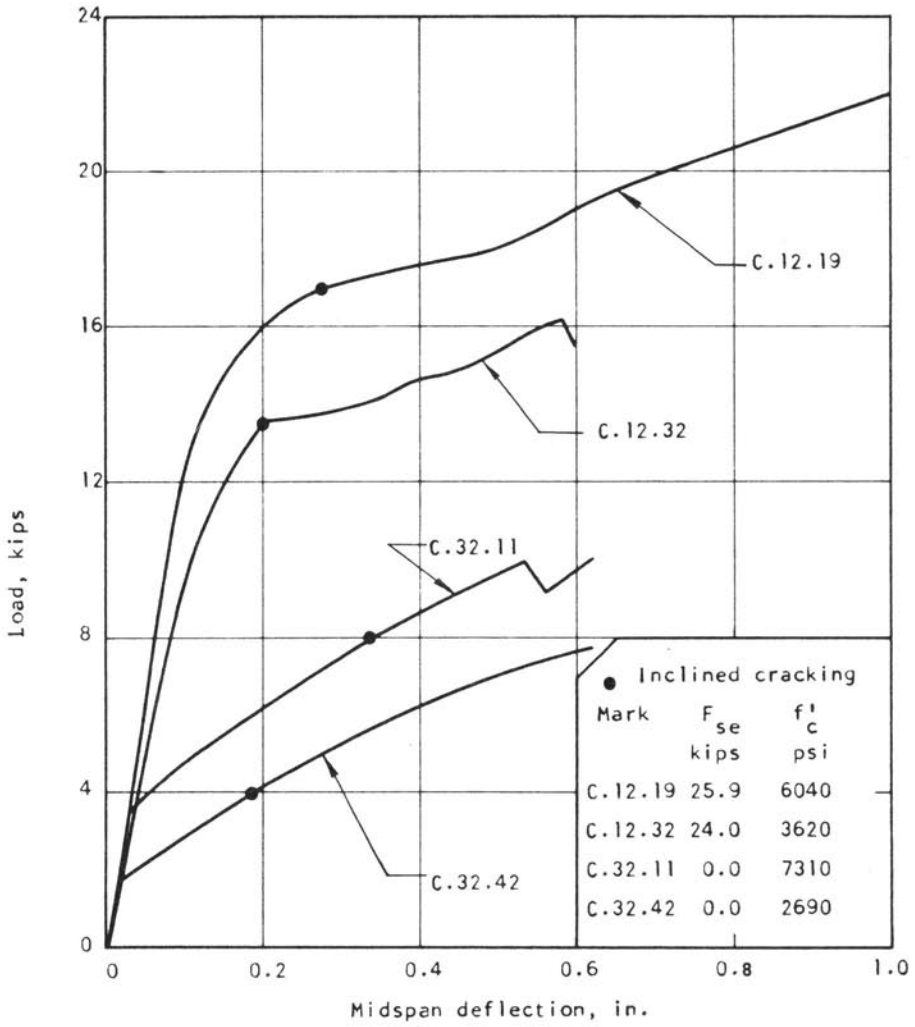

FIGURE 14. EFFECT OF CONCRETE STRENGTH ON INCLINED CRACKING

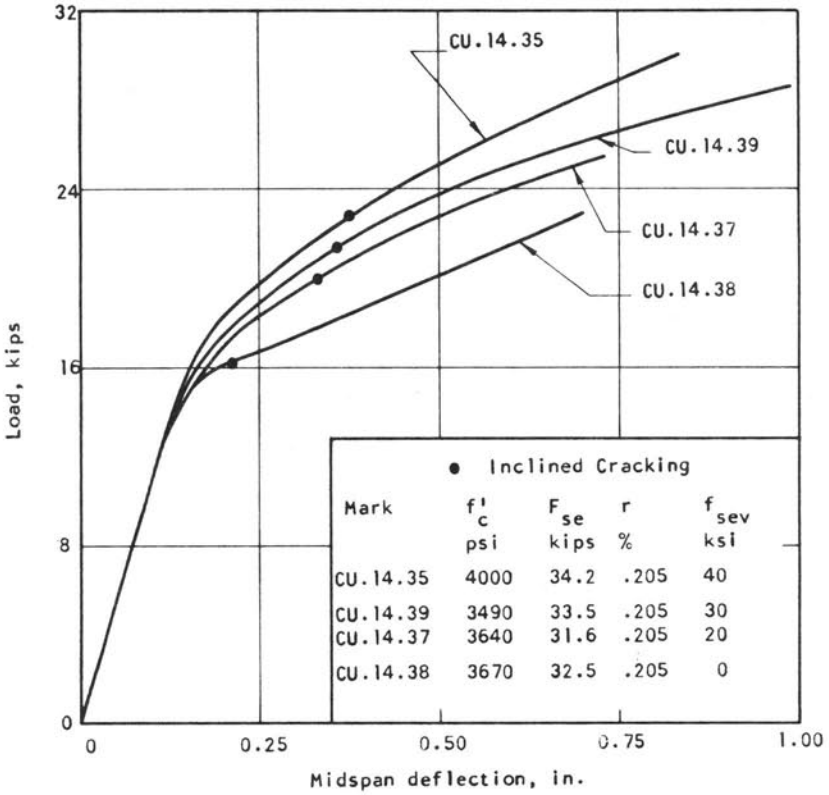

FIGURE 15. EFFECT OF VERTICAL PRESTRESS ON INCLINED CRACKING

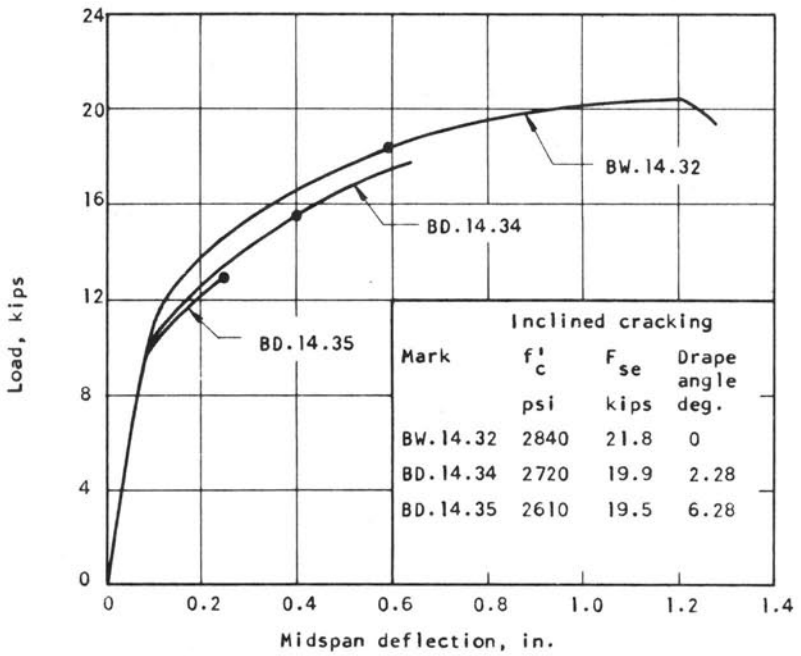

FIGURE 16. EFFECT OF DRAPING OF LONGITUDINAL REINFORCEMENT ON FLEXURE-SHEAR CRACKING

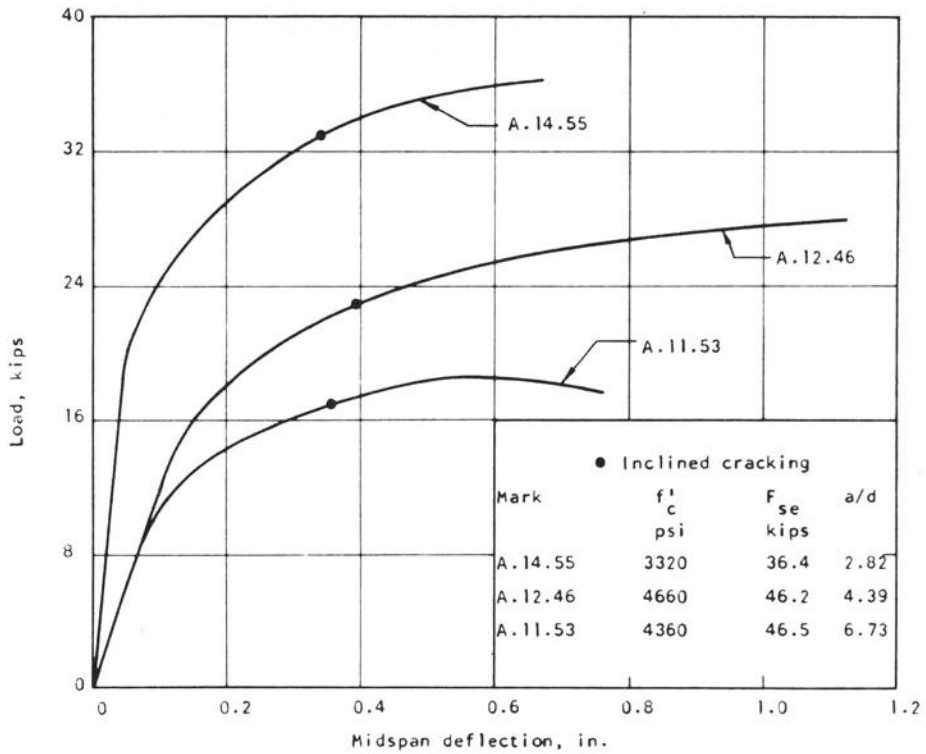

FIGURE 17. EFFECT OF a/d RATIO ON FLEXURE-SHEAR CRACKING

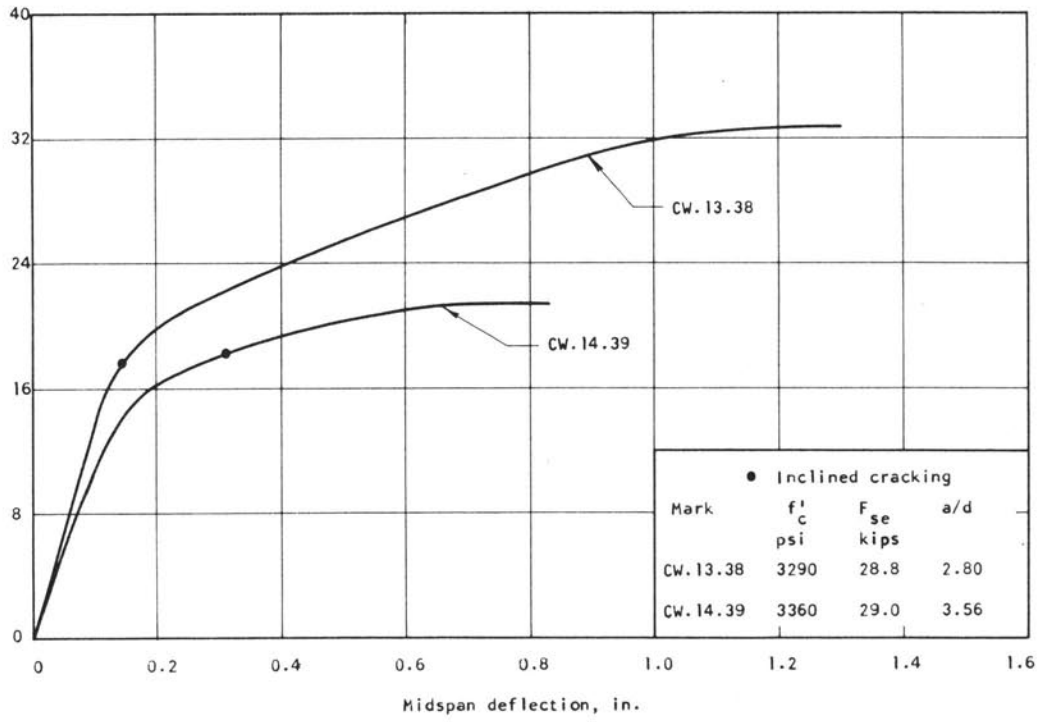

FIGURE 18. EFFECT OF a/d RATIO ON SHEAR CRACKING

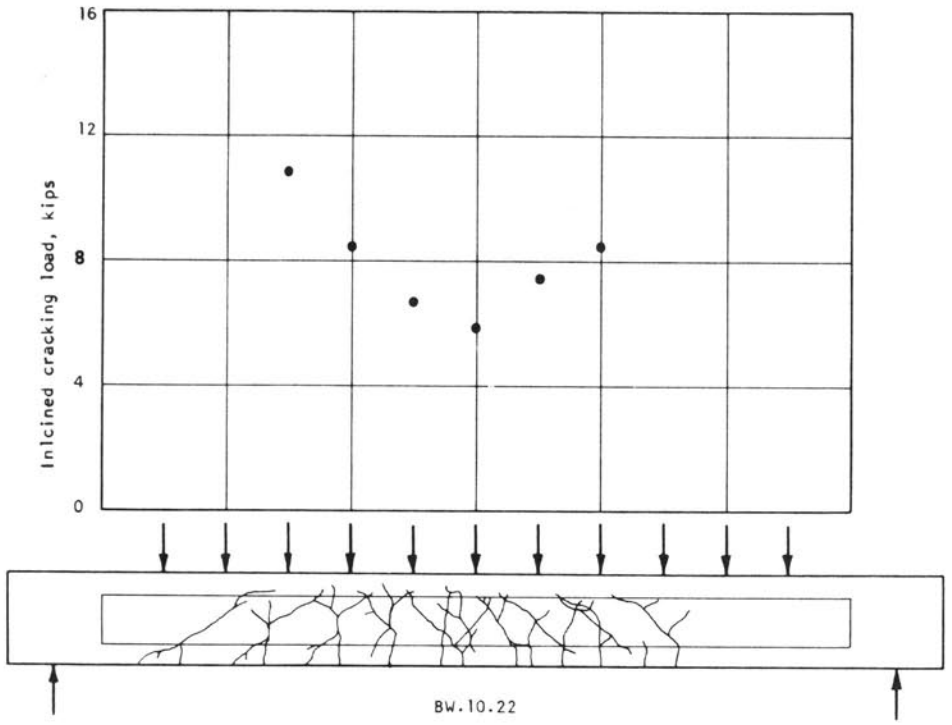

FIGURE 19. INCLINED CRACKING LOAD AS RELATED TO POSITION OF SIMULATED MOVING LOAD

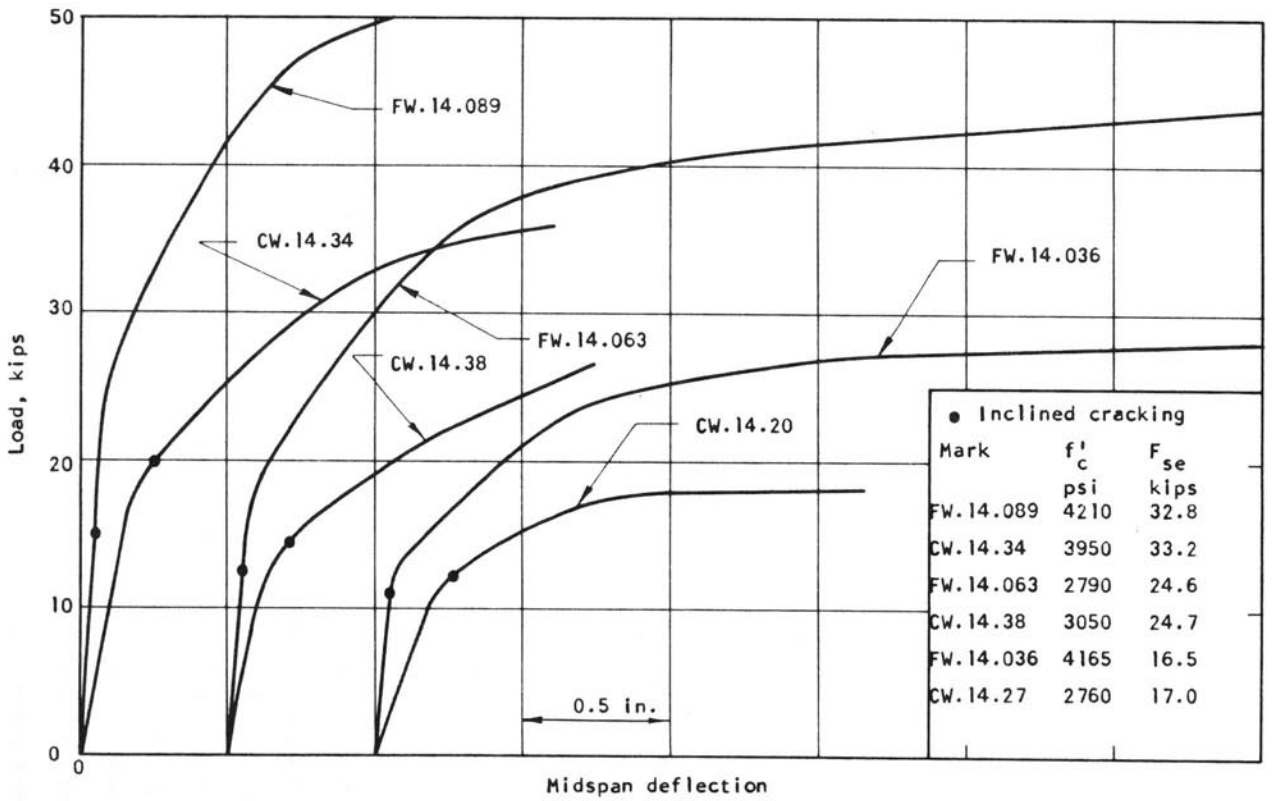

FIGURE 20. EFFECT OF PRESTRESS AND CAST-IN-PLACE SLAB ON SHEAR CRACKING

(a) BW.23.17
rf_y = 0

(b) BW.23.18
rf_y = 48

(c) BW.23.20
rf_y = 96

(d) BW.23.21
rf_y = 133

(e) BW.23.22
rf_y = 176

(f) BW.23.23
rf_y = 206

(g) BW.23.24
bf_y = 246

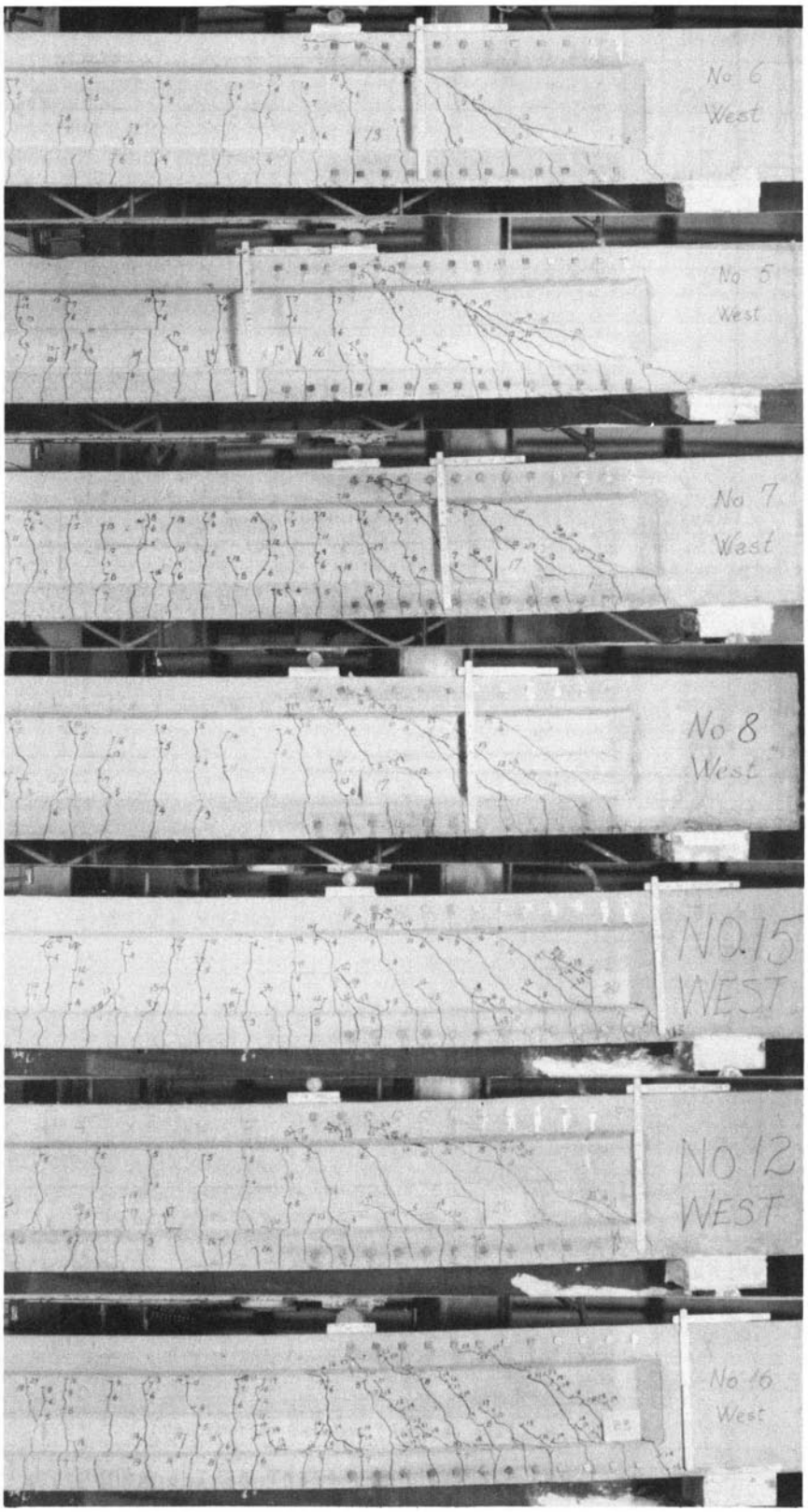

FIGURE 21. CRACK PATTERNS SHOWING EFFECT OF THE AMOUNT OF WEB REINFORCEMENT

(a) B.25.18
$rf_y = 0$

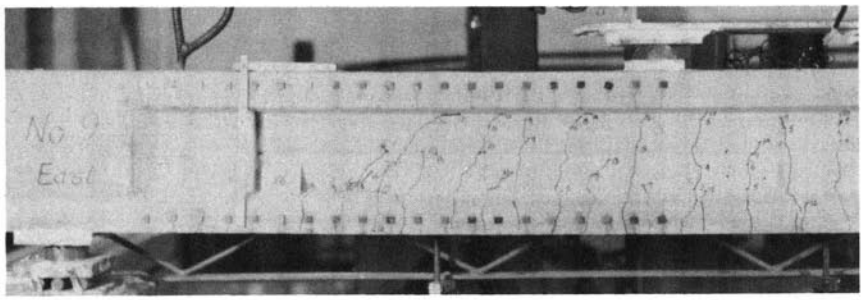

(b) BW.25.19
$rf_y = 48$

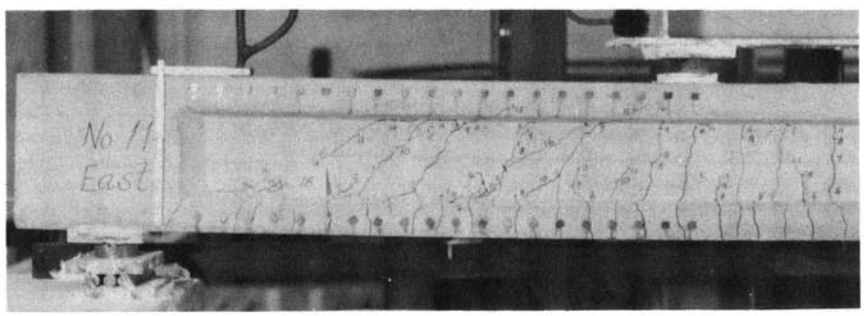

(c) BW.25.20
$rf_y = 96$

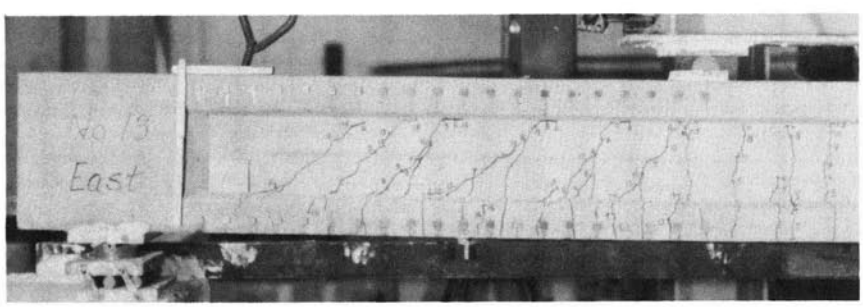

(d) BW.25.21
$rf_y = 133$

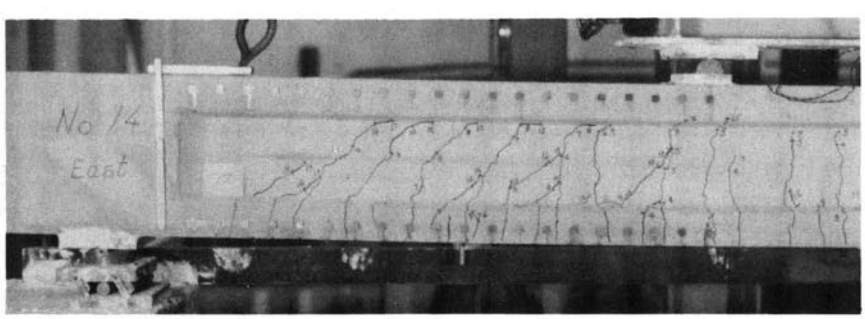

FIGURE 22. CRACK PATTERNS SHOWING NO EFFECT OF THE AMOUNT OF WEB REINFORCEMENT

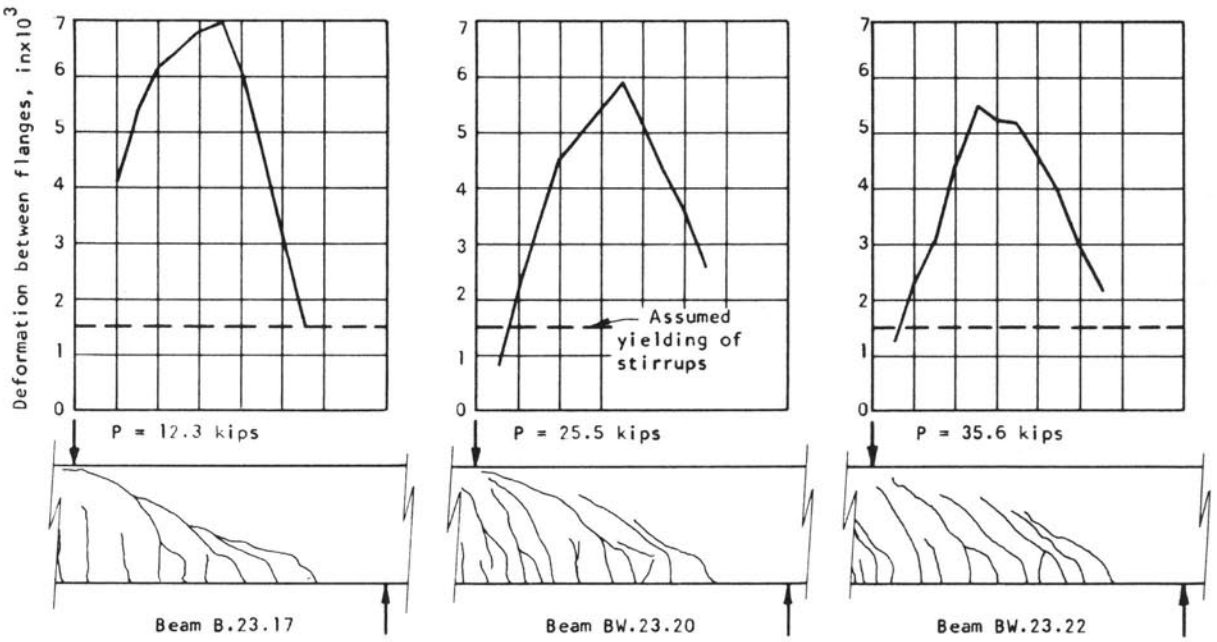

FIGURE 23. CRACK PATTERNS AND RELATED DISTRIBUTION OF DEFORMATIONS BETWEEN FLANGES FOR DIFFERENT AMOUNTS OF WEB REINFORCEMENT

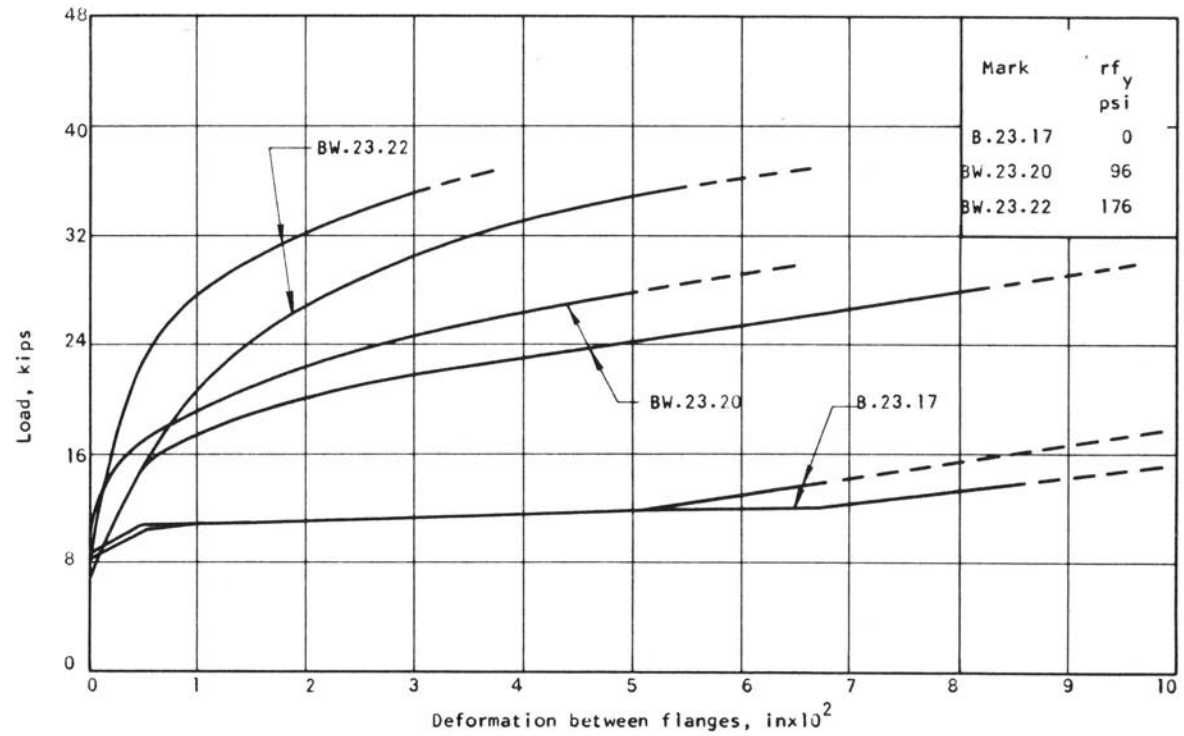

FIGURE 24. LOAD VS. DEFORMATION BETWEEN FLANGES FOR DIFFERENT AMOUNTS OF WEB REINFORCEMENT

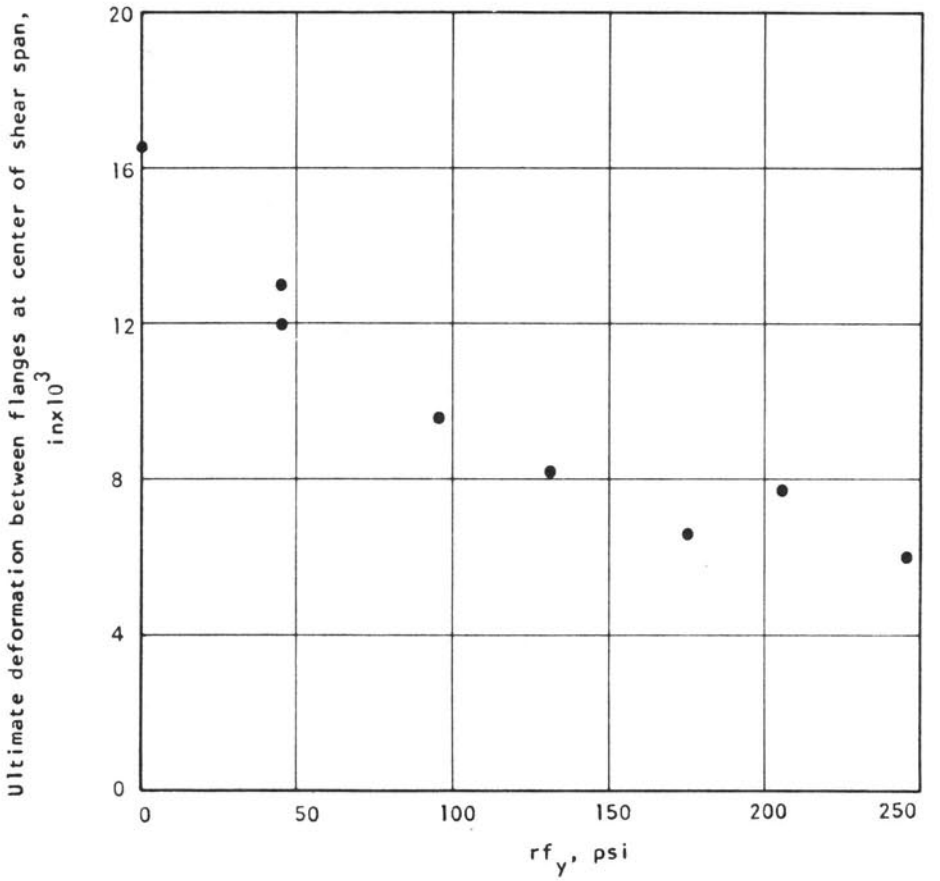

FIGURE 25. ULTIMATE DEFORMATION BETWEEN FLANGES MEASURED AT CENTER OF SHEAR SPAN

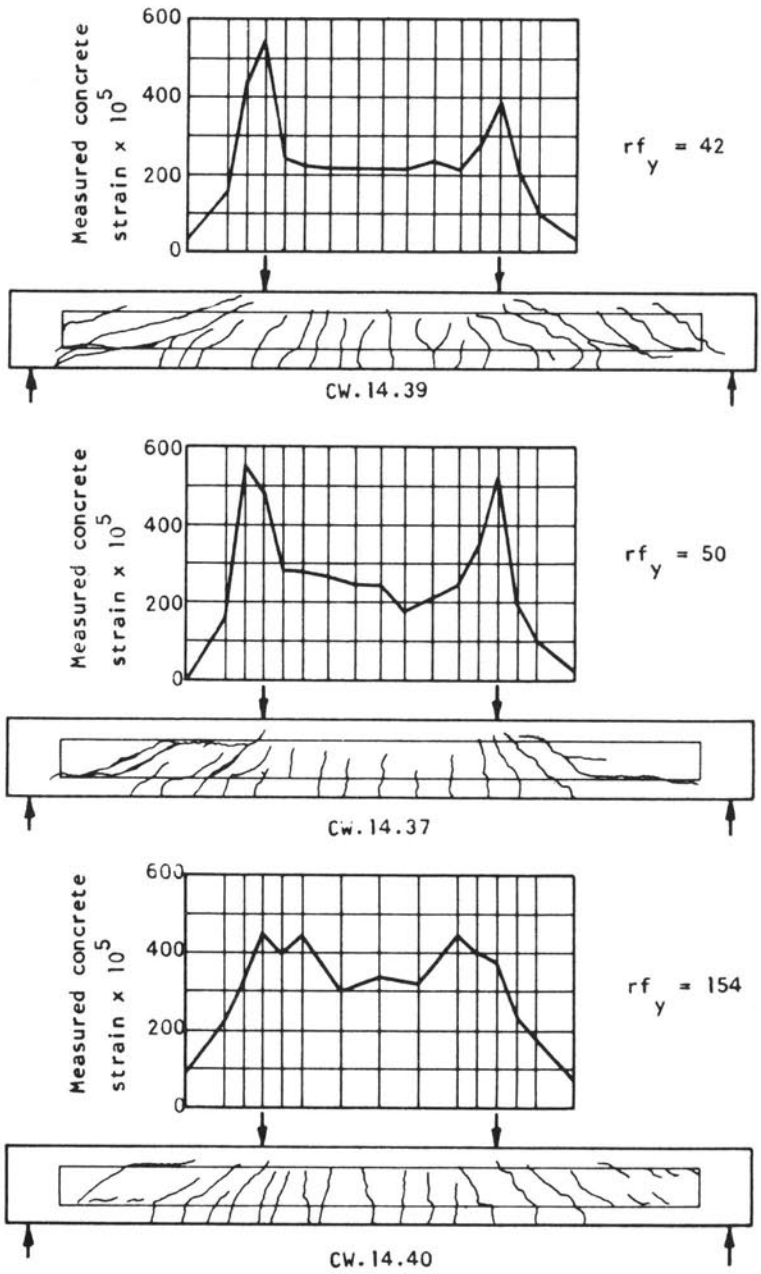

FIGURE 26. EFFECT OF WEB REINFORCEMENT ON DISTRIBUTION OF CONCRETE STRAINS

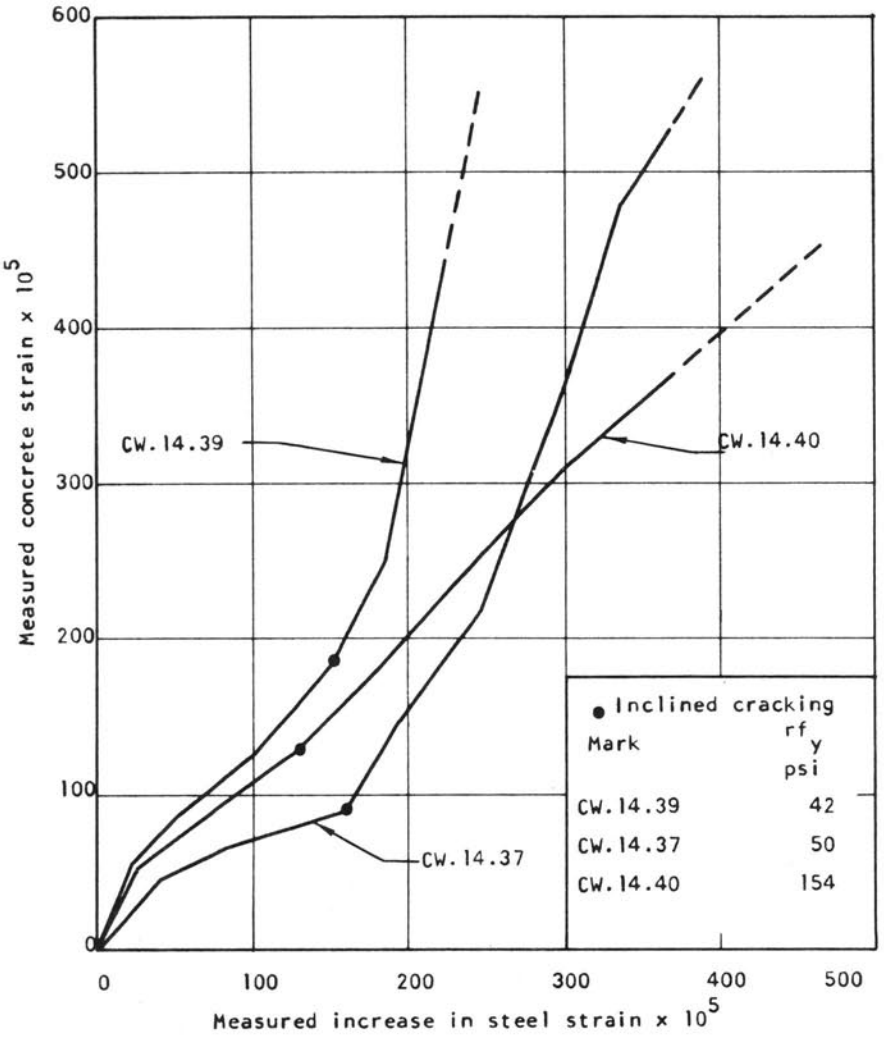

FIGURE 27. EFFECT OF WEB REINFORCEMENT ON RELATION BETWEEN CONCRETE AND STEEL STRAINS

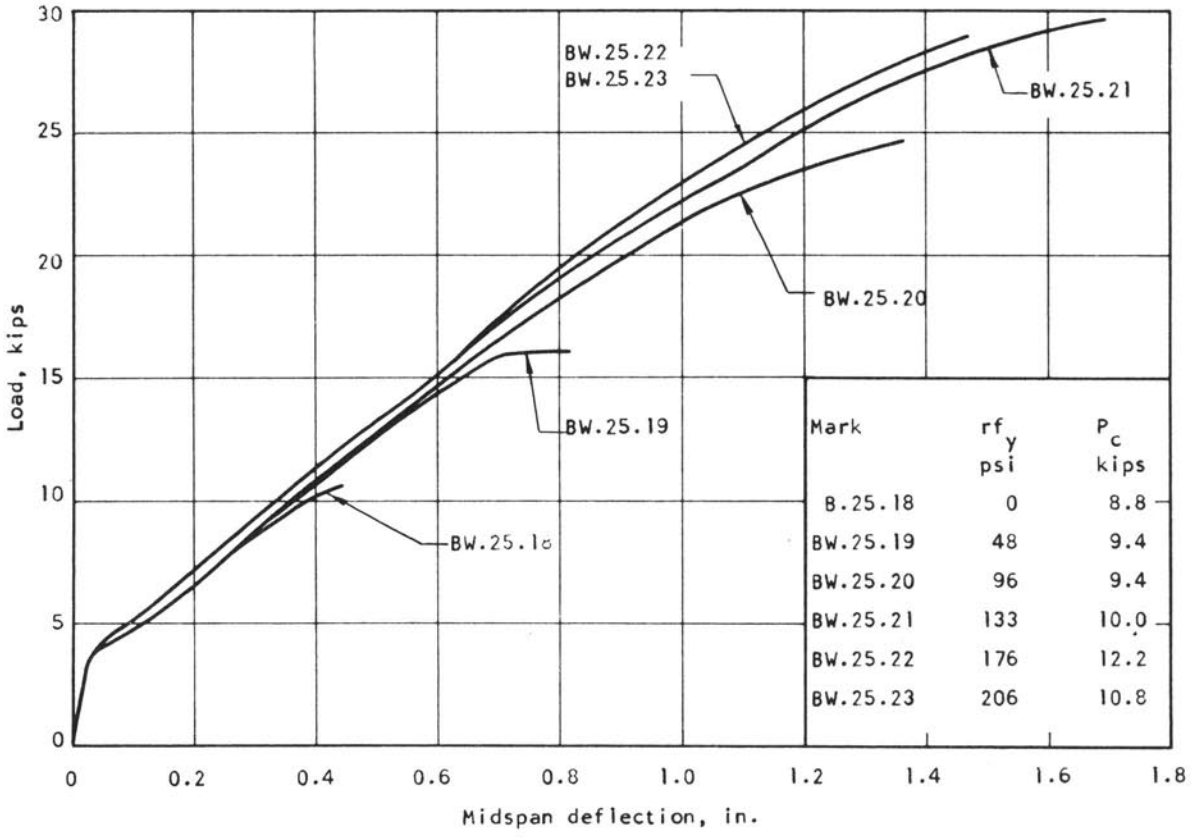

FIGURE 28. EFFECT OF WEB REINFORCEMENT ON LOAD-DEFLECTION CURVE

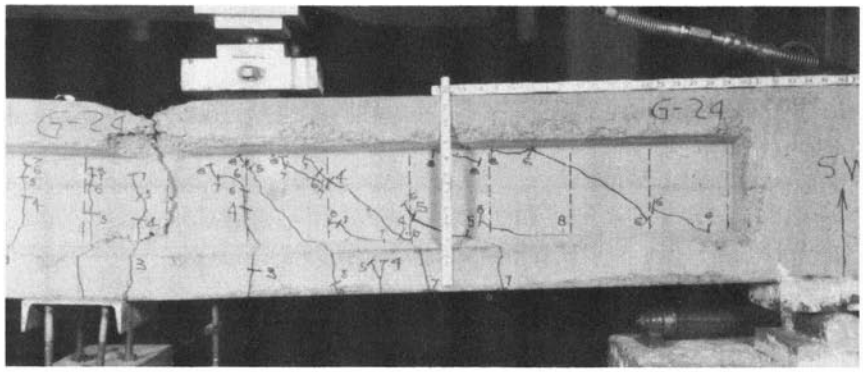

(a) Flexural failure in beam CW.14.40

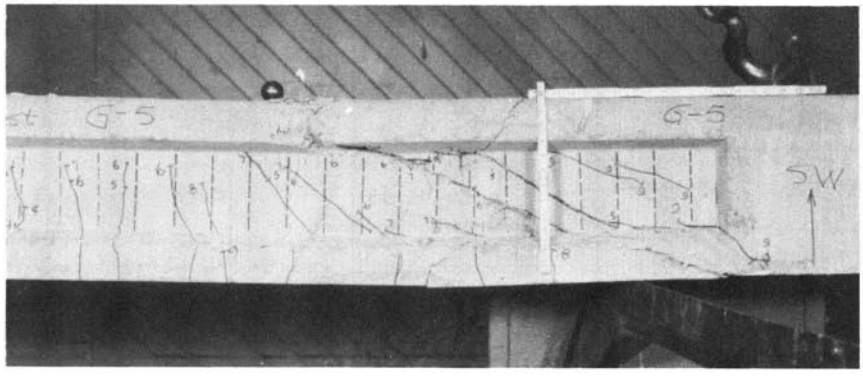

(b) Shear-compression failure in beam CW.14.37

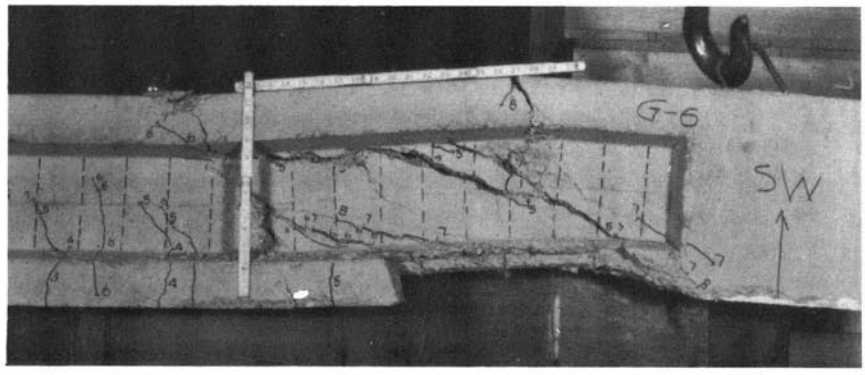

(c) Web-distress failure in beam CW.14.39

FIGURE 29. FAILURES IN FLEXURE, SHEAR-COMPRESSION, AND WEB-DISTRESS

(a) B.25.18
$rf_y = 0$

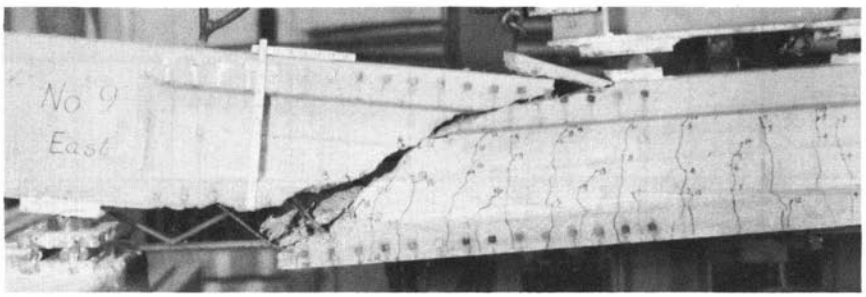

(b) BW.25.19
$rf_y = 48$

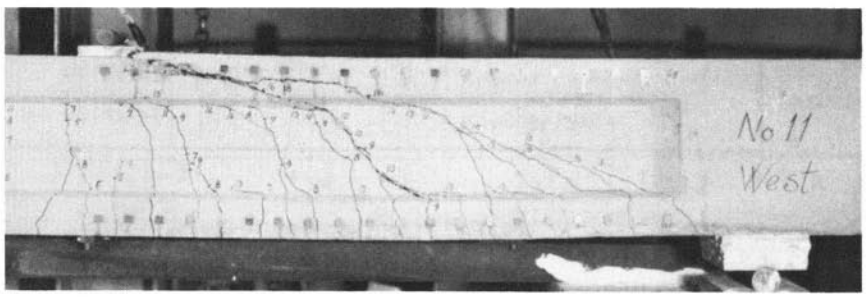

(c) BW.25.20
$rf_y = 96$

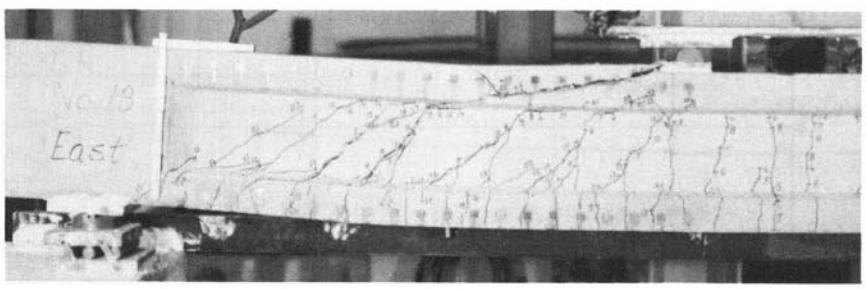

(d) BW.25.21
$rf_y = 133$

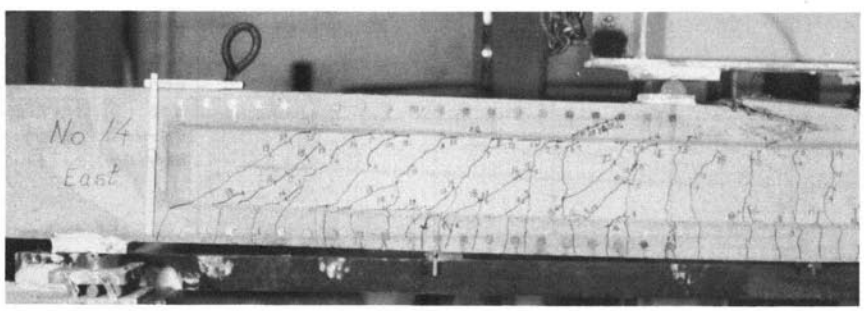

FIGURE 30. EFFECT OF WEB REINFORCEMENT ON FAILURE MODE

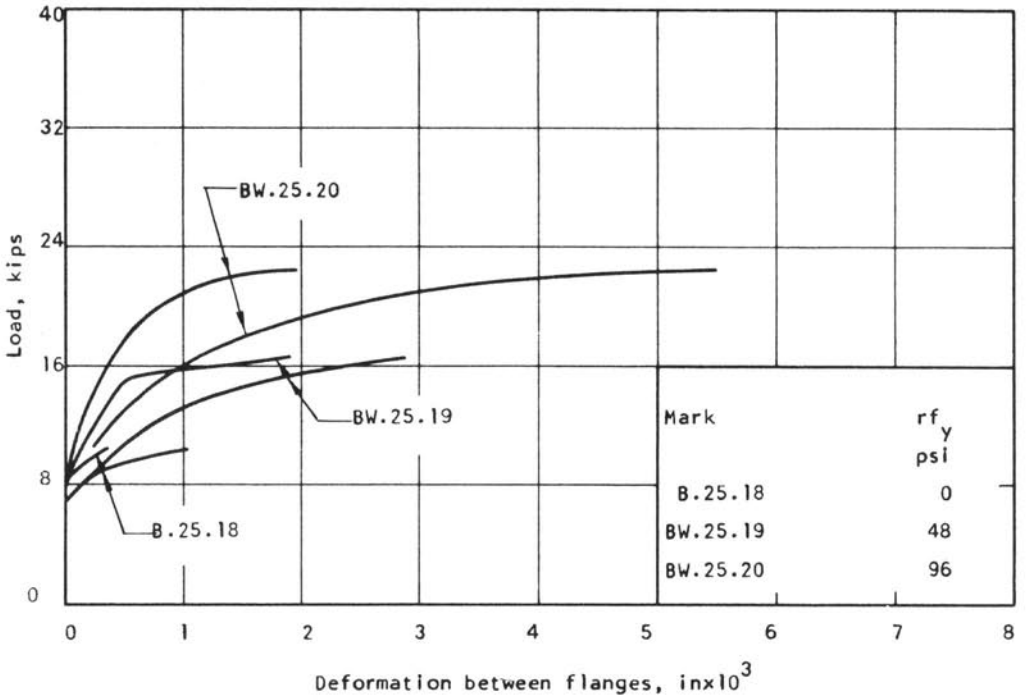

FIGURE 31. INFLUENCE OF FAILURE MODE ON LOAD VS. DEFORMATION BETWEEN FLANGES

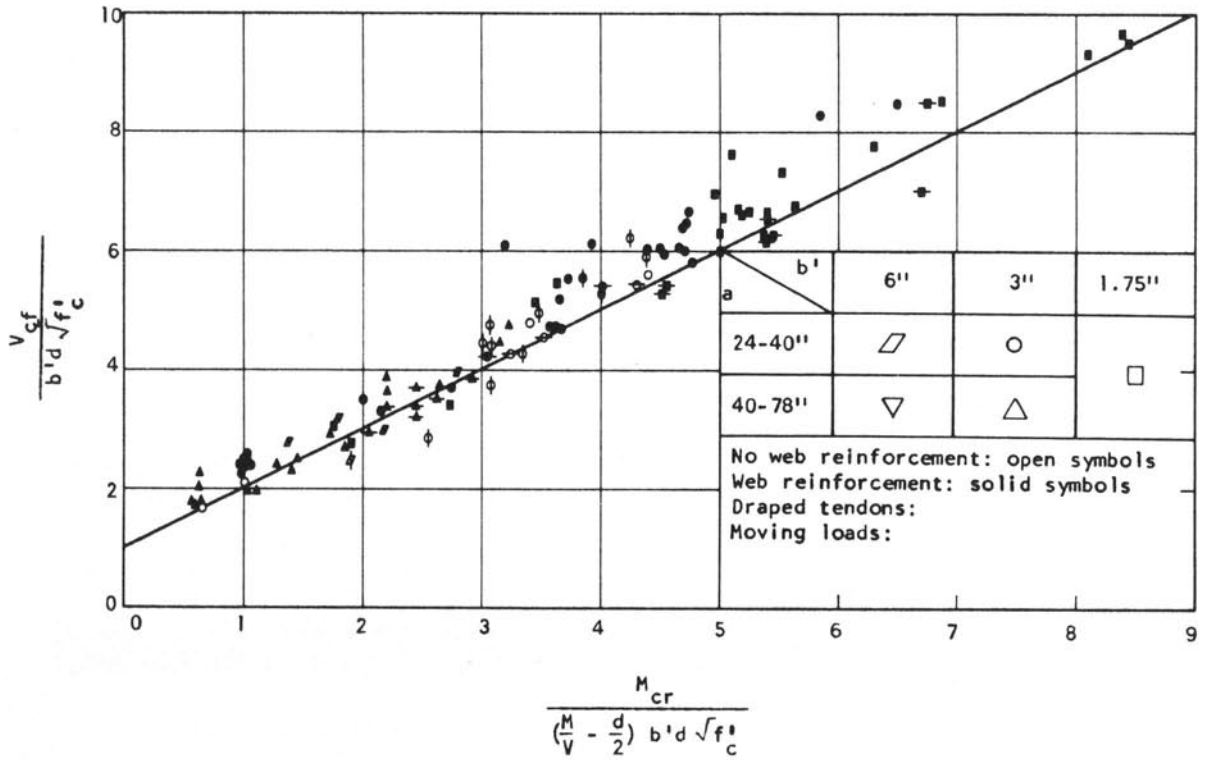

FIGURE 32. SHEAR AT FLEXURE-SHEAR CRACKING IN BEAMS REPORTED IN REFERENCE 1.

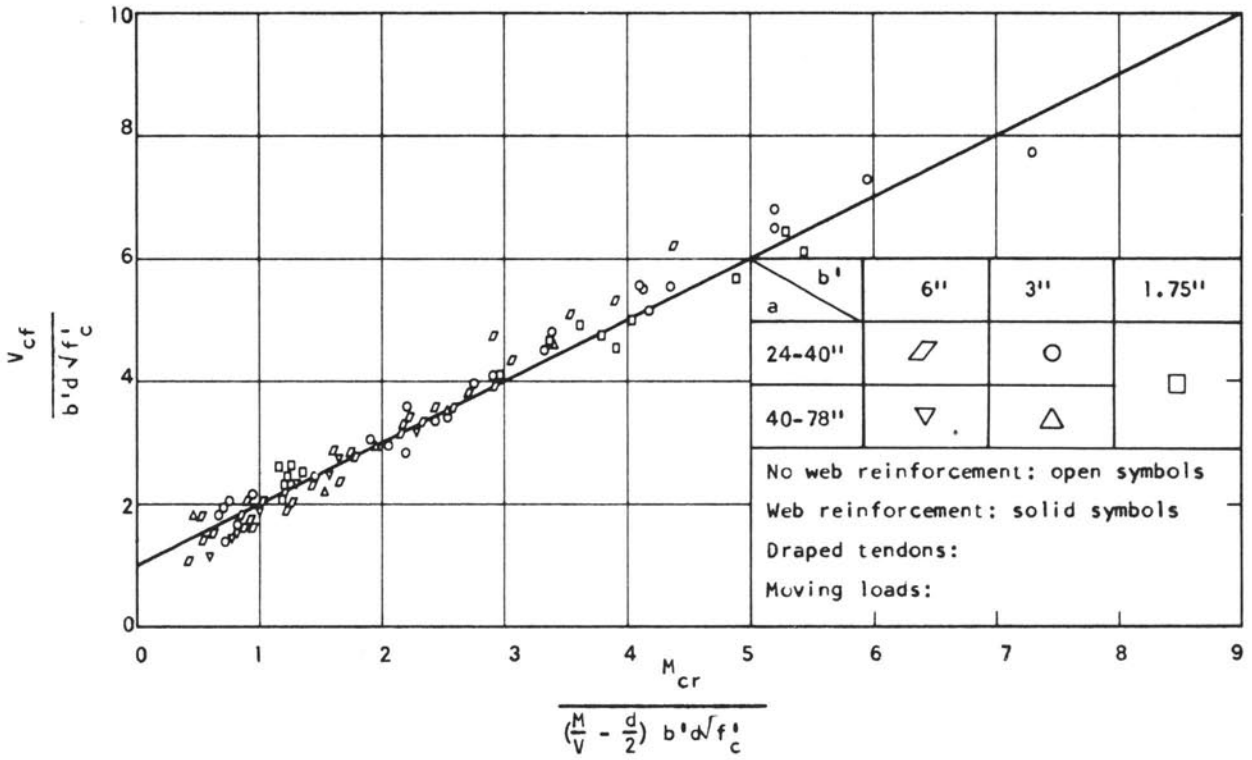

FIGURE 33. SHEAR AT FLEXURE-SHEAR CRACKING IN BEAMS DESCRIBED IN THIS REPORT

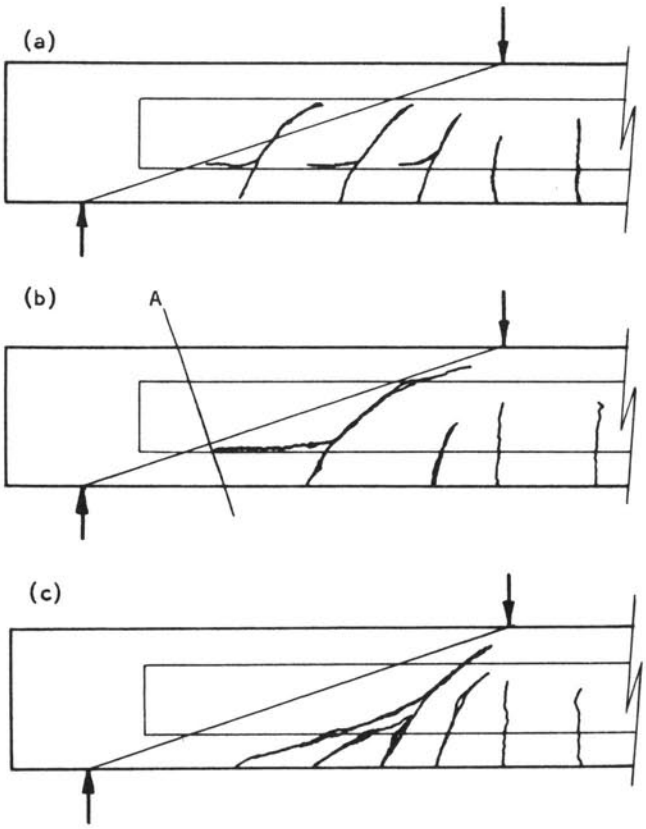

FIGURE 34. IDEALIZED CRACK PATTERNS LEADING TO WEB-DISTRESS AND SHEAR-COMPRESSION FAILURES

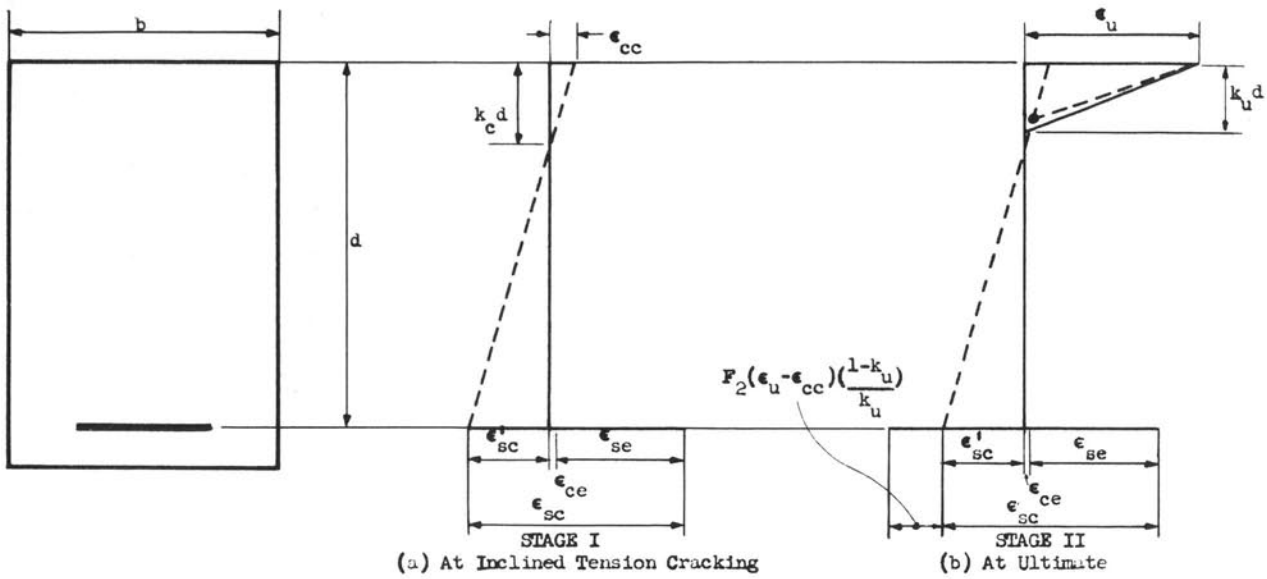

FIGURE 35. IDEALIZED RELATIONSHIPS OF CRITICAL STEEL AND CONCRETE STRAINS FOR BEAM FAILING IN SHEAR COMPRESSION

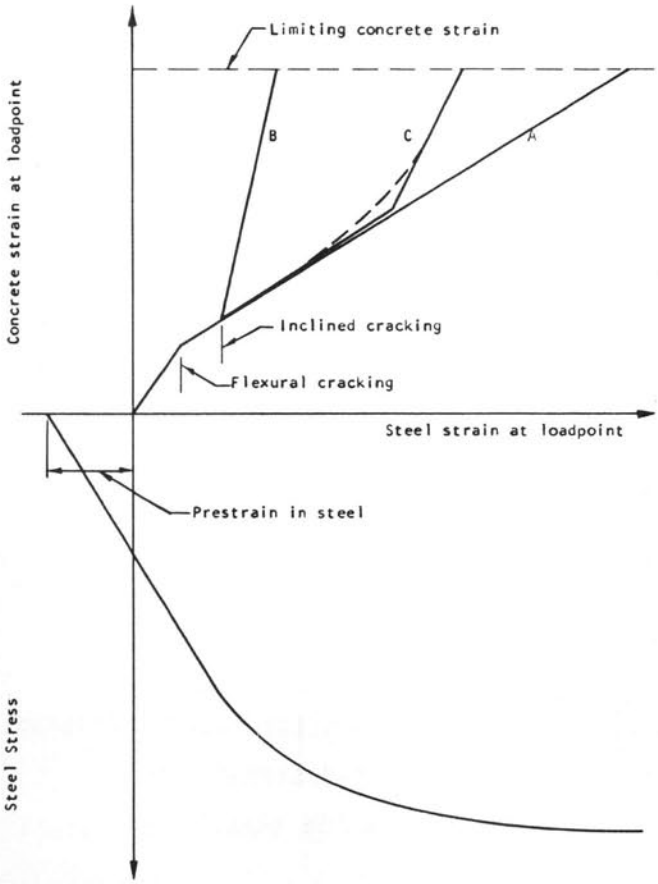

FIGURE 36. IDEALIZED RELATION BETWEEN CONCRETE AND STEEL STRAINS

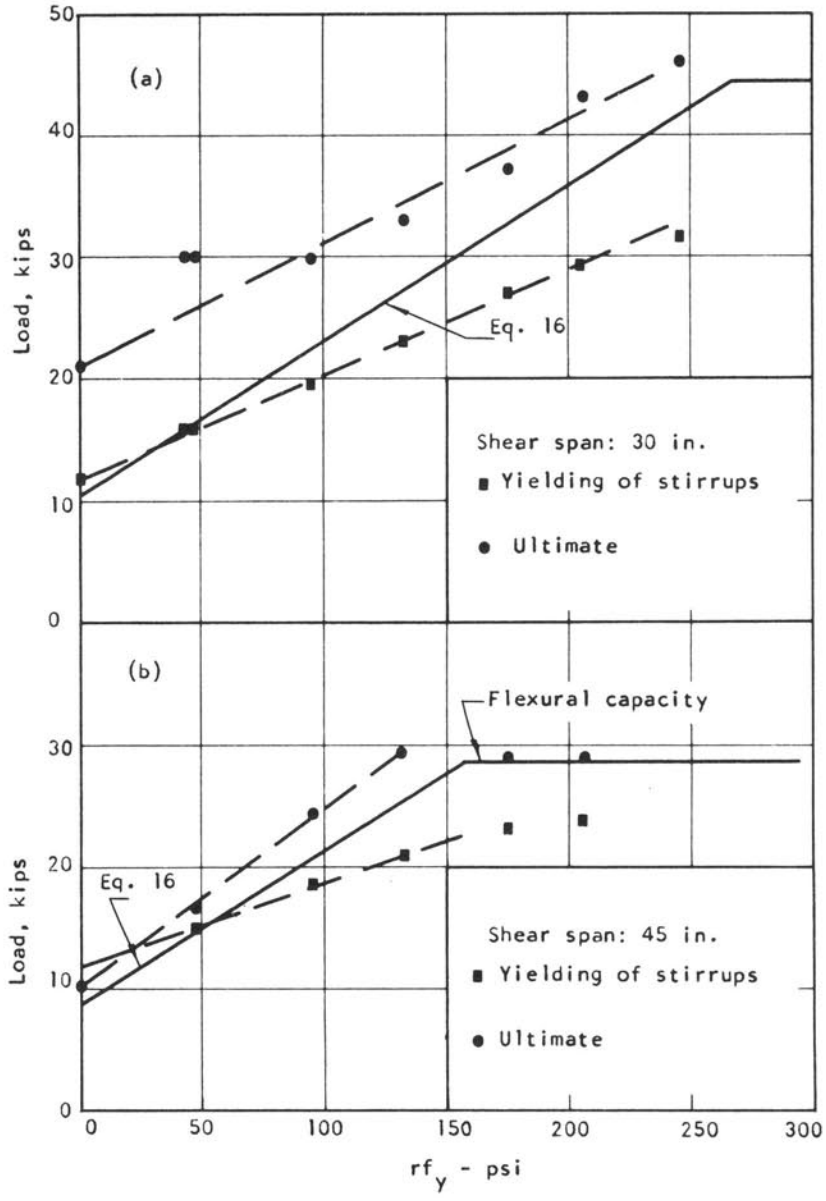

FIGURE 37. INFLUENCE OF WEB REINFORCEMENT ON LOAD AT YIELDING OF STIRRUPS AND AT ULTIMATE

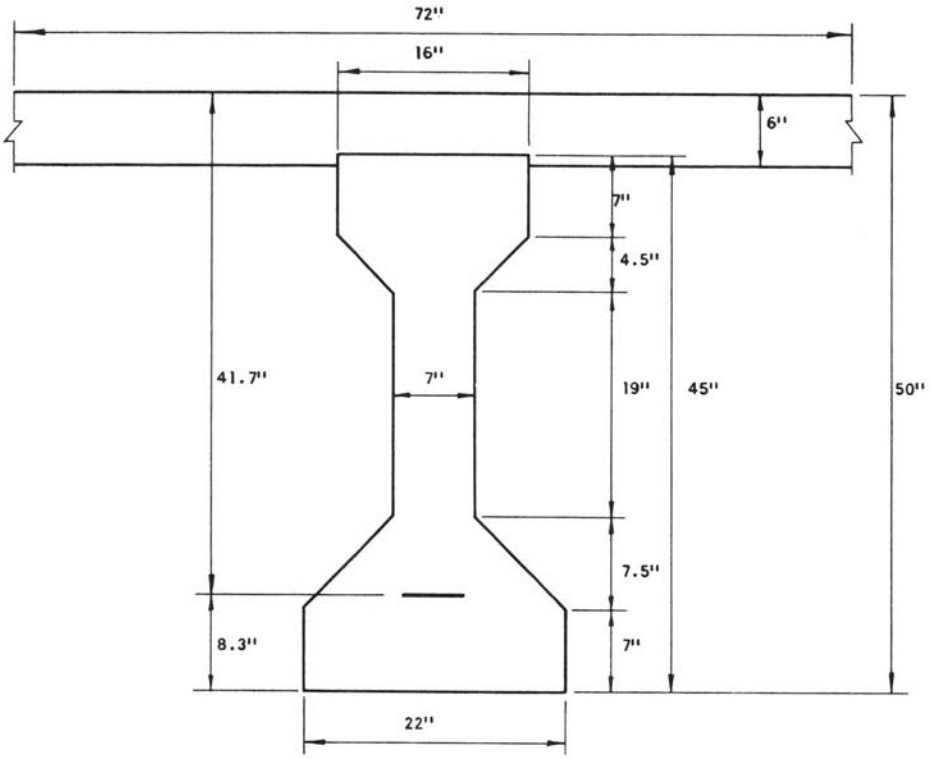

FIGURE 38. AASHO TYPE III GIRDER WITH COMPOSITE SLAB

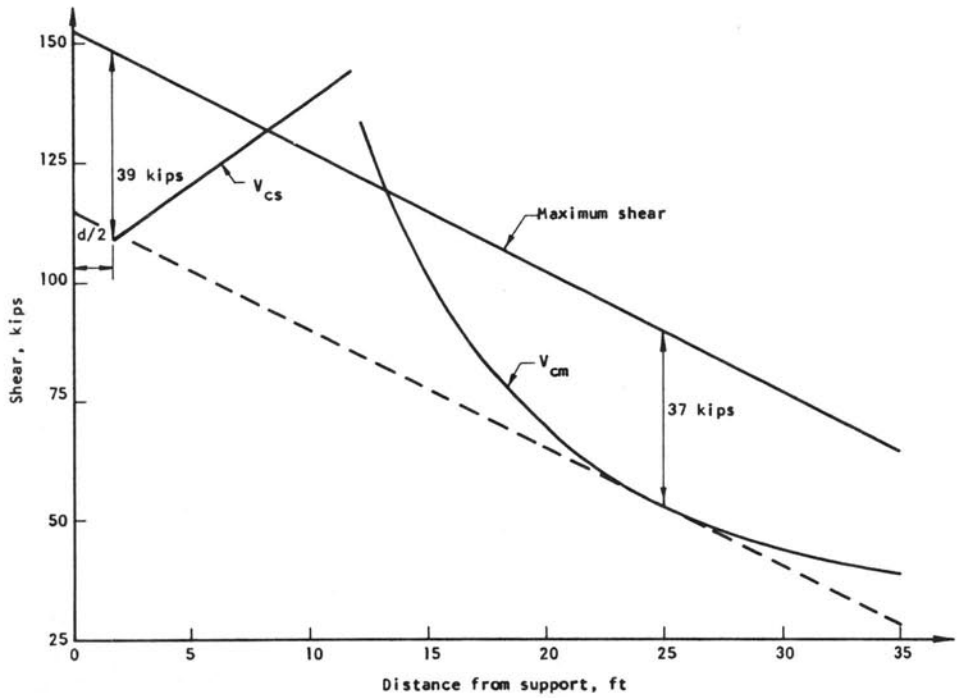

FIGURE 39. SHEAR CAPACITY OF AASHO TYPE III GIRDER WITH COMPOSITE SLAB

APPENDIX

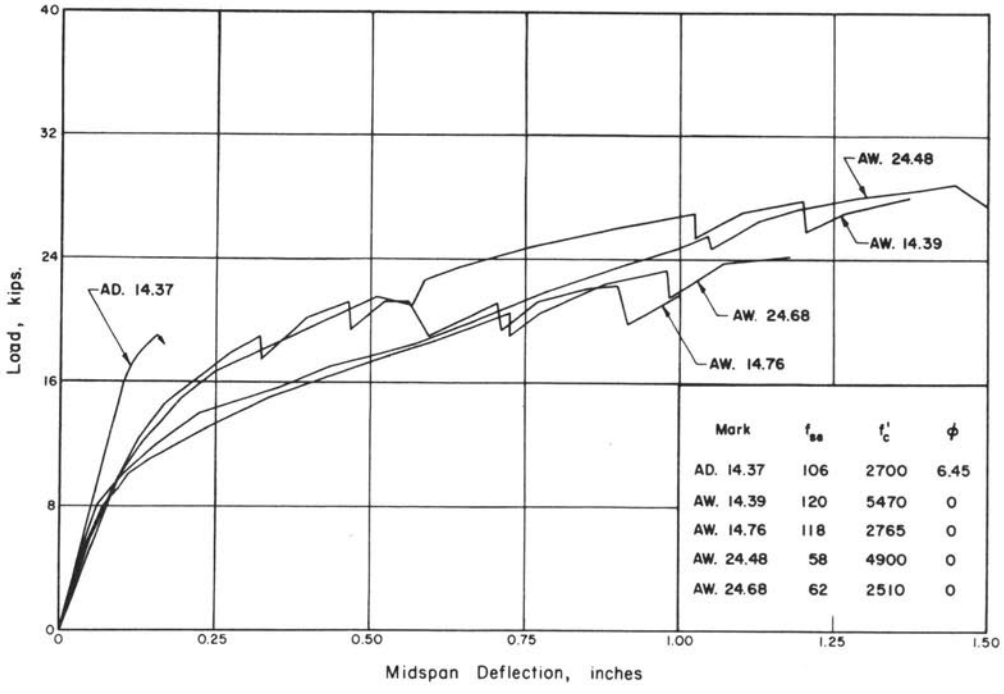

FIGURE A1. LOAD-DEFLECTION CURVES FOR RECTANGULAR BEAMS WITH 36-INCH SHEAR SPANS

(The shear span for AD.14.37 was 32 inches.)

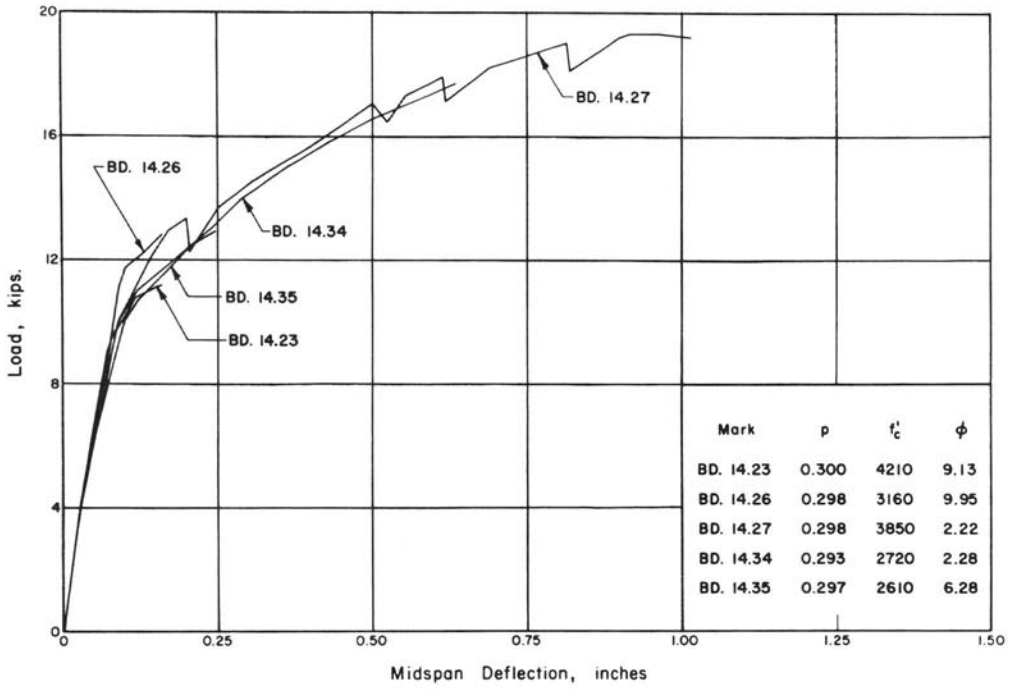

FIGURE A2. LOAD-DEFLECTION CURVES FOR I-BEAMS WITH 3-INCH WEBS AND 36-INCH SHEAR SPANS

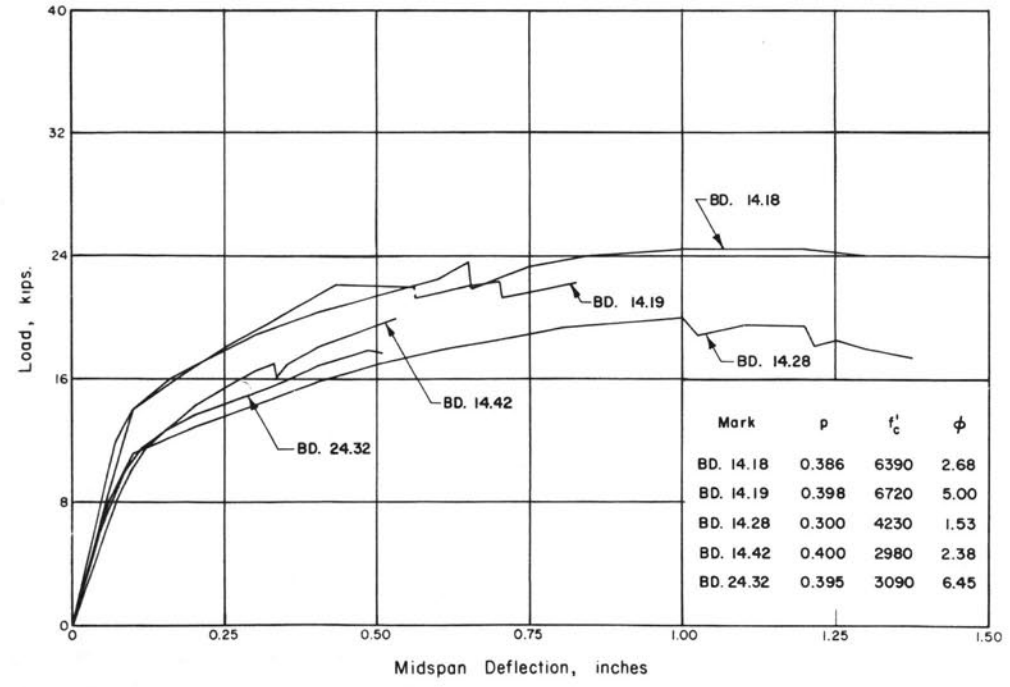

FIGURE A3. LOAD-DEFLECTION CURVES FOR I-BEAMS WITH 3-INCH WEBS AND 36-INCH SHEAR SPANS

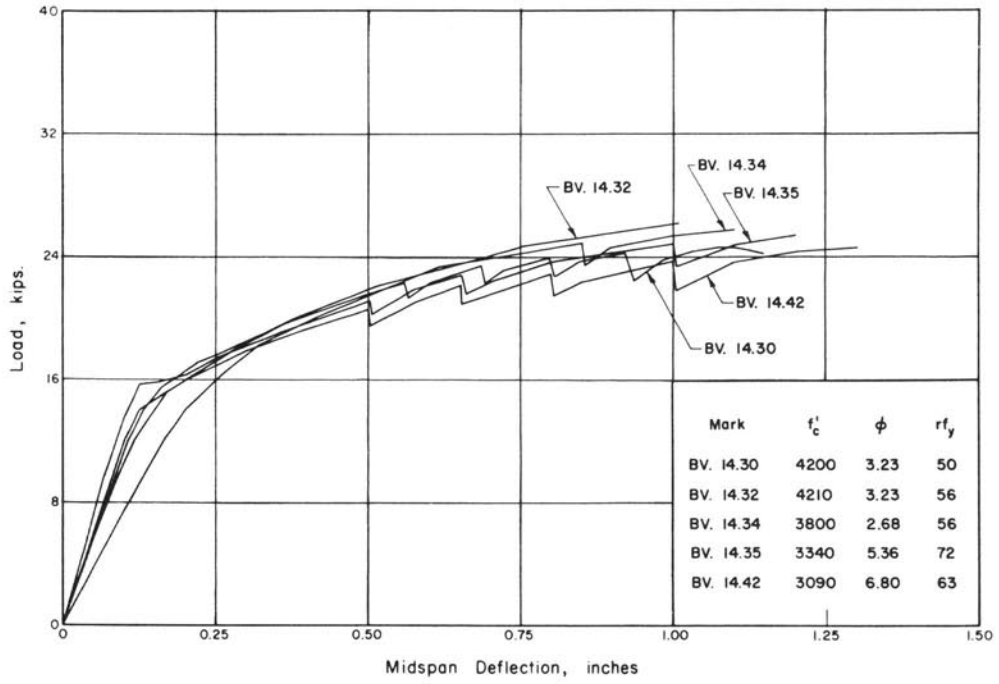

FIGURE A4. LOAD-DEFLECTION CURVES FOR I-BEAMS WITH 3-INCH WEBS AND 36-INCH SHEAR SPANS

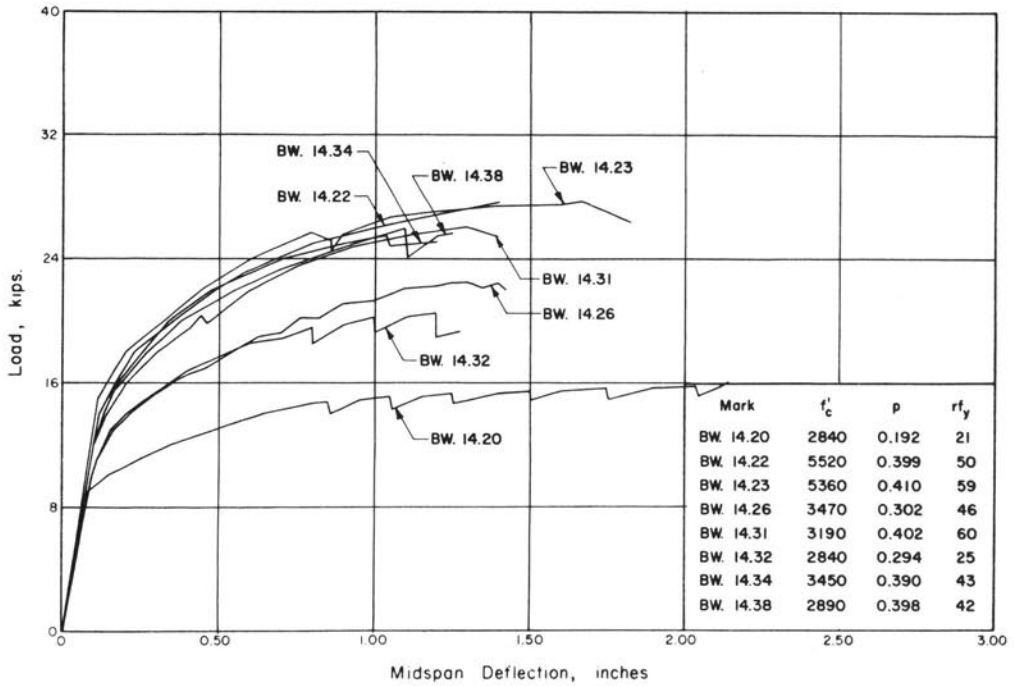

FIGURE A5. LOAD-DEFLECTION CURVES FOR I-BEAMS WITH 3-INCH WEBS AND 36-INCH SHEAR SPANS

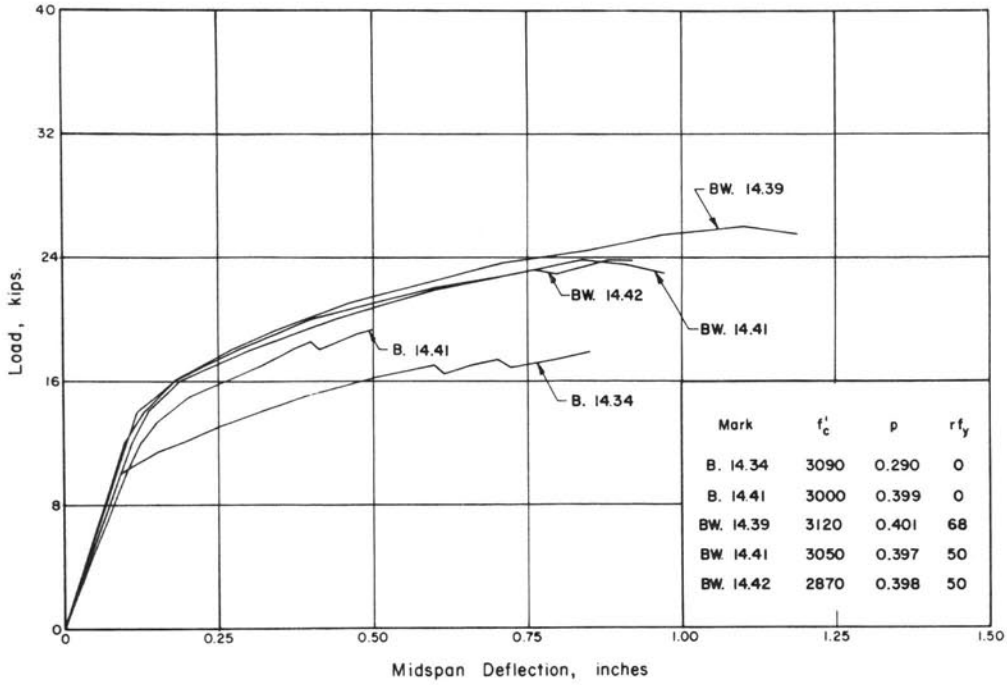

FIGURE A6. LOAD-DEFLECTION CURVES FOR I-BEAMS WITH 3-INCH WEBS AND 36-INCH SHEAR SPANS

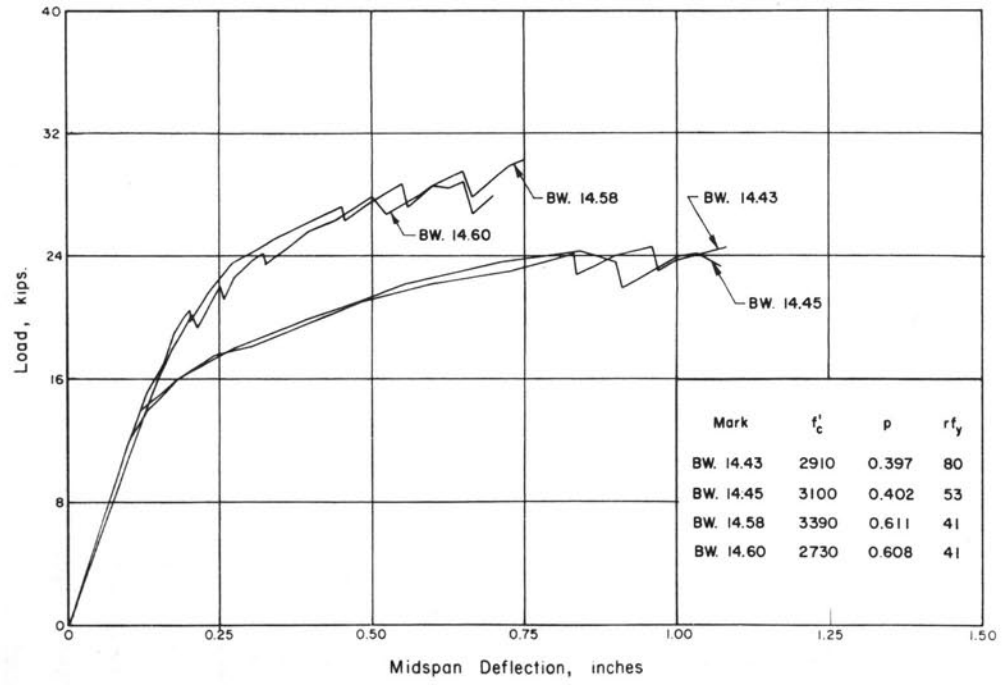

FIGURE A7. LOAD-DEFLECTION CURVES FOR I-BEAMS WITH 3-INCH WEBS AND 36-INCH SHEAR SPANS

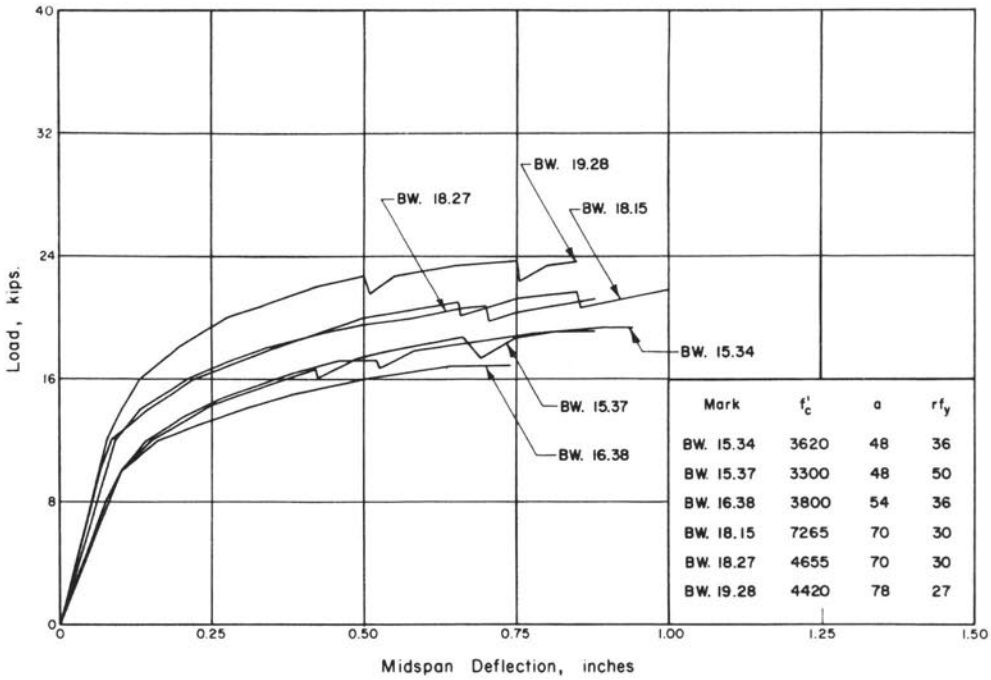

FIGURE A8. LOAD-DEFLECTION CURVE FOR I-BEAMS WITH 3-INCH WEBS

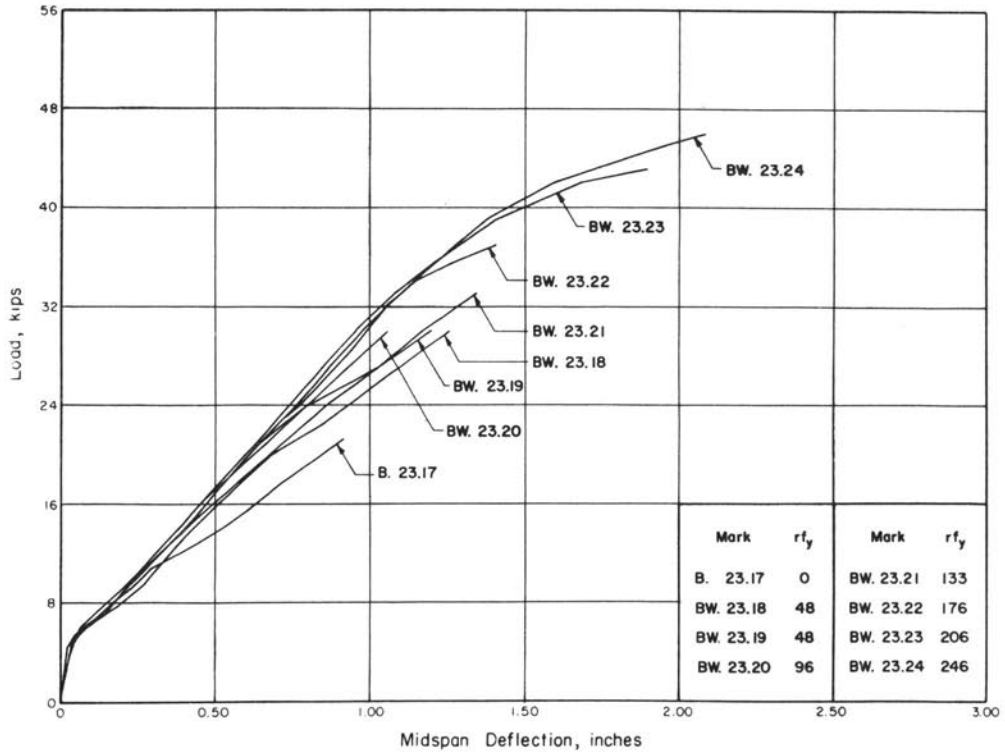

FIGURE A9. LOAD-DEFLECTION CURVES FOR I-BEAMS WITH 3-INCH WEBS, 30-INCH SHEAR SPANS, AND WITHOUT PRESTRESS

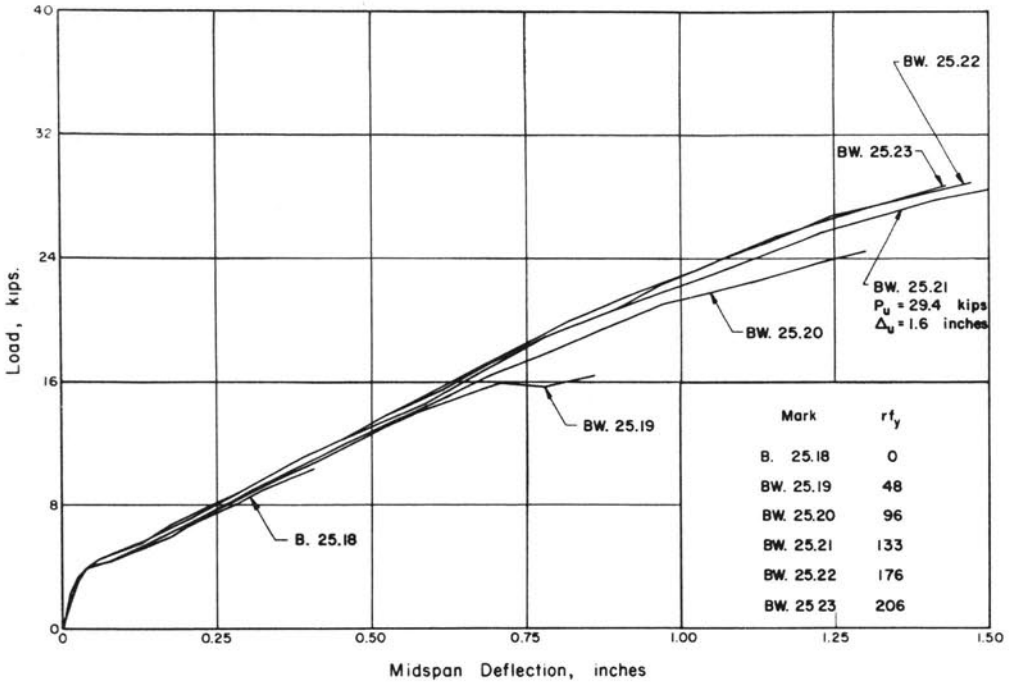

FIGURE A10. LOAD-DEFLECTION CURVES FOR I-BEAMS WITH 3-INCH WEBS, 45-INCH SHEAR SPANS, AND WITHOUT PRESTRESS

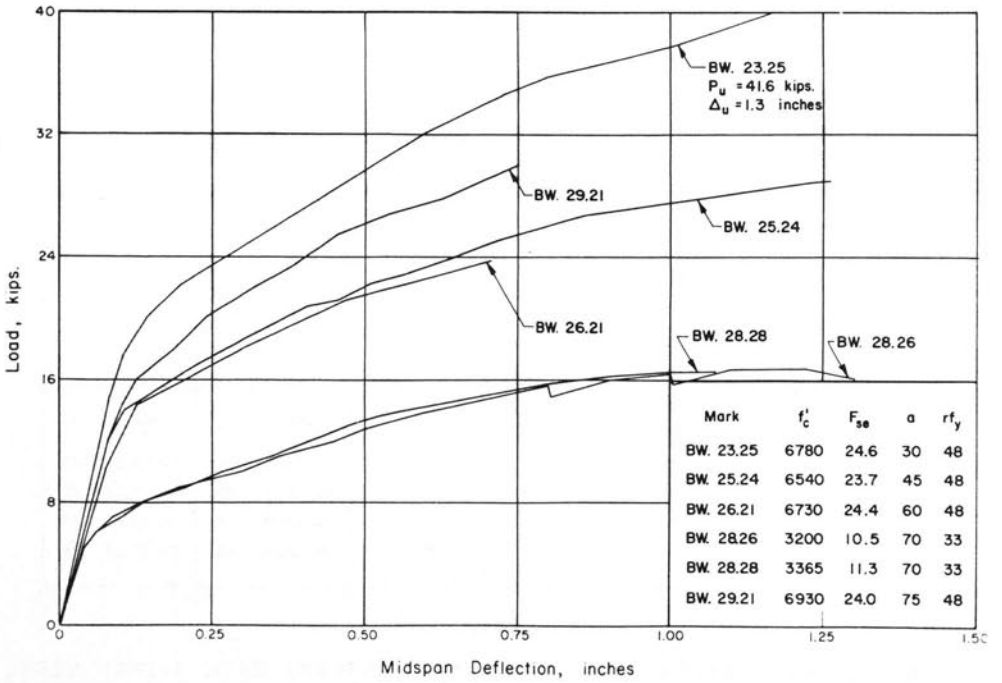

FIGURE A11. LOAD-DEFLECTION CURVES FOR I-BEAMS WITH 3-INCH WEBS

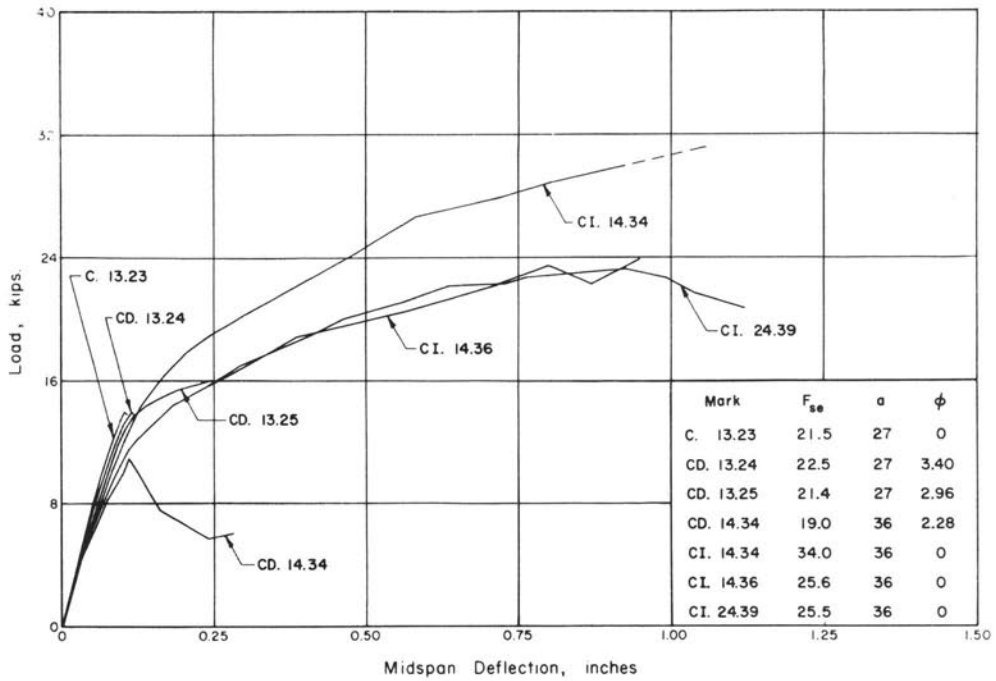

FIGURE A12. LOAD-DEFLECTION CURVES FOR I-BEAMS WITH 1.75-INCH WEBS

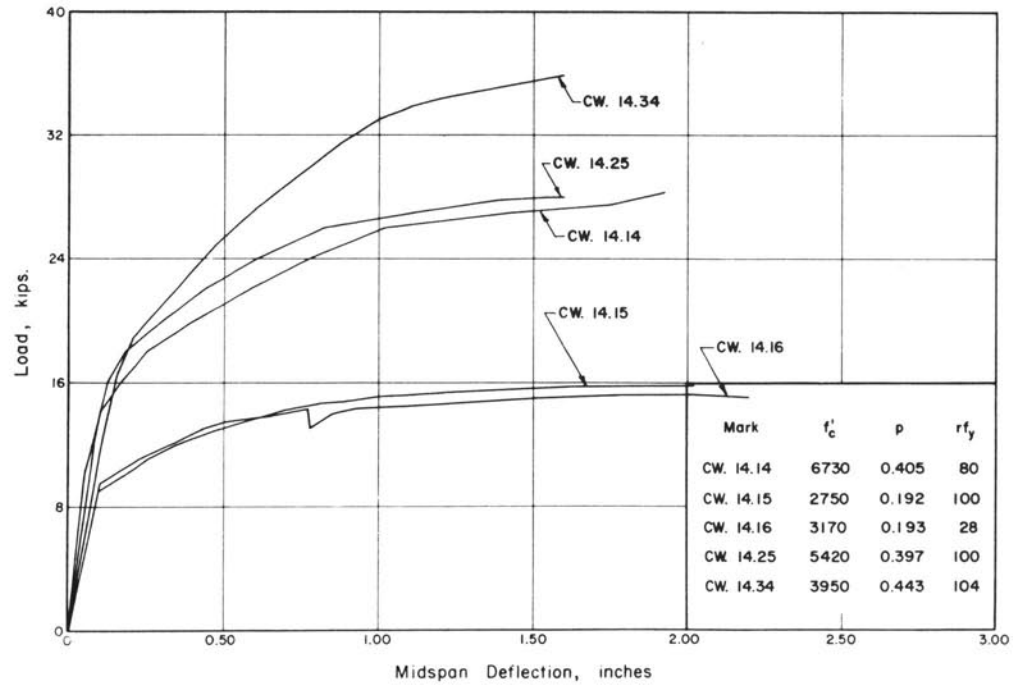

FIGURE A13. LOAD-DEFLECTION CURVES FOR I-BEAMS WITH 1.75-INCH WEBS AND 36-INCH SHEAR SPANS

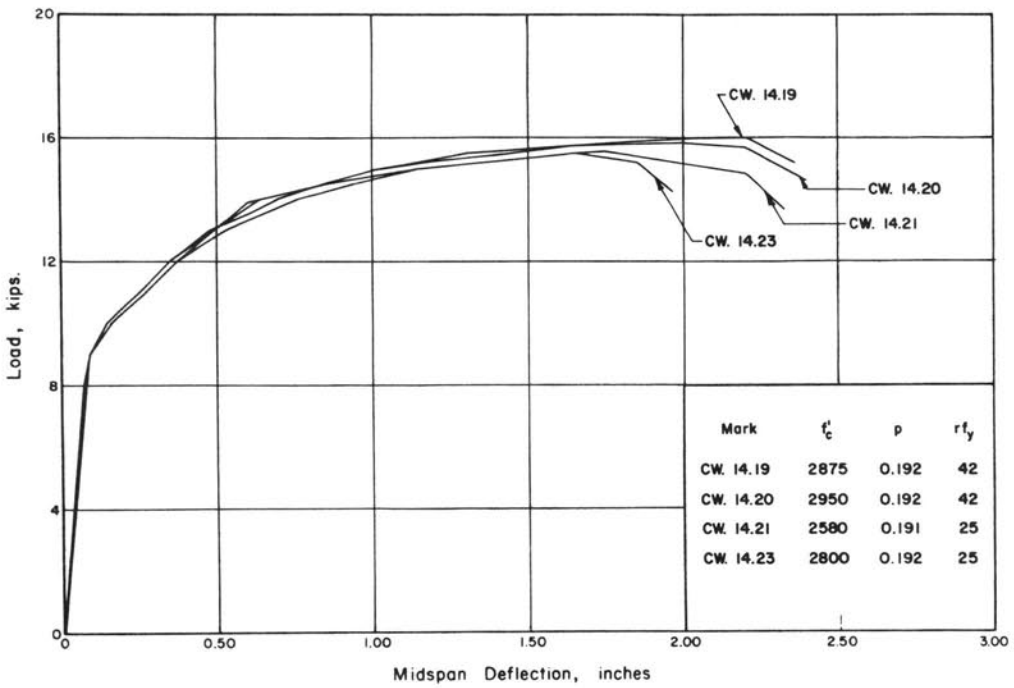

FIGURE A14. LOAD-DEFLECTION CURVES FOR I-BEAMS WITH 1.75-INCH WEBS AND 36-INCH SHEAR SPANS

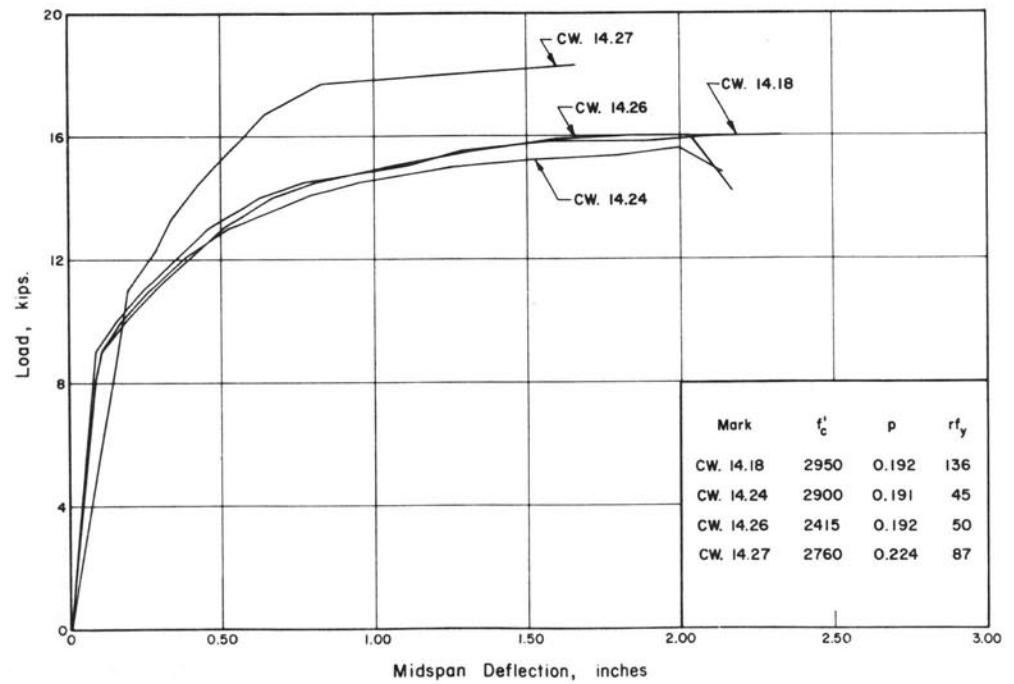

FIGURE A15. LOAD-DEFLECTION CURVES FOR I-BEAMS WITH 1.75-INCH WEBS AND 36-INCH SHEAR SPANS

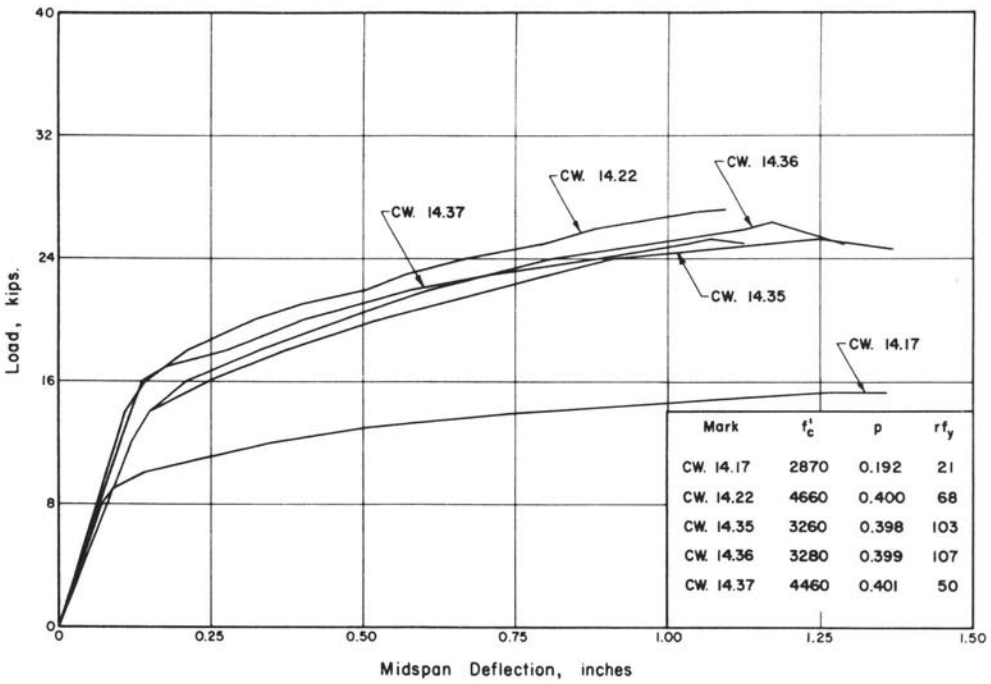

FIGURE A16. LOAD-DEFLECTION CURVES FOR I-BEAMS WITH 1.75-INCH WEBS AND 36-INCH SHEAR SPANS

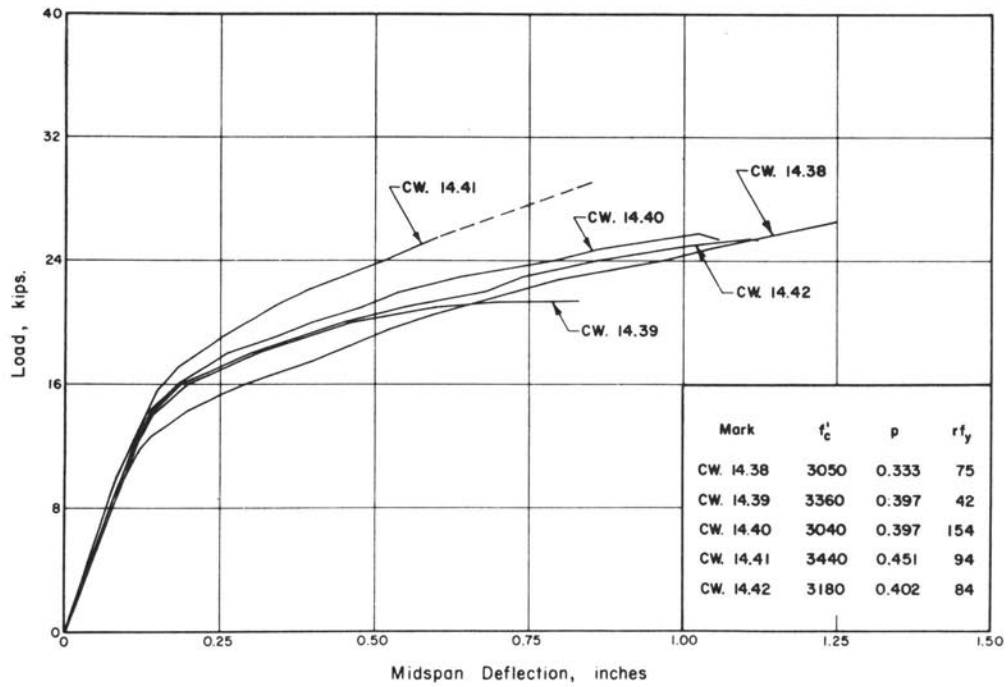

FIGURE A17. LOAD-DEFLECTION CURVES FOR I-BEAMS WITH 1.75-INCH WEBS AND 36-INCH SHEAR SPANS

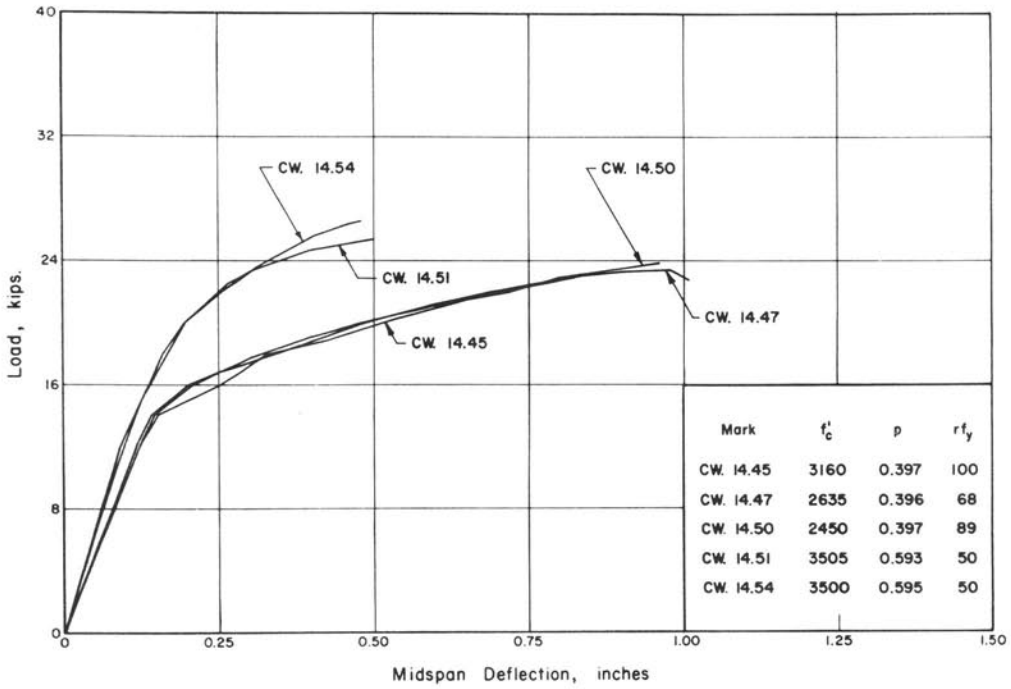

FIGURE A18. LOAD-DEFLECTION CURVES FOR I-BEAMS WITH 1.75-INCH WEBS AND 36-INCH SHEAR SPANS

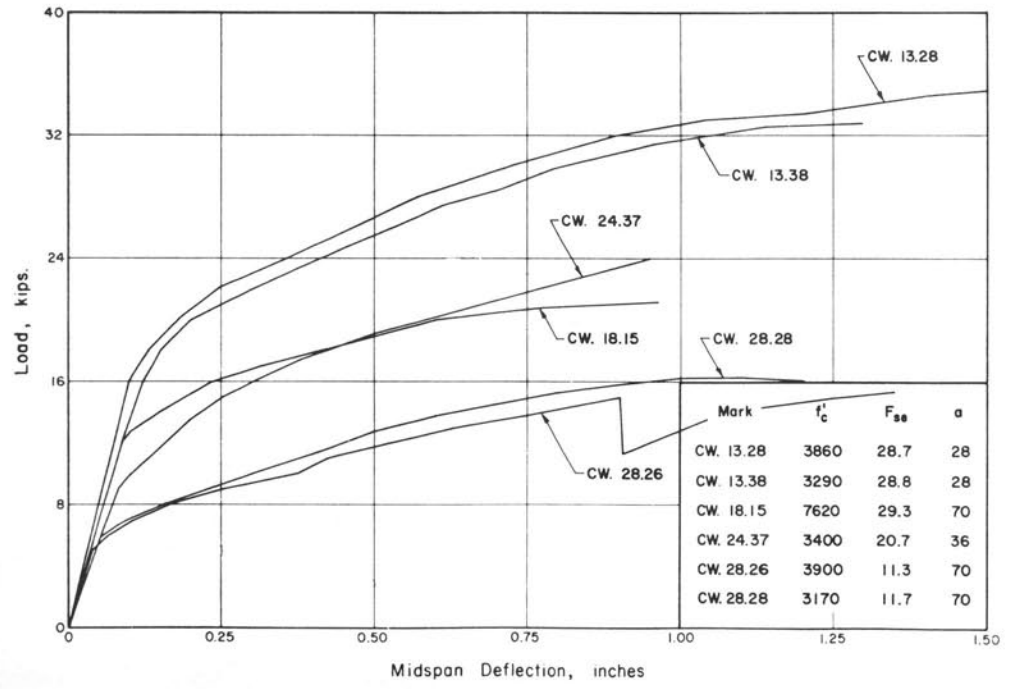

FIGURE A19. LOAD-DEFLECTION CURVES FOR I-BEAMS WITH 1.75-INCH WEBS

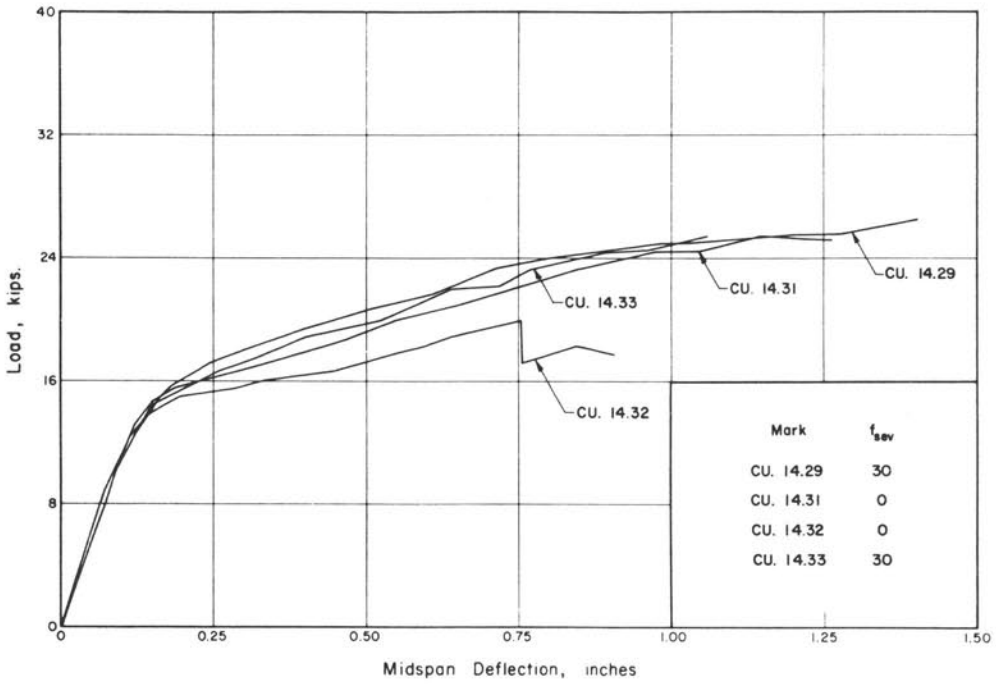

FIGURE A20. LOAD-DEFLECTION CURVES FOR I-BEAMS WITH 1.75-INCH WEBS, 36-INCH SHEAR SPANS, AND PRESTRESSED STIRRUPS

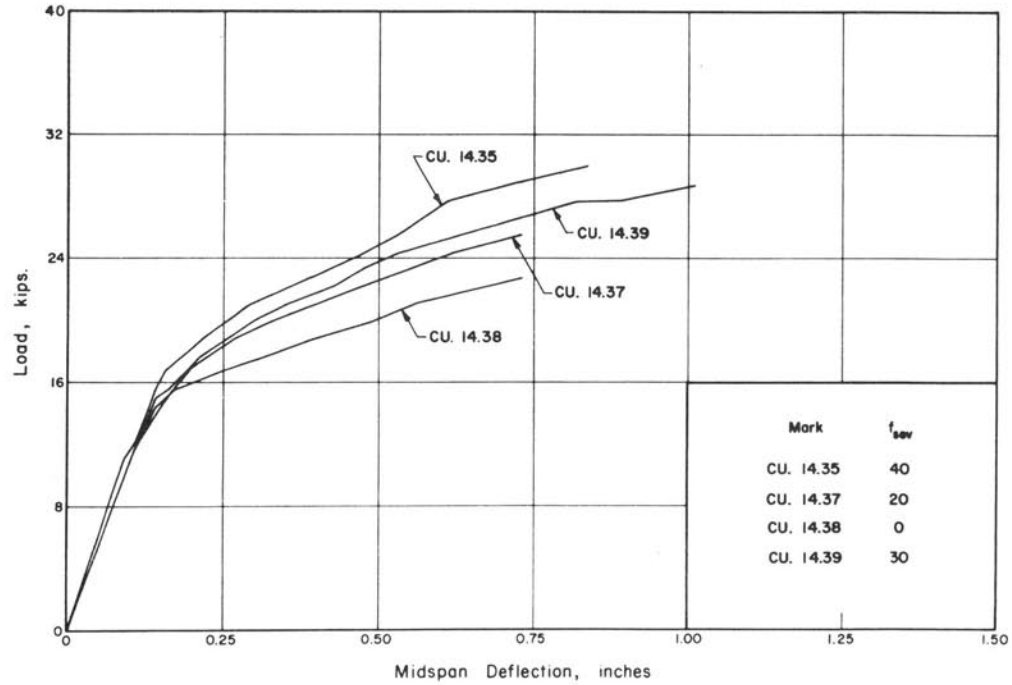

FIGURE A21. LOAD-DEFLECTION CURVES FOR I-BEAMS WITH 1.75-INCH WEBS, 36-INCH SHEAR SPANS, AND PRESTRESSED STIRRUPS

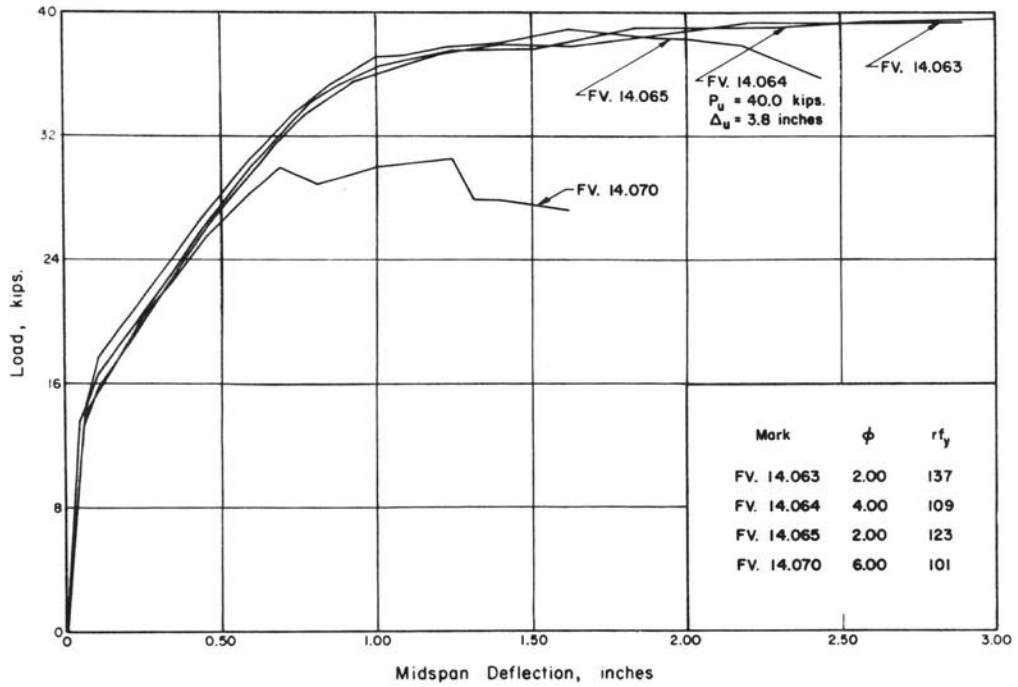

FIGURE A22. LOAD-DEFLECTION CURVES FOR COMPOSITE BEAMS WITH DRAPED TENDONS

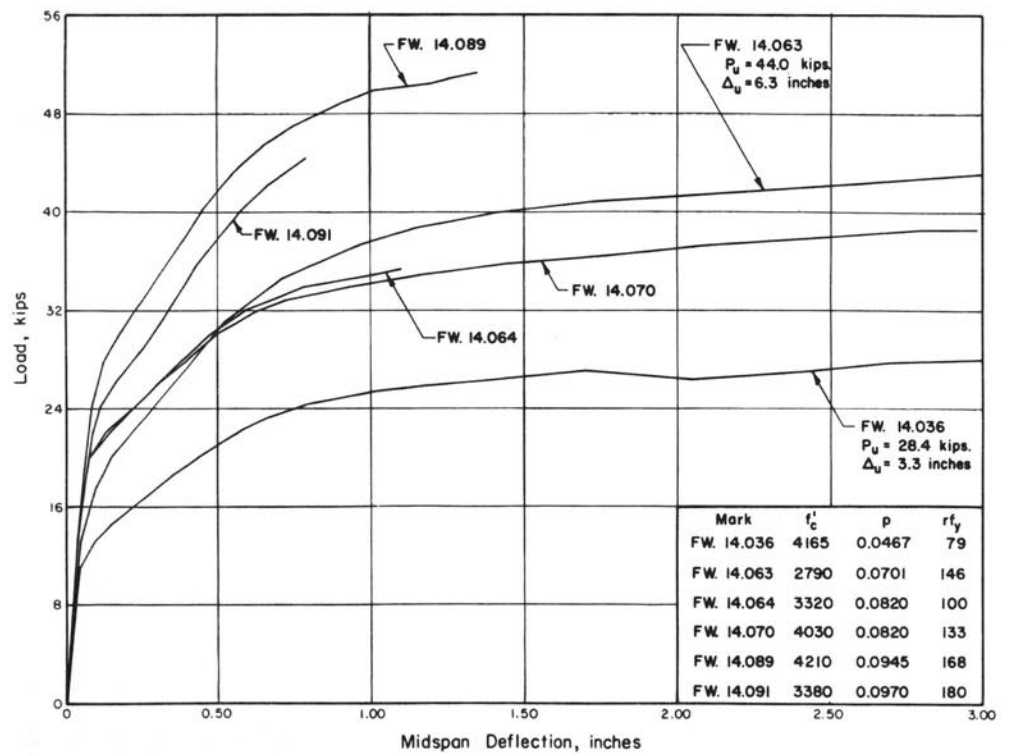

FIGURE A23. LOAD-DEFLECTION CURVES FOR COMPOSITE BEAMS WITH STRAIGHT TENDONS

TABLE 1.

PROPERTIES OF BEAMS

Mark	Concrete Strength f'_c psi a)	Flange width b in.	Web thickness b' in.	Effective depth d in.	Reinforcement Area A_s, in.^{2}	Reinforcement ratio p %	Reinforcement Lot	Effective prestress f_{se} ksi	Steel Area draped %	Drape angle φ degree	Shear span a in.
AD.14.37	2700	6.00	----	10.15	0.242	0.398	11	106	100	6.45	36
AW.14.39	5470	6.00	----	8.53	0.362	0.708	8	120	-	-	36
AW.14.76	2765	6.00	----	8.48	0.362	0.712	8	118	-	-	36
AW.24.48	4900	6.00	----	8.48	0.362	0.712	8	58	-	-	36
AW.24.68	2510	5.95	----	8.54	0.362	0.713	8	62	-	-	36
B. 10.23	5205	6.00	3.00	10.04	0.242	0.405	12	127.4	-	-	ML
B. 10.24	3720	6.04	3.03	10.09	0.181	0.300	12	126.8	-	-	ML
B. 14.34	3090	6.05	3.10	10.30	0.181	0.290	12	115	-	-	36
B. 14.41	3000	6.05	3.00	10.00	0.242	0.399	12	114	-	-	36
B. 23.17	6780	6.06	3.06	10.62	0.285	0.442	17	0.0	-	-	30
B. 25.18	6780	6.06	3.00	10.62	0.285	0.442	17	0.0	-	-	45
BD.14.18	6390	5.95	2.86	10.11	0.237	0.386	13	123	50	2.68	36
BD.14.19	6720	5.95	2.90	10.20	0.242	0.398	12	112	100	5.00	36
BD.14.23	4210	6.00	3.00	10.10	0.181	0.300	11	99	100	9.13	36
BD.14.26	3160	6.00	3.00	10.10	0.181	0.298	11	116	100	9.95	36
BD.14.27	3850	6.00	3.00	10.10	0.181	0.298	11	111	100	2.22	36
BD.14.28	4230	6.00	3.00	10.10	0.181	0.300	11	118	100	1.53	36
BD.14.34	2720	6.05	3.00	10.22	0.181	0.293	11	110	66.7	2.28	36
BD.14.35	2610	6.05	2.95	10.10	0.181	0.297	11	108	100	6.28	36
BD.14.42	2980	6.00	2.90	10.10	0.242	0.400	11	107	100	2.38	36
BD.24.32	3090	6.05	3.00	10.10	0.242	0.395	11	81	100	6.45	36
BV.14.30	4200	5.95	2.95	10.10	0.242	0.403	11	123	50	3.23	36
BV.14.32	4210	5.90	2.85	10.13	0.242	0.403	12	112	50	3.23	36
BV.14.34	3800	5.95	3.00	10.15	0.242	0.400	12	124	50	2.68	36
BV.14.35	3340	5.95	2.92	10.20	0.242	0.398	12	115	100	5.36	36
BV.14.42	3090	6.00	2.88	10.15	0.237	0.387	13	120	100	6.80	36
BW.10.22	4150	6.05	3.05	10.19	0.181	0.295	12	123	-	-	ML
BW.14.20	2840	6.00	2.95	10.47	0.121	0.192	10	126.8	-	-	36
BW.14.22	5520	6.00	3.00	10.10	0.242	0.399	11	119.7	-	-	36
BW.14.23	5360	5.90	3.02	9.97	0.242	0.410	12	119.1	-	-	36
BW.14.26	3470	6.00	2.86	10.11	0.183	0.302	14	121.0	-	-	36
BW.14.31	3190	6.00	3.00	10.02	0.242	0.402	11	116.8	-	-	36

TABLE 1. CONTINUED

Mark	Concrete Strength f'_c psi a)	Flange width b in.	Web thickness b' in.	Effective depth d in.	Reinforcement Area A_s, in.^{2}	Reinforcement ratio p %	Reinforcement Lot	Effective prestress f_{se} ksi	Steel Area draped %	Drape angle φ degree	Shear span a in.
BW.14.32	2840	5.88	2.86	10.21	0.177	0.294	13	123.1	-	-	36
BW.14.34	3450	5.90	2.90	10.10	0.237	0.390	13	122.6	-	-	36
BW.14.38	2890	2.95	2.95	10.11	0.242	0.398	10	120.0	-	-	36
BW.14.39	3120	5.95	2.90	10.11	0.242	0.401	10	120.0	-	-	36
BW.14.41	3050	6.00	2.95	10.15	0.242	0.397	10	121.8	-	-	36
BW.14.42	2870	5.98	2.96	10.14	0.242	0.398	10	121.0	-	-	36
BW.14.43	2910	6.00	2.95	10.12	0.242	0.397	10	120.3	-	-	36
BW.14.45	3100	6.00	3.00	10.03	0.242	0.402	11	120.4	-	-	36
BW.14.58	3390	6.00	2.91	9.97	0.366	0.611	14	109.4	-	-	36
BW.14.60	2730	6.04	2.89	9.98	0.366	0.608	14	109.8	-	-	36
BW.15.34	3620	6.00	3.00	10.15	0.242	0.397	11	122.4	-	-	48
BW.15.37	3300	6.00	3.00	10.12	0.242	0.398	11	122.5	-	-	48
BW.16.38	3800	6.00	3.00	10.05	0.242	0.401	11	122.0	-	-	54
BW.18.15	7265	6.06	3.00	10.04	0.237	0.378	13	105.6	-	-	70
BW.18.27	4655	6.03	3.00	10.15	0.242	0.397	12	122.1	-	-	70
BW.19.28	4420	6.15	3.15	10.15	0.242	0.386	12	120.0	-	-	78
BW.23.18	6290	6.06	3.00	10.62	0.285	0.442	17	0.0	-	-	30
BW.23.19	6660	6.06	3.12	10.62	0.285	0.442	17	0.0	-	-	30
BW.23.20	6500	6.06	3.06	10.62	0.285	0.442	17	0.0	-	-	30
BW.23.21	6810	6.06	3.06	10.62	0.285	0.442	17	0.0	-	-	30
BW.23.22	6850	6.06	3.06	10.62	0.285	0.442	17	0.0	-	-	30
BW.23.23	6730	6.06	3.06	10.62	0.285	0.442	17	0.0	-	-	30
BW.23.24	6450	6.06	3.06	10.69	0.285	0.440	17	0.0	-	-	30
BW.23.25	6780	6.06	3.00	10.55	0.285	0.445	17	86.2	-	-	30
BW.25.19	7030	6.06	3.06	10.69	0.285	0.440	17	0.0	-	-	45
BW.25.20	6180	6.06	3.06	10.62	0.285	0.442	17	0.0	-	-	45
BW.25.21	6960	6.06	3.12	10.62	0.285	0.442	17	0.0	-	-	45
BW.25.22	6790	6.06	3.06	10.62	0.285	0.442	17	0.0	-	-	45
BW.25.23	6690	6.06	3.06	10.62	0.285	0.442	17	0.0	-	-	45
BW.25.24	6540	6.06	3.12	10.56	0.285	0.445	17	83.0	-	-	45
BW.26.21	6730	6.00	2.91	10.56	0.285	0.450	17	85.5	-	-	60
BW.28.26	3200	5.95	3.05	10.20	0.177	0.292	13	59.6	-	-	70
BW.28.28	3365	5.88	2.95	10.18	0.177	0.296	13	64.1	-	-	70
BW.29.21	6930	6.00	3.03	10.50	0.285	0.452	17	84.2	-	-	75
C. 10.27	3300	5.95	1.68	10.21	0.181	0.302	12	123.0	-	-	ML
C. 10.28	4250	6.00	1.88	10.06	0.242	0.400	12	113.0	-	-	ML
C. 13.23	3460	6.05	1.79	10.38	0.181	0.288	12	118.9	-	-	27

TABLE 1. CONTINUED

Mark	Concrete Strength f'_c psi a)	Flange width b in.	Web thickness b' in.	Effective depth d in.	Reinforcement Area A_s, in.^{2}	Reinforcement ratio p %	Reinforcement Lot	Effective prestress f_{se} ksi	Steel Area draped %	Drape angle φ degree	Shear span a in.
CD.13.24	3850	5.92	1.77	10.56	0.181	0.290	12	124.5	100	3.40	27
CD.13.25	3020	6.07	1.82	10.46	0.181	0.286	12	118.2	66.7	2.96	27
CD.14.34	2660	6.00	1.75	10.22	0.181	0.296	11	105.0	66.7	2.28	36
CI.14.34	3880	6.00	1.75	10.63	0.285	0.447	16	19.1	-	-	36
CI.14.36	2670	6.00	1.75	10.62	0.214	0.336	16	119.8	-	-	36
CI.24.39	2840	6.00	1.82	10.11	0.285	0.470	14	89.4	-	-	36
CW.10.26	4160	5.90	1.73	10.00	0.242	0.410	12	119.8	-	-	ML
CW.10.27	4235	6.00	1.72	9.96	0.242	0.405	12	119.1	-	-	ML
CW.13.28	3860	6.00	1.75	10.03	0.242	0.402	11	118.5	-	-	28
CW.13.38	3290	6.00	1.80	10.03	0.242	0.402	11	119.0	-	-	28
CW.14.14	6730	5.92	1.72	10.05	0.242	0.405	12	111.5	-	-	36
CW.14.15	2750	6.00	1.70	10.50	0.121	0.192	10	125.5	-	-	36
CW.14.16	3170	6.00	1.75	10.47	0.121	0.193	11	127.3	-	-	36
CW.14.17	2870	6.00	1.76	10.49	0.121	0.192	10	125.9	-	-	36
CW.14.18	2950	6.00	1.70	10.50	0.121	0.192	10	125.5	-	-	36
CW.14.19	2875	6.00	1.78	10.48	0.121	0.192	10	125.9	-	-	36
CW.14.20	2950	6.00	1.70	10.49	0.121	0.192	10	127.1	-	-	36
CW.14.21	2580	6.00	1.70	10.52	0.121	0.191	10	125.7	-	-	36
CW.14.22	4660	5.95	1.71	10.41	0.242	0.400	10	121.6	-	-	36
CW.14.23	2800	6.00	1.75	10.48	0.121	0.192	10	125.8	-	-	36
CW.14.24	2900	6.05	1.75	10.47	0.121	0.191	10	125.5	-	-	36
CW.14.25	5420	6.00	1.80	10.15	0.242	0.397	11	121.2	-	-	36
CW.14.26	2415	6.00	1.70	10.50	0.121	0.192	10	126.1	-	-	36
CW.14.27	2760	6.00	1.73	10.58	0.142	0.224	16	120.0	-	-	36
CW.14.34	3950	6.10	1.77	10.60	0.285	0.443	16	116.6	-	-	36
CW.14.35	3260	6.05	1.75	10.06	0.242	0.398	11	118.5	-	-	36
CW.14.36	3280	6.00	1.86	10.11	0.242	0.399	10	112.5	-	-	36
CW.14.37	4460	5.95	1.70	10.11	0.242	0.401	10	120.8	-	-	36
CW.14.38	3050	6.00	1.77	10.70	0.214	0.333	16	115.5	-	-	36
CW.14.39	3360	6.00	1.75	10.21	0.242	0.397	10	119.8	-	-	36
CW.14.40	3040	6.00	1.75	10.14	0.242	0.397	11	120.2	-	-	36
CW.14.41	3440	5.95	1.75	10.61	0.285	0.451	16	118.2	-	-	36
CW.14.42	3180	5.95	1.70	10.10	0.242	0.402	10	116.5	-	-	36
CW.14.45	3160	6.00	1.65	10.13	0.242	0.397	10	119.2	-	-	36
CW.14.47	2635	6.00	1.70	10.14	0.242	0.396	10	118.8	-	-	36
CW.14.50	2450	6.00	1.75	10.15	0.242	0.397	10	121.5	-	-	36
CW.14.51	3505	6.03	1.80	9.92	0.355	0.593	13	115.9	-	-	36

TABLE 1. CONTINUED

Mark	Concrete Strength f'_c psi a)	Flange width b in.	Web thickness b' in.	Effective depth d in.	Reinforcement Area A_s, in.^{2}	Reinforcement ratio p %	Reinforcement Lot	Effective prestress f_{se} ksi	Steel Area draped %	Drape angle φ degree	Shear span a in.
CW.14.54	3500	6.00	1.78	9.96	0.355	0.595	13	107.4	-	-	36
CW.18.15	7620	6.08	1.73	10.10	0.232	0.374	13	126.4	-	-	70
CW.24.37	3400	5.90	1.75	10.06	0.244	0.412	14	84.8	-	-	36
CW.28.26	3900	6.00	1.78	10.09	0.177	0.291	13	63.7	-	-	70
CW.28.28	3170	6.00	1.84	10.18	0.177	0.290	13	66.0	-	-	70
CU.14.29	3630	6.00	1.78	10.65	0.214	0.335	16	121.2	-	-	36
CU.14.31	3100	6.05	1.77	10.65	0.214	0.332	16	121.4	-	-	36
CU.14.32	3650	5.99	1.75	10.63	0.214	0.336	16	119.7	-	-	36
CU.14.33	3150	6.02	1.80	10.62	0.214	0.335	16	121.6	-	-	36
CU.14.35	4000	6.02	1.76	10.64	0.285	0.445	16	119.9	-	-	36
CU.14.37	3640	6.00	1.75	10.63	0.285	0.447	16	111.0	-	-	36
CU.14.38	3670	5.96	1.79	10.68	0.285	0.447	16	114.0	-	-	36
CU.14.39	3490	6.00	1.82	10.63	0.285	0.447	16	117.5	-	-	36
FV.14.063	3450	6.05	1.80	12.81	0.214	0.0696	16	110.1	66.7	2	36
FV.14.064	3710	6.00	1.77	12.93	0.214	0.0689	16	101.3	66.7	4	36
FV.14.065	3730	5.98	1.75	12.76	0.214	0.0698	16	121.0	66.7	2	36
FV.14.070	2650	5.95	1.71	12.72	0.214	0.0703	16	99.0	66.7	6	36
FW.14.036	4165	5.95	1.75	12.72	0.142	0.0467	16	116.0	-	-	36
FW.14.063	2790	5.95	1.70	12.72	0.214	0.0701	16	115.2	-	-	36
FW.14.064	3320	24.0	1.75	12.30	0.242	0.0820	11	117.8	-	-	36
FW.14.070	4030	24.0	1.85	12.30	0.242	0.0820	11	123.0	-	-	36
FW.14.089	4210	5.98	1.71	12.56	0.285	0.0945	16	115.0	-	-	36
FW.14.091	3380	5.97	1.78	12.22	0.285	0.0970	16	121.3	-	-	36

a) Strength of concrete in bottom of the beam.

TABLE 2.

PROPERTIES OF WEB REINFORCEMENT

Mark [a]	Stirrup diameter	Stirrup spacing	Stirrup type [c]	Web Reinf. ratio	Steel stress at 1% strain f_y	Steel stress at 2% strain	Ultimate	rf_y	Stirrup prestress f_{sev}
	in.	in.		r	ksi	ksi	ksi		ksi
AW.14.39	0.250	6.5	A	0.252	53.7	55.0	73.6	135	0
AW.14.76	0.250	6.5	A	0.252	53.7	55.0	73.6	135	0
AW.24.48	0.250	6.5	A	0.252	53.7	55.0	73.6	135	0
AW.24.68	0.250	6.5	A	0.252	53.7	55.0	73.6	135	0
BV.14.30	0.161	5.0	D	0.136	36.8	39.0	45.4	50	0
BV.14.32	0.161	4.5	D	0.152	36.8	39.0	45.4	56	0
BV.14.34	0.161	4.5	D	0.152	36.8	39.0	45.4	56	0
BV.14.35	0.161	3.5	D	0.196	36.8	39.0	45.4	72	0
BV.14.42	0.161	4.0	D	0.170	36.8	39.0	45.4	63	0
BW.10.22	0.136	Varies	C'	0.073 [b]	37.2	38.5	49.4	27	0
BW.14.20	0.136	5.0	C	0.048	43.5	46.5	52.0	21	0
BW.14.22	0.161	5.0	D	0.136	36.8	39.0	45.4	50	0
BW.14.23	0.129 [d]	3.75	C'	0.074	79.5	80.0	81.0	59	0
BW.14.26	0.135	4.5	D	0.106	43.0	45.0	64.4	46	0
BW.14.31	0.193	10.0	E	0.146	41.2	43.0	51.0	60	0
BW.14.32	0.161	5.0	C'	0.068	36.8	39.0	45.4	25	0
BW.14.34	0.223	10.5	D	0.125	34.0	36.5	42.1	43	0
BW.14.38	0.136	2.5	C	0.097	43.5	46.5	52.0	42	0
BW.14.39	0.191	2.5	C	0.191	35.7	38.0	46.3	68	0
BW.14.41	0.161	5.0	D	0.136	36.8	39.0	45.4	50	0
BW.14.42	0.161	2.5	C	0.136	36.8	39.0	45.4	50	0
BW.14.43	0.193	5.0	D	0.195	41.2	43.0	51.0	80	0
BW.14.45	0.193	7.5	D	0.130	41.2	43.0	51.0	53	0
BW.14.58	0.135	5.0	D	0.095	43.0	45.0	64.4	41	0
BW.14.60	0.135	5.0	D	0.095	43.0	45.0	64.4	41	0
BW.15.34	0.136	5.0	D	0.097	37.2	38.5	49.4	36	0
BW.15.37	0.161	5.0	D	0.136	36.8	39.0	45.4	50	0
BW.16.38	0.136	5.0	D	0.097	37.2	38.5	49.4	36	0
BW.18.15S	0.129 [d]	Varies	C'	0.069 [b]	79.5	80.0	81.0	55	0
L	0.129 [d]	Varies	C'	0.038 [b]	79.5	80.0	81.0	30	0
BW.18.27S	0.193	5.0	D	0.195	41.2	43.0	51.0	80	0
L	0.136	Varies	C	0.080 [b]	37.2	38.5	49.4	30	0
BW.19.28S	0.193	5.0	D	0.195	41.2	43.0	51.0	80	0
L	0.136	Varies	C	0.072 [b]	37.2	38.5	49.4	27	0

TABLE 2. CONTINUED

Mark [a]	Stirrup diameter	Stirrup spacing	Stirrup type[c]	Web Reinf. ratio	Steel Stress at 1% strain f_y	Steel Stress at 2% strain	Ultimate	rf_y	Stirrup prestress f_{sev}
	in.	in.		r	ksi	ksi	ksi		ksi
BW.23.18	0.162	2.75	C'	0.125	38.6	40.8	47.5	48	0
BW.23.19	0.162	2.75	C'	0.125	38.6	40.8	47.5	48	0
BW.23.20	0.162	2.75	D	0.250	38.6	40.8	47.5	96	0
BW.23.21	0.162	2.0	D	0.344	38.6	40.8	47.5	133	0
BW.23.22	0.253	3.5	D	0.479	36.8	37.6	59.3	176	0
BW.23.23	0.253	3.0	D	0.559	36.8	37.6	59.3	206	0
BW.23.24	0.253	2.5	D	0.670	36.8	37.6	59.3	246	0
BW.23.25	0.162	2.75	C'	0.125	38.6	40.8	47.5	48	0
BW.25.19	0.162	2.75	C'	0.125	38.6	40.8	47.5	48	0
BW.25.20	0.162	2.75	D	0.250	38.6	40.8	47.5	96	0
BW.25.21	0.162	2.0	D	0.344	38.6	40.8	47.5	133	0
BW.25.22	0.253	3.5	D	0.479	36.8	37.6	59.3	176	0
BW.25.23	0.253	3.0	D	0.559	36.8	37.6	59.3	206	0
BW.25.24	0.162	2.75	C'	0.125	38.6	40.8	47.5	48	0
BW.26.21S	0.162	2.0	C'	0.172	38.6	40.8	47.5	66	0
L	0.162	2.75	C'	0.125	38.6	40.8	47.5	48	0
BW.28.26S	0.136	Varies	D	0.161[b]	37.2	38.5	49.4	60	0
L	0.136	Varies	C	0.088[b]	37.2	38.5	49.4	33	0
BW.28.28S	0.161	4.0	D	0.170	36.8	39.0	45.4	63	0
L	0.136	5.5	D	0.088	37.2	38.5	49.3	33	0
BW.29.21S	0.253	3.0	D	0.559	35.8	37.6	59.3	206	0
L	0.162	2.75	C'	0.125	38.6	40.8	47.5	48	0
CI.14.34	0.177	2.5	D[e]	0.461[e]	30.0	32.0	45.0	138	0
CI.14.36	0.177	3.5	D[e]	0.329[e]	30.0	32.0	45.0	99	0
CI.24.39	0.135	3.5	D[e]	0.192[e]	43.0	45.0	64.4	83	0
CW.10.26	0.161	4.5	D	0.151	36.8	39.0	45.4	56	0
CW.10.27	0.161	Varies	D	0.151[b]	36.8	39.0	45.4	56	0
CW.13.28	0.161	2.5	D	0.272	36.8	39.0	45.4	100	0
CW.13.38	0.193	3.0	D	0.325	41.2	43.0	51.0	134	0
CW.14.14	0.129[d]	2.75	C'	0.101	79.5	80.0	81.0	80	0
CW.14.15	0.161	2.5	D	0.272	36.8	39.0	45.4	100	0
CW.14.16	0.161	9.0	D	0.076	36.8	39.0	45.4	28	0
CW.14.17	0.136	5.0	C	0.048	43.5	46.5	52.0	21	0
CW.14.18	0.191	2.5	D	0.382	35.7	38.0	46.3	136	0
CW.14.19	0.136	2.5	C	0.097	43.5	46.5	52.0	42	0

TABLE 2. CONTINUED

Mark [a]	Stirrup diameter	Stirrup spacing	Stirrup type[c]	Web Reinf. ratio	Steel Stress at 1% strain f_y	Steel Stress at 2% strain	Ultimate	rf_y	Stirrup prestress f_{sev}
	in.	in.		r	ksi	ksi	ksi		ksi
CW.14.20	0.136	5.0	D	0.097	43.5	46.5	52.0	42	0
CW.14.21	0.161	5.0	C	0.068	36.8	39.0	45.4	25	0
CW.14.22	0.191	2.5	C	0.191	35.7	38.0	46.3	68	0
CW.14.23	0.161	5.0	C	0.068	36.8	39.0	45.4	25	0
CW.14.24	0.193	9.0	D	0.108	41.2	43.0	51.0	45	0
CW.14.25	0.161	2.5	D	0.272	36.8	39.0	45.4	100	0
CW.14.26	0.161	2.5	C	0.136	36.8	39.0	45.4	50	0
CW.14.27	0.177	3.0	D	0.274	31.8	34.0	44.0	87	0
CW.14.34	0.177	2.5	D	0.328	31.8	34.0	44.0	104	0
CW.14.35	0.257	7.5	D	0.230	44.5	49.0	61.6	103	0
CW.14.36	0.193	3.75	D	0.260	41.2	43.0	51.0	107	0
CW.14.37	0.161	2.5	C	0.136	36.8	39.0	45.4	50	0
CW.14.38	0.177	3.5	D	0.234	31.8	34.0	44.0	75	0
CW.14.39	0.136	2.5	C	0.097	43.5	46.5	52.0	42	0
CW.14.40	0.257	5.0	D	0.346	44.5	49.0	61.6	154	0
CW.14.41	0.250	4.0	C	0.205	46.0	46.5	66.0	94	0
CW.14.42	0.136	2.5	D	0.193	43.5	46.5	52.0	84	0
CW.14.45	0.161	2.5	D	0.272	36.8	39.0	45.4	100	0
CW.14.47	0.191	5.0	D	0.191	35.7	38.0	46.3	68	0
CW.14.50	0.223	5.0	D	0.261	34.0	36.5	42.1	89	0
CW.14.51	0.161	5.0	D	0.136	36.8	39.0	45.4	50	0
CW.14.54	0.161	5.0	D	0.136	36.8	39.0	45.4	50	0
CW.18.15S	0.129[d]	Varies	C'	0.101[b]	79.5	80.0	81.0	80	0
L	0.129[d]	Varies	C'	0.055[b]	79.5	80.0	81.0	44	0
CW.24.37	0.135	3.5	D	0.136	43.0	45.0	64.4	59	0
CW.28.26S	0.136	Varies	D	0.203[b]	37.2	38.5	49.4	76	0
L	0.136	Varies	C'	0.107[b]	37.2	38.5	49.4	40	0
CW.28.28S	0.161	3.25	D	0.209	36.8	39.0	45.4	77	0
L	0.136	4.38	D	0.110	37.2	38.5	49.4	41	0
CU.14.29	0.250	4.0	C	0.205	46.0	46.5	66.0	94	30
CU.14.31	0.250	4.0	C	0.205	46.0	46.5	66.0	94	0
CU.14.32	0.250	4.0	C	0.205	46.0	46.5	66.0	94	0
CU.14.33	0.250	4.0	C	0.205	46.0	46.5	66.0	94	30

TABLE 2. CONTINUED

Mark [a]	Stirrup diameter	Stirrup spacing	Stirrup type[c]	Web Reinf. ratio	Steel Stress at 1% strain f_y	Steel Stress at 2% strain	Ultimate	rf_y	Stirrup prestress f_{sev}
	in.	in.		r	ksi	ksi	ksi		ksi
CU.14.35	0.250	4.0	C	0.205	46.0	46.5	66.0	94	40
CU.14.37	0.250	4.0	C	0.205	46.0	46.5	66.0	94	20
CU.14.38	0.250	4.0	C	0.205	46.0	46.5	66.0	94	0
CU.14.39	0.250	4.0	C	0.205	46.0	46.5	66.0	94	30
FV.14.063	0.177	2.0	B	0.410	33.4	39.0	49.0	137	0
FV.14.064	0.177	2.25	B	0.364	30.0	32.0	45.0	109	0
FV.14.065	0.177	2.0	B	0.410	30.0	32.0	45.0	123	0
FV.14.070	0.177	2.44	B	0.336	30.0	32.0	45.0	101	0
FW.14.036	0.177	3.13	B	0.262	33.4	39.0	49.0	79	0
FW.14.063	0.177	1.88	B	0.436	33.4	39.0	49.0	146	0
FW.14.064	0.161	2.5	B	0.272	36.8	39.0	45.4	100	0
FW.14.070	0.193	3.0	B	0.324	41.2	43.0	51.0	133	0
FW.14.089	0.177	1.63	B	0.503	33.4	39.0	49.0	168	0
FW.14.091	0.177	1.37	B	0.599	30.0	32.0	45.0	180	0

a) In beams loaded with a single unsymmetrically placed load, S refers to the short shear span, L to the long one

b) Adjacent to load point

c) Letters correspond to types of stirrups shown in Figure 4

d) Square bar

e) Stirrups inclined 45^{o} with longitudinal axis. r is based on volume of stirrups

g) Based on flange width of precast section

TABLE 3.

PROPERTIES OF CONCRETE MIXES

Mark	Compressive Strength f'_c psi		Modulus of rupture f_r psi		Splitting Strength f_t psi		Cement:Sand: Gravel	Water/Cement		Slump in.		Age at test days
	1	2	1	2	1	2		1	2	1	2	
AD.14.37	2700	3260	300	282	-	-	1:4.2:4.6	0.91	0.91	1.5	2	12
AW.14.39	5470	5560	510	-	-	-	1:3.3:3.5	0.83	0.83	3.5	3	19
AW.14.76	2765	2795	385	-	-	-	1:3.7:3.9	1.06	1.06	8	8	6
AW.24.48	4900	4400	525	-	-	-	1:3.3:3.5	0.69	0.69	2.5	6	8
AW.24.68	2510	3170	400	-	-	-	1:4.1:4.3	0.96	0.96	5.5	6	10
B. 10.23	5205	5300	425	462	-	-	1:3.9:4.2	0.85	0.85	1	2	36
B. 10.24	3720	3835	375	342	-	-	1:4.1:4.4	0.82	0.87	2	1.5	18
B. 14.34	3090	2640	340	275	-	-	1:4.1:4.4	0.79	0.79	1	1	8
B. 14.41	3000	2890	358	358	-	-	1:4.1:4.4	0.79	0.79	1	1	7
B. 23.17	6780	6280	-	-	506	485	1:2.6:2.9	0.58	0.58	3	3.5	12
B. 25.18	6780	6720	-	-	480	433	1:2.6:2.9	0.58	0.58	2	2.5	12
BD.14.18	6390	6280	517	438	-	-	1:2.9:3.2	0.72	0.71	3	2	6
BD.14.19	6720	6280	519	519	-	-	1:2.8:3.0	0.72	0.74	3	3	7
BD.14.23	4210	3870	337	310	-	-	1:4.0:4.3	0.78	0.78	2	1.5	15
BD.14.26	3160	3460	383	392	-	-	1:4.2:4.6	0.84	0.84	1.5	1	8
BD.14.27	3850	3400	442	416	-	-	1:4.3:4.6	0.79	0.79	1.5	2	9
BD.14.28	4230	3320	457	367	-	-	1:4.0:4.4	0.77	0.78	2	2	8
BD.14.34	2720	2700	404	350	-	-	1:4.2:4.6	0.79	0.79	3	2.5	8
BD.14.35	2610	2610	375	400	-	-	1:4.2:4.6	0.92	0.92	1	1	8
BD.14.42	2980	2870	491	491	-	-	1:4.2:4.5	1.00	1.00	3	2	8
BD.24.32	3090	3800	416	375	-	-	1:4.3:4.6	0.81	0.81	2	2	8
BV.14.30	4200	4020	346	350	-	-	1:3.9:4.2	0.82	0.82	2	3	20
BV.14.32	4210	3800	420	451	-	-	1:3.9:4.2	0.84	0.83	2	3	6
BV.14.34	3800	3620	500	416	-	-	1:4.0:4.2	0.86	0.85	2	2	5
BV.14.35	3340	3410	508	425	-	-	1:3.9:4.2	0.83	0.83	3	3	5
BV.14.42	3090	2910	455	450	-	-	1:3.9:4.2	0.90	0.90	2.5	3	6
BW.10.22	4150	3970	466	469	-	-	1:4.1:4.4	0.91	0.85	2	2	13
BW.14.20	2840	2870	333	350	-	-	1:4.1:4.4	0.80	0.83	1.5	1	7
BW.14.22	5520	5430	517	475	-	-	1:3.2:3.5	0.65	0.62	3	2.5	10
BW.14.23	5360	5525	500	520	-	-	1:2.2:2.6	0.72	0.74	4	6	7
BW.14.26	3470	3505	400	400	-	-	1:3.9:4.2	0.82	0.82	3	3	7
BW.14.31	3190	3870	383	425	-	-	1:4.1:4.4	0.79	0.76	7	3	11
BW.14.32	2840	2830	308	350	-	-	1:3.9:4.2	0.90	0.90	3	3	6
BW.14.34	3450	3560	366	358	-	-	1:3.9:4.2	0.83	0.83	2	2.5	7
BW.14.38	2890	3110	342	316	-	-	1:4.1:4.5	0.91	0.91	1.5	1	7
BW.14.39	3120	3050	358	392	-	-	1:4.2:4.5	0.86	0.86	2	1	8
BW.14.41	3050	2860	466	359	-	-	1:3.9:4.2	0.87	0.85	2.5	2.5	8
BW.14.42	2870	2810	338	342	-	-	1:4.1:4.5	0.84	0.84	2	2	8
BW.14.43	2910	2780	346	392	-	-	1:4.1:4.4	0.88	0.88	1	3	8
BW.14.45	3100	2680	304	304	-	-	1:4.1:4.3	0.80	0.79	2.5	3.5	9
BW.14.58	3390	3165	416	358	-	-	1:4.0:4.3	0.82	0.83	2	3	7
BW.14.60	2730	3025	358	350	-	-	1:4.0:4.3	0.89	0.89	2	2	7
BW.15.34	3620	3550	375	392	-	-	1:4.1:4.3	0.75	0.75	4	2	11
BW.15.37	3300	3210	417	392	-	-	1:4.2:4.4	0.87	0.83	3	3.5	8
BW.16.38	3800	3160	383	267	-	-	1:4.0:4.3	0.88	0.91	1.5	2.5	10

TABLE 3. CONTINUED

Mark	Compressive Strength f'_c psi		Modulus of rupture f_r psi		Splitting Strength f_t psi		Cement:Sand: Gravel	Water/Cement		Slump in.		Age at test days
	1	2	1	2	1	2		1	2	1	2	
BW.18.15	7265	7625	618	558	-	-	1:2.2:2.6	0.59	0.59	3.5	4	18
BW.18.27	4655	4345	533	512	-	-	1:4.0:4.3	0.80	0.80	2	2	12
BW.19.28	4420	4080	444	438	-	-	1:4.1:4.4	0.89	0.86	2	2	12
BW.23.18	6290	6110	-	-	587	538	1:2.6:2.9	0.58	0.58	2	2.5	12
BW.23.19	6660	6720	-	-	-	-	1:2.6:2.9	0.59	0.58	1.5	3	12
BW.23.20	6500	5800	-	-	545	430	1:2.6:2.9	0.58	0.58	1.5	2	12
BW.23.21	6810	6520	-	-	498	449	1:2.6:2.9	0.58	0.58	2.5	4	12
BW.23.22	6850	6910	-	-	-	-	1:2.6:2.9	0.58	0.58	1.5	2	12
BW.23.23	6730	6470	-	-	549	497	1:2.6:2.9	0.58	0.58	1	1	12
BW.23.24	6450	6690	-	-	-	-	1:2.6:2.9	0.58	0.58	2	2	12
BW.23.25	6780	6310	-	-	447	444	1:2.5:2.8	0.52	0.52	4	7	17
BW.25.19	7030	6670	-	-	536	458	1:2.6:2.9	0.59	0.59	1.5	2.5	12
BW.25.20	6180	6400	-	-	-	-	1:2.6:2.9	0.59	0.58	2.5	2.5	12
BW.25.21	6960	6780	-	-	-	-	1:2.6:2.9	0.59	0.58	1.5	2	12
BW.25.22	6790	6880	-	-	-	-	1:2.6:2.9	0.59	0.58	2	2	12
BW.25.23	6690	6640	-	-	-	-	1:2.6:2.9	0.58	0.58	1.5	2	12
BW.25.24	6540	6500	-	-	513	535	1:2.5:2.9	0.57	0.57	2	2	12
BW.26.21	6730	6560	-	-	482	485	1:2.6:2.9	0.58	0.58	2.5	2.5	12
BW.28.26	3200	3425	458	366	-	-	1:3.9:4.2	0.86	0.86	2	2	8
BW.28.28	3365	3120	450	413	-	-	1:3.9:4.2	0.85	0.86	2	3	6
BW.29.21	6930	6980	-	-	480	493	1:2.6:2.9	0.58	0.58	2	2.5	11
C. 10.27	3300	3660	275	300	-	-	1:4.1:4.4	0.85	0.82	2	2	14
C. 10.28	4250	4300	412	316	-	-	1:3.9:4.2	0.89	0.85	1	1	25
C. 13.23	3460	3730	495	425	-	-	1:4.4:4.4	0.87	0.83	1	1.5	13
CD.13.24	3850	3670	467	437	-	-	1:4.4:4.4	0.90	0.90	1	1.5	14
CD.13.24	3020	3460	408	417	-	-	1:4.4:4.4	0.85	0.85	1	1.5	11
CD.14.34	2660	2560	417	420	-	-	1:3.8:4.2	0.91	0.94	2	3	6
CI.14.34	3880	3910	483	533	-	382	1:3.0:3.2	0.71	0.71	2.5	3	6
CI.14.36	2670	2790	325	266	255	257	1:3.8:4.1	0.81	0.81	2.5	2.5	7
CI.24.39	2840	2970	417	433	321	325	-	-	-	-	-	-
CW.10.26	4160	4650	456	460	-	-	1:4.1:4.4	0.84	0.85	2	2	20
CW.10.27	4235	4530	408	417	-	-	1:3.8:4.4	0.94	0.85	1	1.5	16
CW.13.28	3860	4330	408	433	-	-	1:3.9:4.2	0.82	0.82	1.5	1.5	11
CW.13.38	3290	3200	333	367	-	-	1:4.0:4.3	0.86	0.83	4.5	2.5	11
CW.14.14	6730	7205	504	541	-	-	1:2.2:2.6	0.59	0.59	2	2	13
CW.14.15	2750	3280	342	433	-	-	1:4.2:4.6	1.02	1.02	4	5	9
CW.14.16	3170	3230	466	392	-	-	1:3.7:3.9	0.81	0.78	5	3	7
CW.14.17	2870	3140	333	371	-	-	1:4.2:4.5	0.84	0.84	2	2	8
CW.14.18	2950	3100	408	442	-	-	1:4.2:4.4	0.94	0.94	6	3.5	7
CW.14.19	2875	3080	333	366	-	-	1:4.2:4.6	0.86	0.86	2	1.5	8
CW.14.20	2950	3020	400	-	-	-	1:4.2:4.5	0.86	0.86	2	1.5	8
CW.14.21	2580	2990	350	416	-	-	1:4.2:4.4	0.86	0.89	1	1.5	8
CW.14.22	4660	4660	484	458	-	-	1:2.6:3.1	0.70	0.67	7	7	8
CW.14.23	2800	2690	375	342	-	-	1:3.8:4.1	0.87	0.87	1.5	2	7
CW.14.24	2900	2680	416	400	-	-	1:3.7:3.9	0.94	0.94	2.5	4	8
CW.14.25	5420	5050	518	492	-	-	1:3.2:3.5	0.67	0.67	1	2	11
CW.14.26	2415	2310	410	348	-	-	1:4.2:4.5	0.91	0.87	6	2	8
CW.14.27	2760	3450	450	450	-	-	1:3.9:4.1	0.80	0.90	1	1.5	7

TABLE 3. CONTINUED

Mark	Compressive Strength f'_c psi		Modulus of rupture f_r psi		Splitting Strength f_t psi		Cement: Sand: Gravel	Water/Cement		Slump in.		Age at test days
	1	2	1	2	1	2		1	2	1	2	
CW.14.34	3950	3930	384	384	357	367	1:3.9:4.1	0.72	0.72	1.5	2	11
CW.14.35	3260	3420	433	508	-	-	1:3.7:4.0	0.87	0.83	6	2	9
CW.14.36	3280	3300	383	425	-	-	1:3.7:4.0	0.75	0.75	1	2	8
CW.14.37	4460	3240	408	425	-	-	1:4.2:4.5	0.93	0.91	6	1.5	6
CW.14.38	3050	2850	417	417	-	-	1:3.9:4.1	0.89	0.85	4	3.5	12
CW.14.39	3360	3010	408	425	-	-	1:4.2:4.5	0.93	0.91	1	3	8
CW.14.40	3040	3010	421	383	-	-	1:3.7:4.0	0.80	0.80	2	2.5	8
CW.14.41	3440	3360	400	392	374	304	1:3.6:3.8	0.73	0.70	1.5	1.5	8
CW.14.42	3180	2840	375	342	-	-	1:4.2:4.5	0.89	0.89	3	8	8
CW.14.45	3160	2640	333	366	-	-	1:4.3:4.5	0.95	0.95	5	3	9
CW.14.47	2635	2535	366	317	-	-	1:4.2:4.5	0.91	0.95	1	1	8
CW.14.50	2450	2400	400	367	-	-	1:3.9:4.2	0.92	0.88	4.5	2.5	8
CW.14.51	3505	3260	333	266	-	-	1:3.9:4.2	0.88	0.89	3	3.5	13
CW.14.54	3500	3300	358	342	-	-	1:3.9:4.2	0.82	0.83	2	2.5	8
CW.18.15	7620	7425	633	609	-	-	1:2.2:2.6	0.59	0.60	2.5	2.5	19
CW.24.37	3400	3180	400	367	327	306	-	-	-	-	-	-
CW.28.26	3900	3370	433	292	-	-	1:3.9:4.2	0.80	0.81	2	3	10
CW.28.28	3170	3085	433	334	-	-	1:4.0:4.2	0.86	0.86	2	2.5	8
CV.14.29	3630	3500	408	425	390	390	1:3.8:4.1	0.81	0.81	3	3	13
CV.14.31	3100	3170	333	352	283	262	1:3.8:4.1	0.81	0.81	2.5	3	12
CV.14.32	3650	3190	418	401	391	272	1:3.8:4.0	0.82	0.80	5	5	22
CV.14.33	3150	3060	333	366	284	-	1:3.8:4.1	0.81	0.81	2	2	10
CV.14.35	4000	3870	550	533	388	357	1:3.6:3.8	0.70	0.70	1	1.5	8
CV.14.37	3640	3590	483	400	362	426	1:3.6:3.8	0.79	0.76	1	1	5
CV.13.38	3670	3540	482	482	410	409	1:3.8:4.1	0.81	0.81	2	3	14
CV.14.39	3490	3490	416	400	288	369	1:2.8:3.0	0.67	0.67	3.5	4	4
FV.14.063												
beam	3450	3460	417	384	388	385	1:3.8:4.1	0.81	0.81	1.5	1.5	16
slab	3280	-	375	-	300	-	1:3.8:4.1	0.81	-	4	-	13
FV.14.064												
beam	3710	3490	400	400	405	335	1:3.8:4.1	0.81	0.81	1.5	2.5	17
slab	3230	-	367	-	290	-	1:3.8:4.1	0.81	-	1.5	-	12
FV.14.065												
beam	3730	3640	417	542	305	293	1:3.5:3.7	0.79	0.79	5.5	6	12
slab	3240	-	500	-	326	-	1:3.4:3.7	0.78	-	1.5	-	8
FV.14.070												
beam	2650	2710	358	334	221	232	1:3.8:4.1	0.81	0.81	6	4	15
slab	3040	-	375	-	294	-	1:3.8:4.0	0.80	-	2	-	7
FW.14.036												
beam	4165	4240	450	450	420	442	1:3.9:4.1	0.79	0.77	1.5	2	24
slab	3940	3960	467	-	362	437	1:3.6:3.9	0.72	0.72	1	1	19
FW.14.063												
beam	2790	2705	417	400	-	-	1:3.9:4.1	0.75	0.75	2	2	18
slab	3360	-	-	-	327	-	1:3.8:4.1	0.77	-	1.5	-	9
FW.14.064												
beam	3320	3910	425	362	-	-	1:4.1:4.3	0.82	0.79	3	2	12
slab	3000	-	383	-	-	-	1:3.9:4.0	0.78	-	2.5	-	6
FW.14.070												
beam	4030	3520	433	275	-	-	1:4.1:4.3	0.80	0.79	2.5	4.5	15
slab	3280	-	333	-	-	-	1:3.8:4.1	0.75	-	1	-	9

TABLE 3. CONTINUED

Mark	Compressive Strength f'_c psi		Modulus of rupture f_r psi		Splitting Strength f_t psi		Cement:Sand: Gravel	Water/Cement		Slump in.		Age at test days
	1	2	1	2	1	2		1	2	1	2	
FW.14.089												
beam	4210	3660	458	367	397	388	1:3.9:4.1	0.62	0.66	1	1	13
slab	3325	3040	-	-	357	367	1:3.9:4.1	0.72	0.72	1	1	7
FW.14.091												
beam	3380	3100	508	525	361	301	1:3.5:3.7	0.79	0.79	1.5	2.5	11
slab	3070	-	467	-	290	-	1:3.4:3.7	0.79	-	6	-	6

TABLE 4.

PROPERTIES OF LONGITUDINAL REINFORCEMENT

Lot	Manufacturer	Heat Analysis C %	Mn %	P %	S %	Si %	Diameter in.	Stress at 1% strain ksi	Ultimate stress ksi
8	AS and W[a)]	0.83	0.75	0.010	0.035	0.20	0.196	217	255
10	AS and W	0.81	0.76	0.010	0.027	0.23	0.196	222	267
11	AS and W	0.85	0.65	0.010	0.027	0.18	0.196	219	256
12	AS and W	0.88	0.79	0.024	0.033	0.25	0.196	228	255
13	AS and W	0.82	0.72	0.018	0.032	0.21	0.194	218	258
14	Union[b)]	0.85	0.84	0.010	0.029	0.18	0.197	242	280
16	AS and W	0.07	0.36	0.008	0.28	-	0.250	244	274
17	AS and W	0.07	0.36	0.008	0.28	-	0.250	234	265

a) American Steel and Wire Division of the U. S. Steel Corporation

b) Union Wire Rope Corporation

TABLE 5.

COMPUTED AND MEASURED VALUES OF INCLINED CRACKING LOAD

Mark	Shear span a in.	Calc. shear cracking load V_{cs} kips	Calc. flexure-shear cracking load V_{cf} kips	Measured inclined cracking load V_{cm} kips	Type of crack observed d)	$\frac{V_{cm}}{V_c}$ c)
AD.14.37	36	22.0[a]	9.17	8.00	F	0.87
AW.14.39	36	29.0	12.0	11.3	F	0.94
AW.14.76	36	22.8	10.1	10.6	F	1.05
AW.24.48	36	22.7	8.43	10.0	F	1.19
AW.24.68	36	18.0	7.13	8.21	F	1.15
B. 10.23	38	15.0	10.0	9.85	F	0.99
	46	15.0	8.49	8.35	F	0.98
	54	15.0	7.46	6.93	F	0.93
B. 10.24	30	12.2	9.86	10.1	F	1.02
	38	12.2	7.93	7.93	F	1.00
	46	12.2	6.74	6.59	F	0.98
	54	12.2	5.94	6.26	F	1.05
	46	12.2	6.74	6.59	F	0.98
	38	12.2	7.93	7.93	F	1.00
B. 14.34	36	11.1	7.79	8.49	F	1.09
B. 14.41	36	12.0	8.84	9.21	F	1.04
B. 23.17	30	10.6	5.36	5.6	F	1.04
B. 25.18	45	10.6	4.29	4.4	F	1.03
BD.14.18	36	17.1[a]	9.98	10.9	F	1.09
BD.14.19	36	18.3[a]	10.1	11.2	F	1.11
BD.14.23	36	14.8[a]	6.94	5.60	F	1.24
BD.14.26	36	14.8[a]	6.92	6.38	F	1.09
BD.14.27	36	12.7[a]	7.63	8.95	F	1.17
BD.14.28	36	13.1[a]	8.12	(10.2)[b]	-	(1.19)
BD.14.34	36	11.3[a]	7.15	7.90	F	1.10
BD.14.35	36	12.4[a]	6.60	6.49	F	0.98
BD.14.42	36	12.8[a]	8.38	9.95	F	1.19
BD.24.32	36	13.1[a]	6.89	7.45	F	1.08
BV.14.30	36	15.5[a]	9.66	10.2	F	1.06
BV.14.32	36	14.7[a]	9.07	10.4	F	1.14
BV.14.34	36	14.8[a]	9.66	10.5	F	1.09
BV.14.35	36	14.0[a]	8.75	9.80	F	1.12
BV.14.42	36	15.5[a]	8.50	9.60	F	1.13
BW.10.22	30	12.6	10.1	10.8	F	1.07
	38	12.6	8.11	8.46	F	1.04
	46	12.6	6.91	6.70	F	0.97
	54	12.6	6.11	5.85	F	0.96
	46	12.6	6.91	7.45	F	1.08
	38	12.6	8.11	8.46	F	1.04
BW.14.20	36	9.90	6.49	(8.25)[b]	-	(1.27)
BW.14.22	36	15.0	10.4	10.6	F	1.02
BW.14.23	36	14.9	10.1	10.3	F	1.02
BW.14.26	36	11.8	7.96	7.99	F	1.00
BW.14.31	36	12.4	9.14	10.2	F	1.12
BW.14.32	36	10.9	7.69	9.54	F	1.24
BW.14.34	36	12.8	9.46	10.4	F	1.10
BW.14.38	36	12.1	9.20	10.4	F	1.13

TABLE 5. CONTINUED

Mark	Shear span a in.	Calc. shear cracking load V_{cs} kips	Calc. flexure-shear cracking load V_{cf} kips	Measured inclined cracking load V_{cm} kips	Type of crack observed d)	$\frac{V_{cm}}{V_c}$ c)
BW.14.39	36	12.4	9.33	10.5	F	1.12
BW.14.41	36	12.3	9.44	9.90	F	1.07
BW.14.42	36	12.1	9.29	9.35	F	1.01
BW.14.43	36	12.1	9.24	10.7	F	1.16
BW.14.45	36	12.4	9.26	9.90	F	1.07
BW.14.58	36	14.2	11.6	14.0	F	1.21
BW.14.60	36	13.3	11.3	12.8	F	1.13
BW.15.34	48	13.1	7.54	8.15	F	1.08
BW.15.37	48	12.7	7.40	8.35	F	1.13
BW.16.38	54	13.3	6.81	7.00	F	1.03
BW.18.15	70	15.9	6.13	5.93	F	0.97
	38	15.9	9.59	9.50	F	0.99
BW.18.27	70	14.2	5.95	5.63	F	0.95
	38	14.2	9.70	10.8	F	1.11
BW.19.28	78	13.9	5.16	5.28	F	1.02
	30	13.9	12.0	12.8	F	1.07
BW.23.18	30	10.2	5.10	6.25	F	1.22
BW.23.19	30	10.5	5.35	6.10	F	1.14
BW.23.20	30	10.4	5.24	6.20	F	1.18
BW.23.21	30	10.6	5.36	6.70	F	1.25
BW.23.22	30	10.6	5.37	6.50	F	1.21
BW.23.23	30	10.6	5.34	6.40	F	1.20
BW.23.24	30	10.3	5.23	6.70	F	1.28
BW.23.25	30	15.5	12.3	14.4	F	1.17
BW.25.19	45	10.8	4.44	4.70	F	1.06
BW.25.20	45	10.1	4.15	4.70	F	1.13
BW.25.21	45	10.7	4.45	5.00	F	1.12
BW.25.22	45	10.6	4.35	6.10	F	1.40
BW.25.23	45	10.5	4.32	5.40	F	1.25
BW.25.24	45	15.1	8.50	9.70	F	1.14
BW.26.21	60	15.3	6.86	7.40	F	1.08
	48	15.3	8.08	9.87	F	1.22
BW.28.26	70	9.50	3.54	3.43	F	0.97
	38	9.50	5.28	6.18	F	1.17
BW.28.28	70	9.83	3.62	3.46	F	0.96
	38	9.83	5.46	5.75	F	1.05
BW.29.21	75	15.9	6.02	6.42	F	1.07
	33	15.9	11.1	16.2	F	1.46
C. 10.27	22	7.17	12.7	7.16	S	1.00
C. 10.28	22	8.35	15.2	8.90	S	1.07
C. 13.23	27	7.21	10.3	8.30	S	1.15
CD.13.24	27	8.93[a]	9.90	9.90	S	1.11
CD.13.25	27	7.99[a]	9.22	9.89	S	1.24
CD.14.34	36	7.09[a]	5.95	5.45	S	0.92
CI.14.34	36	8.71	11.0	8.33	S	0.96
CI.14.36	36	6.97	8.47	7.22	S	1.04
CI.24.39	36	7.12	8.05	8.05	S	1.13
CW.10.26	30	8.45	11.0	8.69	S	1.03
	38	8.45	8.61	9.42	F	1.11
	46	8.45	7.15	6.95	F	0.97

TABLE 5. CONTINUED

Mark	Shear span a in.	Calc. shear cracking load V_{cs} kips	Calc. flexure-shear cracking load V_{cf} kips	Measured inclined cracking load V_{cm} kips	Type of crack observed d)	$\frac{V_{cm}}{V_c}$ c)
	54	8.45	6.16	6.00	F	0.97
	46	8.45	7.15	8.34	F	1.16
	38	8.45	8.61	9.42	F	1.11
	30	8.45	11.0	8.74	S	1.03
CW.10.27	30	8.48	11.0	9.50	S	1.12
	38	8.48	8.55	7.78	F	0.92
	46	8.48	7.09	6.90	F	0.97
	54	8.48	6.12	5.92	F	0.97
	46	8.48	7.09	7.30	F	1.03
CW.13.28	28	8.21	11.7	9.90	S	1.20
CW.13.38	28	7.80	11.5	8.90	S	1.14
CW.14.14	36	9.74	9.46	9.60	F	1.01
CW.14.15	36	6.01	5.87	6.25	F	1.06
CW.14.16	36	6.38	6.20	6.75	F	1.09
CW.14.17	36	6.12	5.95	5.95	F	1.00
CW.14.18	36	6.17	5.96	6.50	F	1.09
CW.14.19	36	6.12	5.96	6.94	F	1.16
CW.14.20	36	6.17	6.00	6.45	F	1.07
CW.14.21	36	5.89	5.82	6.05	F	1.04
CW.14.22	36	8.82	9.56	9.45	S	1.07
CW.14.23	36	6.07	5.92	7.40	F	1.24
CW.14.24	36	6.13	5.94	6.20	F	1.04
CW.14.25	36	9.27	9.85	10.5	F	1.13
CW.14.26	36	5.76	5.74	6.45	F	1.12
CW.14.27	36	6.22	6.37	6.11	S	0.98
CW.14.34	36	8.68	10.8	10.0	S	1.15
CW.14.35	36	7.73	8.78	6.65	S	0.86
CW.14.36	36	7.63	8.59	8.65	F	1.13
CW.14.37	36	8.68	9.34	9.40	S	1.08
CW.14.38	36	7.22	8.50	7.22	S	1.00
CW.14.39	36	7.85	8.98	9.10	S	1.16
CW.14.40	36	7.60	8.90	9.15	F	1.20
CW.14.41	36	8.22	10.7	8.89	S	1.07
CW.14.42	36	7.65	8.68	9.25	S	1.21
CW.14.45	36	7.68	8.80	8.90	S	1.16
CW.14.47	36	7.23	8.60	8.80	S	1.22
CW.14.50	36	7.11	8.71	8.15	S	1.14
CW.14.51	36	9.03	11.4	9.99	S	1.10
CW.14.54	36	8.79	10.9	10.1	S	1.15
CW.18.15	70	10.4	5.67	5.20	F	0.92
	38	10.4	9.70	9.55	F	0.98
CW.24.37	36	7.11	7.08	7.09	S	1.00
CW.28.26	70	6.38	3.08	2.88	F	0.94
	38	6.38	4.97	5.78	F	1.16
CW.28.28	70	5.95	2.99	2.83	F	0.95
	38	5.95	4.86	5.75	F	1.18
CU.14.29	36	10.1	8.97	9.72	F	1.08
CU.14.31	36	7.37	8.77	7.78	S	1.06
CU.14.32	36	7.76	8.84	7.50	S	0.97
CU.14.33	36	9.83	8.77	9.45	F	1.08
CU.14.35	36	12.1	11.1	11.4	F	1.03
CU.14.37	36	10.1	10.3	10.0	S	0.99

TABLE 5. CONTINUED

Mark	Shear span a in.	Calc. shear cracking load V_{cs} kips	Calc. flexure-shear cracking load V_{cf} kips	Measured inclined cracking load V_{cm} kips	Type of crack observed d)	$\frac{V_{cm}}{V_c}$ c)
CU.14.38	36	8.41	10.6	8.10	S	0.96
CU.14.39	36	10.9	10.8	10.8	F	1.00
FV.14.063	36	6.77[a]	12.8	6.95	S	1.03
FV.14.064	36	7.46[a]	11.7	7.78	S	1.04
FV.14.065	36	7.17[a]	13.8	8.05	S	1.12
FV.14.070	36	7.50[a]	10.4	8.33	S	1.11
FW.14.036	36	6.14	10.3	5.56	S	0.91
FW.14.063	36	5.55	13.2	6.66	S	1.20
FW.14.064	36	6.40	14.2	10.3	S	1.61
FW.14.070	36	6.94	15.0	9.71	S	1.40
FW.14.089	36	7.04	15.3	7.78	S	1.11
FW.14.091	36	6.82	17.5	7.75	S	1.14

a) Includes vertical component of prestressing force

b) No critical inclined crack developed. Ultimate shear is given

c) V_c is taken as the smaller of V_{cs} and V_{cm}

d) F indicates a flexure-shear crack
S indicates a shear crack

TABLE 6.

COMPUTED AND MEASURED CAPACITIES

Mark	Calc. shear at incl. cracking V_c kips	$rf_y bd$ kips	$V_c + rf_y bd$ V_{us} kips	Calc. shear at flex. failure V_f kips	Meas. shear at failure V_{um} kips	Failure mode b)	$\frac{V_{um}}{V_{us}}$	$\frac{V_{um}}{V_f}$
AD.14.37	9.17	-	9.17	13.3	8.52	S	0.93	-
AW.14.39	12.0	6.91	18.9	15.8	14.2	F	-	0.90
AW.14.76	10.1	6.88	17.0	13.2	11.4	F	-	0.86
AW.24.48	8.43	6.88	15.3	14.5	14.7	F	-	1.01
AW.24.68	7.13	6.92	14.1	13.0	12.4	F	-	0.95
B. 10.23	7.46	0	7.46	9.68	7.73	S	1.04	-
B. 10.24	5.94	0	5.94	7.41	7.11	S	1.20	-
B. 14.34	7.79	0	7.79	10.8	9.11	S	1.17	-
B. 14.41	8.84	0	8.84	12.9	9.84	S	1.11	-
B. 23.17	5.36	0	5.36	22.1	10.6	S	1.98	-
B. 25.18	4.29	0	4.29	14.3	5.15	S	1.20	-
BD.14.18	9.98	0	9.98	14.2	12.4	S	1.24	-
BD.14.19	10.1	0	10.1	15.1	11.4	S	1.13	-
BD.14.23	6.94	0	6.94	10.7	5.78	S	0.83	-
BD.14.26	6.92	0	6.92	10.6	6.55	S	0.95	-
BD.14.27	7.63	0	7.63	10.5	9.84	S	1.29	-
BD.14.28	8.12	0	8.12	10.5	10.2	F	-	0.97
BD.14.34	7.15	0	7.15	10.4	9.00	S	1.26	-
BD.14.35	6.60	0	6.60	10.2	6.67	S	1.01	-
BD.14.42	8.38	0	8.38	12.7	10.1	S	1.20	-
BD.24.32	6.89	0	6.89	13.5	9.16	S	1.33	-
BV.14.30	9.66	3.03	12.7	13.6	12.5	B	-	-
BV.14.32	9.07	3.40	12.5	14.1	13.0	B	-	-
BV.14.34	9.66	3.41	13.1	13.7	13.1	F	-	0.96
BV.14.35	8.75	4.42	13.2	13.7	12.8	F	-	0.93
BV.14.42	8.50	3.81	12.3	12.7	12.5	F	-	0.98
BW.10.22	6.91	1.66	8.57	8.88	8.74	S	1.02	-
BW.14.20	6.49	1.31	7.80	8.05	8.25	F	-	1.02
BW.14.22	10.4	3.03	13.4	14.1	14.1	F	-	1.00
BW.14.23	10.1	3.52	13.6	14.5	14.1	F	-	0.97
BW.14.26	7.96	2.79	10.8	11.7	11.5	T	11.06	0.98
BW.14.31	9.14	3.62	12.8	13.5	13.1	F	-	0.97
BW.14.32	7.69	1.53	9.22	10.2	10.5	F	-	1.03
BW.14.34	9.46	2.57	12.0	13.2	12.9	S	1.07	-
BW.14.38	9.20	2.56	11.8	13.2	13.2	S	1.12	-
BW.14.39	9.33	4.14	13.5	13.1	13.2	F	-	1.01
BW.14.41	9.44	3.05	12.5	12.9	12.2	F	-	0.95
BW.14.42	9.29	3.05	12.3	12.6	12.2	F	-	0.97
BW.14.43	9.24	4.88	14.1	12.6	12.6	F	-	1.00
BW.14.45	9.26	3.22	12.5	12.2	12.4	T	0.99	1.02
BW.14.58	11.6	2.44	14.0	15.6	15.3	S	1.09	-
BW.14.60	11.3	2.44	13.7	15.5	14.6	S	1.07	-
BW.15.34	7.54	2.20	9.74	10.1	9.95	F	-	0.99
BW.15.37	7.40	3.04	10.4	9.75	9.83	F	-	1.01
BW.16.38	6.81	2.17	8.98	8.57	8.68	F	-	1.01
BW.18.15	9.59	3.31	12.9	13.7	13.7	-	-	-
	6.13	1.82	7.95	7.43	7.46	S	0.94	-

TABLE 6. CONTINUED

Mark	Calc. shear at incl. cracking V_c kips	$rf_y bd$ kips	$V_c + rf_y bd$ V_{us} kips	Calc. shear at flex. failure V_f kips	Meas. shear at failure V_{um} kips	Failure mode b)	$\frac{V_{um}}{V_{us}}$	$\frac{V_{um}}{V_f}$
BW.18.27	9.70	4.89	14.6	13.6	13.6	F	-	1.00
	5.95	1.81	7.76	7.38	7.38	F	-	1.00
BW.19.28	12.0	4.89	16.9	17.3	17.3	F	-	1.00
	5.16	1.63	6.79	6.65	6.64	F	-	1.00
BW.23.18	5.10	3.07	8.17	22.1	15.0	S	1.84	-
BW.23.19	5.35	3.07	8.42	22.2	15.1	S	1.79	-
BW.23.20	5.24	6.15	11.4	22.1	14.9	S	1.31	-
BW.23.21	5.36	8.46	13.8	22.2	16.6	S	1.20	-
BW.23.22	5.37	11.23	16.6	22.2	18.5	S	1.11	-
BW.23.23	5.34	13.10	18.4	22.2	21.5	S	1.17	-
BW.23.24	5.23	15.80	21.0	22.2	23.0	F	-	1.04
BW.23.25	12.3	3.05	15.3	22.1	20.8	S	1.36	-
BW.25.19	4.44	3.09	7.53	14.3	8.30	S	1.10	-
BW.25.20	4.15	6.15	10.3	14.3	12.3	S	1.19	-
BW.25.21	4.45	8.46	12.9	14.3	14.7	F	-	1.03
BW.25.22	4.35	11.23	15.6	14.3	14.5	F	-	1.01
BW.25.23	4.32	13.10	17.4	14.3	14.4	F	-	1.01
BW.25.24	8.50	3.06	11.6	14.8	14.5	T	1.25	0.98
BW.26.21	8.08	4.20	12.3	13.8	13.2	-	-	-
	6.86	3.06	9.92	11.0	10.5	S	1.06	-
BW.28.26	5.28	3.67	8.95	9.92	10.2	T	1.14	1.03
	3.54	2.00	5.54	5.38	5.57	-	-	-
BW.28.28	5.46	3.82	9.28	9.74	10.3	F	-	1.06
	3.62	2.00	5.62	5.28	5.61	F	-	1.06
BW.29.21	11.1	12.95	24.1	20.3	20.8	-	-	-
	6.02	3.04	9.06	8.92	9.17	T	1.01	1.03
C. 10.27	7.17	0	-	10.5	5.97	S	-	-
C. 10.28	8.35	0	-	9.49	5.76	S	-	-
C. 13.23	7.21	0	7.21	15.1	10.0	S	1.39	-
CD.13.24	8.93	0	8.93	15.5	10.4	S	1.16	-
CD.13.25	7.99	0	7.99	15.3	10.7	S	1.34	-
CD.14.34	5.95	0	5.95	10.5	5.61	S	0.94	-
CI.14.34	8.71	8.83	17.5	16.5	15.7	T	0.90	0.95
CI.14.36	6.97	6.29	13.2	11.9	12.2	F	-	1.02
CI.24.39	7.12	5.01	12.1	12.3	11.8	T	0.98	0.96
CW.10.26	6.16	3.33	9.49	9.46	9.11	F	-	0.96
CW.10.27	6.12	3.32	9.44	9.45	9.26	F	-	0.98
CW.13.28	8.21	6.02	14.2	17.7	17.7	S	1.25	-
CW.13.38	7.80	8.06	15.9	16.9	16.6	F	-	0.98
CW.14.14	9.46	4.84	14.3	15.0	14.3	F	-	0.95
CW.14.15	5.87	6.30	12.2	8.22	8.16	F	-	0.99
CW.14.16	6.20	1.76	7.96	7.80	8.00	F	-	1.03
CW.14.17	5.95	1.31	7.26	8.16	7.89	S	1.09	-
CW.14.18	5.96	8.59	14.6	8.16	8.22	F	-	1.01
CW.14.19	5.96	2.65	8.61	8.11	8.25	F	-	1.02
CW.14.20	6.00	2.65	8.65	8.11	8.20	F	-	1.01
CW.14.21	5.82	1.58	7.40	8.14	8.03	T	1.08	0.99
CW.14.22	8.82	4.26	13.1	14.5	13.8	S	1.05	-
CW.14.23	5.92	1.57	7.49	8.03	7.97	S	1.06	-
CW.14.24	5.94	2.80	8.74	8.03	8.03	F	-	1.00

TABLE 6. CONTINUED

Mark	Calc. shear at incl. cracking V_c kips	$rf_y bd$ kips	$V_c + rf_y bd$ V_{us} kips	Calc. shear at flex. failure V_f kips	Meas. shear at failure V_{um} kips	Failure mode b)	$\frac{V_{um}}{V_{us}}$	$\frac{V_{um}}{V_f}$
CW.14.25	9.27	6.08	15.4	14.2	14.2	F	-	1.00
CW.14.26	5.74	3.15	8.89	7.89	8.22	F	-	1.04
CW.14.27	6.22	5.52	11.7	9.56	9.31	F	-	0.97
CW.14.34	8.68	6.63	15.3	18.1	18.2	S	1.19	-
CW.14.35	7.73	6.17	13.9	13.3	12.9	T	0.93	0.97
CW.14.36	7.63	6.50	14.1	13.3	13.4	F	-	1.01
CW.14.37	8.68	3.04	11.7	13.2	12.9	S	1.10	-
CW.14.38	7.22	4.78	12.0	13.5	13.5	S	1.12	-
CW.14.39	7.85	2.58	10.4	12.9	10.9	S	1.05	-
CW.14.40	7.60	9.37	17.0	12.9	13.1	F	-	1.01
CW.14.41	8.22	6.01	14.2	15.9	14.5	S	1.02	-
CW.14.42	7.65	5.08	12.7	12.5	12.9	F	-	1.03
CW.14.45	7.68	6.09	13.8	12.2	11.7	F	-	0.96
CW.14.47	7.23	4.15	11.4	12.0	12.0	S	1.05	-
CW.14.50	7.11	5.41	12.5	11.7	12.1	S	0.97	-
CW.14.51	9.03	2.98	12.0	15.7	12.9	S	1.07	-
CW.14.54	8.79	2.99	11.8	15.5	13.4	S	1.13	-
CW.18.15	9.70	4.87	14.6	13.4	13.7	F	-	1.02
	5.67	2.65	8.32	7.27	7.46	F	-	1.02
CW.24.37	7.08	3.53	10.6	14.2	12.1	S	1.14	-
CW.28.26	4.97	4.56	9.53	9.71	9.83	T	1.03	1.01
	3.08	2.41	5.49	5.27	5.35	-	-	-
CW.28.28	4.86	4.70	9.56	9.68	10.3	F	-	1.06
	2.99	2.50	5.49	5.26	5.62	F	-	1.06
CU.14.29	8.97	2.10[a]	11.1	13.6	13.4	T	1.21	0.98
CU.14.31	7.37	6.03	13.4	13.0	13.0	S	0.97	-
CU.14.32	7.76	6.02	13.8	13.0	10.2	S	0.77	-
CU.14.33	8.77	2.10[a]	10.9	12.7	13.0	T	1.19	1.02
CU.14.35	11.1	0.79[a]	11.9	17.3	15.2	F	-	0.88
CU.14.37	10.1	3.40[a]	13.5	15.5	13.2	S	0.98	-
CU.14.38	8.41	6.05	14.5	15.3	11.5	S	0.79	-
CU.14.39	10.8	2.09[a]	12.9	14.9	14.7	T	1.14	0.99
FV.14.063	6.77	10.53	17.3	20.4	20.1	S	1.16	-
FV.14.064	7.46	8.48	15.9	20.4	20.0	F	-	0.98
FV.14.065	7.17	9.41	16.6	20.3	19.6	F	-	0.97
FV.14.070	7.50	7.69	15.2	20.2	16.3	T	1.07	0.81
FW.14.036	6.14	6.68	12.8	13.7	14.2	F	-	1.04
FW.14.063	5.55	11.12	16.7	20.1	22.0	F	-	1.09
FW.14.064	6.40	7.38	13.8	20.6	18.2	S	1.32	-
FW.14.070	6.94	9.85	16.8	20.6	19.7	F	-	0.96
FW.14.089	7.04	12.65	19.7	25.7	25.8	S	1.31	-
FW.14.091	6.82	13.19	20.0	24.8	22.2	S	1.11	-

a) The difference between the yield stress and the effective prestress in the stirrups is used for f_y

b) S refers to a shear failure
F refers to a flexural failure
T refers to a transition failure
B refers to a bond failure

This page is intentionally blank.

cracks developed in all three beams, but the effect of these cracks were different. Large strain concentrations were measured at the top of the inclined crack in the two beams with light web reinforcement. Both these beams failed in shear. The web reinforcement in the third beam was sufficient to restrain the opening of the inclined crack and the measured strain concentrations were therefore much smaller. As a result, this beam reached its full flexural capacity.

The same trend can be seen in Figure 27 which shows the concrete strain at the load point versus the steel strain at midspan for the same three beams. The deviation of the curves for CW.14.37 and CW.14.39 from the curve for CW.14.40 then shows that the insufficiently restrained inclined crack caused higher strains in the compression zone than would be deduced from the assumption of a linear strain distribution over the depth of the beam.

The overall effect of web reinforcement is illustrated by the load-deflection curves in Figure 28. It must be admitted that these beams are extreme cases since the prestress is zero. It was chosen so as to make the difference between the flexural capacity and the capacity of the beam without web reinforcement as large as possible. It was then possible to obtain a shear failure with a fairly large range of rf_y values.

It appears from Figure 28 that the inclined cracking load increases slightly with the amount of web reinforcement. The trend, however, is not consistent. The determination of the inclined cracking load for these beams was extremely difficult since no abrupt change in behavior was associated with it. Therefore, it seems justified to neglect any effect of the web reinforcement on inclined cracking.

The ultimate load as well as the ultimate deflection increased almost linearly with rf_y until sufficient web reinforcement was provided to develop a flexural failure.

3.4 FAILURE MODES

The types of failure observed during this investigation can be classified in three groups:

(1) flexural failure

(2) shear-compression failure

(3) web-distress failure

A beam was said to have failed in flexure if it failed by crushing of the concrete or fracture of the longitudinal reinforcement as a result of bending stresses (Figure 29a). The concrete strains at failure were nearly uniform in the constant moment region and no serious strain concentrations were observed as a result of inclined cracks.

A shear-compression failure was said to have occurred if the beam failed by crushing of the concrete at or near the top of an inclined crack. Figure 29b shows such a failure. In beams with an insufficient amount of web reinforcement, this type of failure was always accompanied by large concentrations of strains at the top of the inclined crack. Usually the ultimate load was considerably higher than the inclined cracking load, or for beams with web reinforcement, higher than the load at which yielding of the stirrups took place. In beams with high longitudinal reinforcement ratio or a high concrete strength, the failure was often very violent but in most other cases the shear-compression failure was relatively gentle.

Figure 29c shows a beam which failed by web distress. This type of failure was chiefly observed in I-beams where it might follow immediately after the formation of an inclined crack or, in beams with web rein-

forcement, right after yielding of the stirrups.

In Reference 1, Section 23 it was described that a fully developed inclined crack transformed a beam without web reinforcement into a tied arch with a thrust line which was essentially a straight line between the load point and the support. This structure could fail if the connection between the arch and the tie was destroyed or if the thrust could not be resisted by the rib of the arch. In beams without web reinforcement it was possible to distinguish between three categories of web distress failures: secondary inclined tension cracking, separation of the tension flange from the web, and web crushing. The two former categories describe to a certain extent the cause of failure while the last merely reflects an effect of the failure.

The same classification was not possible for beams with web reinforcement. Separation of the tension flange from the web was never observed to an extent that made this phenomenon the direct cause of failure. The stirrups restrained the widening of inclined cracks with the result that the load could be increased and new cracks developed. No distinction could therefore be made between secondary inclined tension cracking failure and web-crushing failure.

Web-distress failures were explosive. In some cases a vertical crack was observed immediately before failure in the compression zone between the support and the center of the shear span but otherwise there was little warning. The existence of tensile stresses in the top flange as a result of arch action was confirmed by measurements of the concrete strains along the shear span. Curve D in Figure 10 shows a typical result of such measurements. The compressive strain at D increased until the formation of the inclined crack. As the load was increased further, the strain decreased and finally reversed its sign.

It was mentioned earlier that web distress failures were observed mainly in beams with thin webs and high prestressing forces. Under such conditions, the thrust in the tied arch would become large and it would often act with a large eccentricity with respect to the centroid of the effective section of the arch. In several cases, it was observed that an increase in the amount of web reinforcement could increase the stability of the thrust. Thus a web-distress failure could be avoided and the beam would instead fail in shear-compression because of concentration of strains close to the load point. Finally, as the amount of web reinforcement was further increased, the restraint on the opening of the inclined cracks could become effective enough to prevent a strain concentration and the beam could develop its full flexural capacity. An example of this sequence is shown in the photographs in Figure 29. The distribution of concrete strains for these three beams was given in Figure 26.

Web-distress failures were also observed in a few beams with 3-inch webs and with no prestress. Photographs of these beams, taken shortly before failure, are shown in Figure 22. Although beam B.25.18 had no web reinforcement, it appears that the ability of the longitudinal reinforcement to transfer at least part of the shear across the inclined crack enables the beam to carry the load mainly by beam action until close to failure. As the doweling force began to cause cracks along the longitudinal reinforcement, the beam was transformed gradually into a tied arch. At this stage, cracks with fairly steep inclinations had developed in a large portion of the shear span. The thrust was therefore forced to act with a large eccentricity which resulted in a sudden and violent web-distress

failure (Figure 30a).

In beam BW.25.19 a small amount of web reinforcement was used. Until yielding of the stirrups occurred, the effect of the web reinforcement was to delay the transformation from beam action to the tied-arch action. Soon after yielding of the stirrups the transformation took place and again the result was a web-distress failure.

A characteristic feature of a web-distress failure is illustrated in Figure 31 which shows plots of deformation between the flanges versus the load for three of the beams shown in Figure 30. These curves may be compared with the curves in Figure 24 which relate to beams with the same section properties but a shorter shear span. From Figure 31 it is seen that beam B.25.18 failed at a rather small deformation between the flanges indicating instability. Beam BW.25.19 failed soon after yielding of the stirrups (Figure 30b) but for an ultimate deformation which was still much smaller than for the comparable beam with the short shear span.

In beam BW.25.20 a sufficient amount of web reinforcement was provided to keep the tied arch stable at deformations considerably higher than those corresponding to yielding of the stirrups. The failure mechanism for this beam (Figure 30c) contains elements of both web-distress and shear-compression failures. However, the large ultimate deformation between the flanges indicates a shear-compression failure caused by a strain concentration at the load point. The web reinforcement in beam BW.25.21 was sufficient to develop the full flexural capacity (Figure 30d).

Shear failure in a beam with web reinforcement may thus develop either as a web-distress or a shear-compression failure. If a beam without web reinforcement fails by web distress, it furthermore appears that the addition of more and more web reinforcement will change the failure mode first to a shear-compression failure and then to a flexural failure.

• • •

IV. INCLINED CRACKING LOAD

In the discussion of the behavior of prestressed beams, it was demonstrated how an inclined crack could transform a beam without web reinforcement into a structure which carries the load in a manner similar to a tied arch. Although the beam without web reinforcement has been observed in some cases to sustain a considerable increase in load after inclined cracking, its behavior is modified so drastically that the inclined cracking load rather than the maximum load attained should be considered as the useful capacity of the beam. This is especially true for beams which fail by web distress since the formation of an inclined crack in such a beam usually leads to collapse with only a slight increase in load. Therefore, the quantitative prediction of this load is essential.

In the following two sections, analytical expressions are derived for the loads corresponding to shear and flexure-shear cracks.

4.1 SHEAR CRACKS

A shear crack was defined as an inclined crack which occurs in the web before flexural cracking in its vicinity (Figure 8c). The qualitative observations pertaining to the formation of a shear crack suggested that the corresponding load relates to the principal tensile stress in the web. Since the part of the beam under consideration is uncracked, the principal tensile stress at any given point may be found with sufficient accuracy by the conventional methods of strength of materials:

$$\sigma_\theta = \frac{\sigma_x + \sigma_y}{2} + \sqrt{\tau^2 + \left(\frac{\sigma_x - \sigma_y}{2}\right)^2} \qquad (3)$$

where

σ_θ = principal stress
σ_x = the normal longitudinal stress
σ_y = the normal transverse stress
τ = the shearing stress

Tensile stresses are defined as positive. The term σ_x involves stresses caused by prestress, dead load, and live load. At shear cracking this term may be expressed as

$$\sigma_x = -\frac{F_{se}}{A_c} - \frac{F_{se}\, ey}{I} + \frac{M_D\, y}{I} + \frac{(V_{cs} - V_D)\,\frac{M}{V}\, y_t}{I_t}$$

where

F_{se} = effective prestressing force
A_c = area of prestressed concrete section
e = eccentricity of prestressing force with respect to elastic centroid of prestressed section (positive downwards)
y = distance from centroid of prestressed section to point considered (positive downwards)
I = moment of inertia of prestressed section
y_t = distance from centroid of total section (section including cast-in-place slab) to point considered (positive downwards)

I_t = moment of inertia of total section
M_D = dead load moment at section considered
V_D = dead load shear at section considered
V_{cs} = total shear at shear cracking
M/V = ratio of live load moment to shear at section considered

The term σ_y includes stresses from a vertical prestress (e.g., prestressed stirrups) and bearing stresses acting near loads and reactions. The region in which the bearing stresses are significant extends, according to an elastic analysis, about 0.75h on either side of the load point. In beams with shear spans shorter than 1.5h the bearing stresses will affect the principal tensile stresses in the region where the shear crack may develop. However, in beams of practical proportions, with shear spans longer than twice the depth of the beam, the bearing stresses will have little or no influence on the stresses causing shear cracking.

The shearing stress τ at shear cracking may be found from the expression:

$$\tau = \frac{V_D Q}{I b'} + \frac{(V_{cs} - V_D)Q_t}{I_t b'} \qquad (5)$$

where Q = first moment of area beyond point considered with respect to centroid of prestressed section
Q_t = first moment of area beyond point considered with respect to centroid of total section
b' = width of web at point considered

The total shear, V_{cs}, may be modified to take into account the effect of draped reinforcement. As long as the drape angle is small, the prestressing force on a section of the beam may be considered as the resultant of a force normal to the section with the same magnitude as the prestressing force and a shear force in the plane of the section. This shear force will counteract the shear from the dead load and applied load so that the effect of draped reinforcement can be found by using in Equations 4 and 5:

$$V_{cs} = V' - F_{se} \sin \Phi \qquad (6)$$

where V' = shear corresponding to dead load and applied load
Φ = drape angle, angle between the longitudinal axis of the beam, and the resulting prestressing force

With the aid of Equations 3 through 6, the principal tensile stress at any point in the beam may be determined. If it is assumed that the initiation of the shear crack is a stress problem only, it follows that the shear crack will form when the largest principal tensile stress exceeds the tensile strength of the concrete. The process of determining the point at which this maximum stress exists is very tedious because of the changing combinations of shearing and flexural stresses. In an attempt to simplify the procedure a study was made of the beams, reported here and in Reference 1, in which shear cracks developed. The principal tensile stress was calculated at points along the trajectory of the actual shear cracks. For the I-beams these computations showed that the ratio at inclined cracking between the maximum principal tensile stress and the principal tensile stress at the centroid was close to unity. In 20 of the 30 beams the maximum stress actually occurred at the centroid while the ratio in the remaining cases varied between 1.00 and 1.23. The maximum tensile stress in these ten beams occurred at points below the centroid. At the same time, however, the properties of the beams were such that a flexure crack became more and more likely to develop concurrently with the shear crack. The few beams with a high ratio between the maximum tensile stress and the principal tensile stress at the centroid thus represent a transition region between shear cracking and flexure-shear cracking. Shear cracking

in I-beams may, therefore, be predicted with sufficient accuracy on the basis of the principal tensile stress at the centroid.

The composite beams consisted of a precast, prestressed I-beam and a cast-in-place slab which was added after the prestress was released. The centroid of the total section was in the flange of the precast I-beam. If a shear crack developed in a composite beam, it was always observed first at the junction between the web and the flange. The distance from the load point to the top of the shear crack was nearly the same as the distance from the top of the beam to the top of the web. Hence, it was assumed that the maximum tensile stress at shear cracking would occur at the point in the web closest to the centroid along a line passing through the top of the beam at the load point and forming a 45° angle with the longitudinal axis.

With these simplifying assumptions, it is possible to determine the maximum tensile stress in the web for a given load. And if the tensile strength f_t of the concrete is known, the shear V_{cs} at which the shear crack develops can be obtained. For I-beams, the expression for V_{cs} reduces to:

$$V_{cs} = \frac{Ib'f_t}{Q}\sqrt{\left(1 + \frac{F_{se}}{A_c f_t}\right)\left(1 - \frac{\sigma_y}{f_t}\right)} \qquad (7)$$

where f_t = tensile strength of concrete.

The corresponding expression for a composite section reduces to (neglecting the term σ_y):

$$V_{cs} = \frac{I_t b'}{Q_t}\left[f_t\sqrt{1 - \frac{\sigma_x}{f_t} - V_D\frac{Q}{I\,b'}}\right] + V_D \qquad (8)$$

where σ_x is found from Equation 4. If the centroid of the composite section is in the web, the last term in Equation 4 is equal to zero and V_{cs} can be determined directly. If the centroid of the composite section is in the flange, V_{cs} enters in both Equation 4 and Equation 8 and a solution is obtained readily by a trial-and-error procedure.

It appears that the state of stress leading to a shear crack in the web is best simulated by the cylinder splitting-test. Consequently, in all calculations pertaining to a shear crack, it was decided to use the tensile strength determined from Equation 2 (Figure 2):

$$f_t = 5\sqrt{f'_c} \qquad (2)$$

The shears required to produce a shear crack according to Equations 2 through 8 are listed in Table 5. The correlation with test results will be discussed in Section 4.3.

4.2 FLEXURE-SHEAR CRACKS

The second type of inclined crack was always observed in connection with a flexure crack developing between the load point and the support. If the principal tensile stresses in the web at this stage of the loading was high, the stress redistribution caused by the formation of the flexure crack was often such that an inclined crack could develop for a slight increase in load. In other cases, depending on the properties of the beam, the load at inclined cracking could be much greater than the load at which the critical flexure crack formed.

The position of the critical flexure crack was found to depend on the properties of the beam. Its distance from the load point ranged from approximately one-half the height of the beam to about one-third the shear span. The distance was generally small when the load causing the critical flexure crack approached the computed load at shear cracking and it increased as the difference between these loads increased.

Determination of the stresses in a beam

in the vicinity of a crack is rather involved and especially sensitive to the assumptions necessary to describe the conditions at the top of the crack. In view of the scatter in the test data and the sensitivity of the results of an "exact" analysis to the assumptions that have to be made, determination of the flexure-shear cracking load on the basis of an "exact" stress analysis of the cracked web is not justified.

On the other hand, it can be stated on the basis of the observations that the flexure-shear cracking load is larger than the load which produces the critical flexure crack. The horizontal projection of the crack must be longer than the depth of the beam for the inclined crack to have a significant effect on the behavior. A flexure crack in the shear span at a distance closer than d/2 from the load point should not affect the tensile stresses along a potential trajectory for an inclined crack. Therefore, flexural cracking at a distance d/2 in the direction of decreasing moment from the section considered may be assumed as being critical. For the test beams, the dead load was small compared with the live load and the total shear at the formation of the critical flexural crack may be expressed as follows:

$$V = \frac{M_{cr}}{\frac{M}{V} - \frac{d}{2}} \qquad (9)$$

where M_{cr} is the flexural cracking moment for a section located a distance d/2 from the point considered in direction of decreasing moment.

The additional shear required to form the inclined crack can be evaluated from the test results. Figures 32 and 33 show non-dimensional plots of the measured total shear at inclined cracking versus the calculated total shear at the formation of the critical flexure crack. A sufficiently accurate representation of the test data was obtained by the expression:

$$V_{cf} = \frac{M_{cr}}{\frac{M}{V} - \frac{d}{2}} + b'd\sqrt{f'_c} \qquad (10)$$

The cracking moment M_{cr} was computed using Equation 1 for the modulus of rupture and the moment of inertia was based on plain concrete section. Computed as well as measured values of the flexure-shear cracking load are listed in Table 5. The correlation will be discussed in Section 4.3.

The dead load for beams of practical proportions is usually comparable to the live load. To avoid the ambiguity of the moment-shear ratio in Equations 9 and 10, the dead-load shear and the live-load shear may be separated. Equation 10 then becomes:

$$V_{cf} = \frac{M'_{cr}}{\frac{M}{V} - \frac{d}{2}} + V_D + b'd\sqrt{f'_c} \qquad (11)$$

where M'_{cr} is the cracking moment available to resist live load and M/V is the moment-shear ratio corresponding to live load alone.

4.3 COMPARISON BETWEEN COMPUTED AND MEASURED INCLINED CRACKING LOADS

Computed and measured inclined cracking loads and the type of the inclined cracks observed are given in Table 5. For each beam, the calculated inclined cracking loads corresponding to both a shear crack and a flexure-shear crack are listed. The smaller of these loads indicates the predicted value as well as the expected type of inclined crack.

Inclined cracks developed in 127 beams. In 122 of these beams, the predicted type of crack agreed with that observed.

A total of 42 beams developed shear cracks. The average ratio of measured to predicted cracking loads was 1.10 with a standard deviation of 0.12. The average ratio as well as the mean deviation for the composite beams

were larger than for the remaining beams. A possible reason for this difference may be the presence of differential shrinkage stresses in the composite beams. The shrinkage in the slab of these beams acts as an additional prestressing force introducing compressive stresses at the junction between the flanges and the web. Assuming a differential shrinkage strain in the flange of 0.0001, the increase in the calculated shear cracking load would be about 10 per cent. However, since the shrinkage strain may vary considerably from beam to beam, it was neglected in the calculations.

Flexure-shear cracks were observed in 87 beams (2 beams with moving loads developed both shear and flexure-shear cracks). The average ratio of measured to computed cracking loads was 1.10 and the standard deviation was 0.087.

It should be noted that the last term in Equation 10 includes only a few of the variables which may affect the shear carried after the critical flexural crack has developed. However, in beams with medium or high levels of prestress, the term in Equation 10 containing the flexural cracking moment is predominant and the second term is relatively unimportant. This probably accounts for the good agreement between computed and measured inclined cracking loads in beams with a reasonably high prestress. In beams without prestress, the flexural cracking moment is small and the last term in Equation 10 becomes important. The simplifications made in this term may thus result in a less accurate prediction of the inclined cracking load. Consequently, Equation 10 is not directly applicable to ordinary reinforced concrete members.

● ● ●

V. ULTIMATE LOAD

The shear failures observed in the tests were classified as web-distress failures or shear-compression failures. The following two sections describe qualitatively how an analysis of the ultimate load may be developed on the basis of the observed failure mechanisms. It should be pointed out that such an analysis has little practical value. It is mentioned here for the purpose of describing more fully the failure mechanisms and the factors affecting shear. This was deemed very important considering that the simplified design procedure developed in Section 5.4 usually has been associated with a completely different failure mechanism.

5.1 WEB-DISTRESS FAILURES

This mode of failure is essentially a result of arch action in the beam, and questions therefore arise as to the geometry of the arch and the location of the thrust at each section along the shear span. Idealized crack patterns for three beams shortly before failure are shown in Figure 34. It is evident that a considerable loss of shear flow has taken place in all three beams along a large part of the shear span so that at least some arch action must be present. The actual loss of shear flow, however, is difficult to determine since part of the shear may still be transferred across the inclined crack by doweling in the longitudinal reinforcement or by the web reinforcement. Since the thrust line is determined by the loss of shear flow, its position is also uncertain. The actual geometry of the arch is extremely difficult to predict since it depends on the development of cracks.

If total loss of shear flow is assumed in the three cases shown in Figure 34, the thrust line would be a straight line between the load point and the reaction. Such a line would fall outside the rib of the arch in case (a), in fact, this beam would fail before the shear flow within the beam was completely lost. In cases (b) and (c) the thrust line falls inside the rib, but it may have a large eccentricity with respect to the centroid of the rib as in case (b). An interaction diagram between axial load and bending moment could then be constructed for the critical section of the arch. The effect of stirrups on such a diagram is twofold: the thrust line is raised reducing the eccentricity, and the magnitude of the thrust is decreased as a result of the shear flow through the stirrups.

The eccentricity of the thrust in case (b) is so large that failure is likely to be initiated by high tensile stresses in the top flange at point A. This failure would be called web-distress. The thrust in case (c) may be resisted by the arch so that a web-distress failure becomes unlikely. The same situation could arise in cases (a) and (b) if sufficient web reinforcement was provided. A shear-compression failure is then the most

likely result.

5.2 SHEAR-COMPRESSION FAILURES

The conditions at ultimate for a shear-compression failure were observed to be essentially similar to those for a flexural failure. The analysis of the strength of beams failing in shear-compression could, therefore, be carried out in a manner similar to the analysis of flexural strength.

In the case of pure flexure, it is usually assumed that strains are distributed linearly over the entire cross section at any stage of the loading. An analysis based on this assumption gives sufficiently accurate results for sections subjected to pure flexure, since the assumption with respect to distribution of strains over such a section is in good agreement with measurements. Furthermore, the flexural strength of a moderately reinforced concrete section is rather insensitive to small deviations from the assumed linear strain distribution. Measurements show that the strain distribution in a region subjected to combined bending and shear is nearly linear up to inclined cracking. However, as the load is increased further, the concrete strains tend to concentrate at the top of the inclined crack (Figure 10) because an angle change in the compression zone takes place over a very short distance, while the corresponding deformations in the reinforcement is distributed over a distance equal at least to the horizontal projection of the inclined crack at the level of the steel. The beam thus undergoes two stages of behavior governed by two different relations between strains in steel and concrete. Referring to Figure 35 these compatibility equations may be written as

$$\epsilon_{sc} = F_1 \epsilon_{cc} \left[\frac{1 - k_c}{k_c} \right] + \epsilon_{ce} + \epsilon_{se} \qquad (12)$$

$$\epsilon_{su} = \epsilon_{sc} + F_2 (\epsilon_u - \epsilon_{cc}) \left[\frac{1-k_u}{k_u} \right] \qquad (13)$$

where the compatibility factors F_1 and F_2 express the relation between the concrete strain in the top fiber and the steel strain at a section through the top of the inclined crack. If F_1 and F_2 are set equal to unity, Equations 12 and 13 become familiar expressions corresponding to a linear strain distribution over the section.

The equilibrium conditions for this section can be written in the same way as for a section unaffected by the inclined crack:

$$pbdf_{su} = bk_u df_{cu} \quad \text{or}$$

$$k_u = \frac{pf_{su}}{f_{cu}} \qquad (14)$$

and

$$M_u = A_s f_{su} d(1-k_2 k_u) \qquad (15)$$

Equations 12 through 15 can be solved to yield the strength of the beam, if F_1, F_2, k_c, f_{cu}, ϵ_{cc}, and ϵ_u are assumed or known.

Such an analysis was used for beams without web reinforcement in Reference 1 where the necessary assumptions and the sensitivity of the analysis to these assumptions were discussed in detail. For the purpose of this report it is sufficient to note that the analysis of the ultimate load for a beam failing in shear-compression with the assumptions made becomes identical to the computation of the flexural capacity, except that a compatibility factor smaller than unity is used after inclined cracking. Thus, for both the flexural and shear-compression analyses, the failure criterion is that the ultimate load is reached when the strain in the extreme fiber of the compression zone exceeds a limiting value.

How the shear-compression analysis as defined in Reference 1 can be modified to incorporate the effect of web reinforcement is illustrated with the help of the curves shown in Figure 36. The curves in this figure idealize the relationships between concrete and steel strains as indicated for three similar beams with different amounts of web reinforcement. Curve A refers to a flexural failure where the ratio between concrete and steel strain is nearly constant from flexural cracking to failure. This ratio corresponds to an almost fixed position of the neutral axis and a compatibility factor close to unity. Curve B refers to a shear failure in a beam with no web reinforcement and Curve C to a beam with some web reinforcement although not enough to develop the flexural capacity. All three beams behave in the same manner up to inclined cracking. For higher loads the amount of web reinforcement has a marked influence on the strain relationship. The inclined crack is effectively restrained against opening as long as the stress in the stirrups is in the elastic range. Curve C will therefore be close to Curve A between points corresponding to inclined cracking and yielding of the web reinforcement. Beyond this point the beam with intermediate amount of web reinforcement behaves in a manner similar to the beam without web reinforcement. Since yielding of all the stirrups crossed by the inclined crack is a gradual process, Curve C should have a smooth transition as indicated by the broken line. However, the strain relation may be thought of as having a compatibility factor equal to unity up to yielding of the web reinforcement thus replacing the broken line with two straight lines.

It is interesting to consider the result of a dogmatic application of the shear-compression analysis to two identical beams loaded to have different lengths of shear span. If the inclined crack develops as a flexure-shear crack, the corresponding moment (Equation 10) and hence the steel strain at inclined cracking would be nearly the same in the two cases. There is no significant change in the relationship between the critical concrete and steel strains until the web reinforcement yields. Again on the basis of the shear-compression analysis, the yielding of the web reinforcement is influenced primarily by the moment. Consequently, the web reinforcement should yield in both beams at the same moment. Curve C in Figure 36 could thus represent the relation between steel and concrete strains in both beams. This implies that the increase in steel strain and, therefore, the increase in moment caused by the stirrups should be independent of the length of the shear span. Accordingly, the increase in shear capacity provided by a certain amount of stirrups should be inversely proportional to the a/d ratio.

It is difficult to conduct tests which conclusively support or repudiate this inference. Experimental scatter and the possibility of having different failure modes are the principal sources of these difficulties. The test results presented in Figure 37 reflect both sources. However, certain trends may be observed.

Figure 37 shows the influence of web reinforcement on the load at ultimate and at yielding of the stirrups. Each part of the figure represents a series of beams with constant length of shear span: 30 inches or 45 inches. All the beams had similar properties except that the amount of web reinforcement for each shear span was varied from zero to an amount sufficient to develop the flexural capacity of the beam.

Yielding of the stirrups was said to have occurred when an average strain between

the flanges of 0.0015 was measured along a length of the shear span equal to the effective depth of the beam. The corresponding load increased linearly with the amount of web reinforcement. Furthermore, the rate of increase was nearly inversely proportional to the length of the shear span. It should be noted that yielding of the stirrups is a matter of definition. If another criterion is used, the load at yielding will change for a beam with a large amount of web reinforcement but stay almost constant for a beam with a small amount of stirrups (Figure 24). The slope of the broken lines would thus change but it appears that the ratio between the slopes corresponding to 30-inch and 45-inch shear span is almost constant as long as a reasonable and consistent definition of yielding in the stirrups is used. Thus, the measured yield loads seem to agree with the results from the shear-compression analysis.

A similar comparison between predicted and measured ultimate loads is not possible since beams B.25.18 and BW.25.19 failed by web distress (Figure 31).

It is rather obvious that a shear-compression analysis as outlined here is of little value in design. However, the analysis provides a better understanding of the failure mechansim, and hence may serve as a good basis for a simplified analysis. The following section describes in detail the development of a design criterion and discusses its limitations.

5.3 BASIC DESIGN CONSIDERATIONS

Design of beams without web reinforcement is usually based on the inclined cracking load as the useful shear capacity of the beam rather than the ultimate load, although the ultimate load may be as high as twice the inclined cracking load in some cases. This is a reasonable approach for two reasons. The mode of failure in shear is difficult to predict and, even if this obstacle could be removed, the corresponding failure load cannot be found with certainty. Furthermore, the behavior of the beam after inclined cracking is often so poor that the beam has lost its usefulness as a structural member.

A similar argument is true to a certain extent for beams with web reinforcement as long as the beam still fails in shear. Once the web reinforcement in a beam yields, the crack propagation can take place without much restraint. The behavior of such a beam after the web reinforcement has started to yield is very similar to the behavior after inclined cracking of a beam without web reinforcement. To be consistent with the design of beams without web reinforcement, it might be suggested that the load at which the stirrups yield be considered as the useful capacity of a beam with web reinforcement.

The same conclusion could be arrived at by a slightly different approach. Figure 36 shows that yielding of the stirrups before the flexural capacity is reached means in principle that the ultimate steel strain and therefore the deflection at failure will be smaller than expected for a flexural failure. If the longitudinal reinforcement ratio is fairly small it is possible to have a significant reduction in ultimate strain with only a few per cent decrease in ultimate steel stress and thus in failure load.

The ductility of a member is of prime importance in many structures and will probably be so more and more with the increased use of limit design. The design procedure must ensure that the necessary load capacity as well as a reasonable ductility can be obtained. The last requirement, however, can only be satisfied if the ultimate steel strain

is at least nearly as high as it would be expected for a flexural failure. In some cases the proportions of a section are determined on the basis of service load conditions. The factor of safety against a flexural failure is then higher than required. To ensure a ductile failure of this member, it is necessary to provide at least the same factor of safety against a shear failure as the actual design provides against a flexural failure.

On the basis of a ductility requirement, it might be desirable to limit the useful capacity of a beam with web reinforcement to the load at which the stirrups yield. However, as the amount of web reinforcement is increased up to that which is needed to prevent a shear failure, the load at yielding of the stirrups loses some of its significance. As mentioned before, this yielding occurs gradually and the corresponding load for beams with a large amount of web reinforcement is sensitive to the definition of yielding. The available test results also seem to indicate that this sensitivity is reflected in the strain relationship (Figure 36). Apparently, the change in compatibility factor at yielding of the stirrups decreased as the amount of web reinforcement was increased. The upper part of a Curve C' in Figure 36 corresponding to a beam with a large amount of web reinforcement may have a slope only slightly different from Curve A, although the stirrups may have yielded before the flexural capacity was reached.

The gradual yielding of the stirrups is a possible physical explanation of this behavior. However, at least one other factor seems to be important. Even in a beam with an amount of web reinforcement much larger than needed to prevent a shear failure, it is possible that at least some stirrups will yield when the stress in the longitudinal steel exceeds the proportional limit. The cracks will then open much more rapidly. If these cracks have any inclination at all, which is almost always the case in a region subjected to combined bending and shear, their opening will result in an increase in the distance between the flanges and therefore a strain in the stirrups. An indication of this effect is provided in Figure 37b which shows that an increase in rf_y from 176 to 206 in this particular case has almost no effect on the load at which the stirrups yielded.

To recapitulate, it can be said that (1) a member should be designed to fail in flexure, (2) if the inclined cracking load is smaller than the flexural capacity, web reinforcement must be provided to ensure both flexural strength and ductility, (3) available test results show reasonably well how much web reinforcement is needed to develop the flexural strength, and (4) to provide the ductility corresponding to a flexural failure, it may be necessary to use more web reinforcement than would be required in order to develop the flexural strength.

5.4 A DESIGN EXPRESSION

A hypothesis for the mechanism of the action of web reinforcement was discussed in Section 5.2. Ideally, it would be desirable to formulate a design procedure on the basis of that mechanism. On the other hand, it is necessary that the design procedure be no more complicated than would be justified by the certainty of the theory and the economy of the end results. Consequently, the "deus ex machina" contained in the following expression, which has been used successfully in design as well as in analysis of test results for a long time, should be examined

in the light of the hypothesis presented in this report.

$$V_u = V_c + rf_y bd \qquad (16)$$

Equation 16 has been justified on the basis of diverse reasoning in essentially the form shown above but with different definitions of V_c. It should be emphasized that this equation is used here strictly as an expression to determine the amount of web reinforcement which is needed to prevent a shear failure. The equation should not be expected to predict the ultimate load corresponding to a shear failure in a beam with any given amount of web reinforcement, although it will be shown that in most practical cases, Equation 16 will indicate a lower bound to this quantity. Thus, the lines in Figure 37 corresponding to Equation 16 are drawn only for the purpose of comparing the design criterion with the effect of the major variables on the test results.

Figure 37a shows that the slope of the line representing the design equation may be greater than the rate of increase in the ultimate load for a shear failure. This is generally true when failure occurs in shear-compression. If beams with small amounts of web reinforcement fail by web distress (Figure 37b), the rate of increase in failure load with an increase in rf_y will be larger because of the change in failure mode from a web-distress to a shear-compression failure. As mentioned in Chapter III, a transition region of shear-compression failures will always separate ranges of rf_y in which web-distress and flexural failures are obtained. The mechanism of web-distress failures may be ignored in considerations related to design.

From Figure 37a, it is seen that the line representing Equation 16 is steeper than the lines referring to yielding of the stirrups and to ultimate load. This raises the questions as to whether the difference between the flexural capacity V_f and the inclined cracking load V_c can be large enough so that the amount of web reinforcement required by Equation 16 may be too small to ensure a flexural failure. In terms of the difference between V_f and V_c, the beams referred to in Figure 37 are extreme cases since they are not prestressed. In fact, the main consideration in the design of these beams was to make the difference between the flexural capacity and the inclined cracking load as large as possible in order to obtain shear failures with a large range of rf_y. Even for this extreme condition, Equation 16 yields an amount of web reinforcement large enough to develop the flexural strength. The primary reason for this was that the beams with high values of rf_y failing in shear-compression were able to support loads significantly higher than that at which the stirrups started to yield. A shear-compression failure is always associated with large deformations between the flanges. Since these deformations can take place only in connection with a considerable increase in load, it is reasonable to expect that a relatively large difference between loads at ultimate and at yielding of the stirrups is a general feature of shear-compression failures in beams with high rf_y. The magnitude of this additional capacity compared with the difference between the flexural capacity and the inclined cracking load determines the degree of conservatism involved in using Equation 16. The smaller the difference between V_f and V_c, the more conservative is the amount of web reinforcement required by Equation 16.

The shear-compression approach described

in Section 5.2 leads to the conclusion that the effectiveness of the stirrups may decrease as the length of the shear span increases. This is not directly reflected in Equation 16. The increase in the length of the shear span automatically decreases the difference between the flexural capacity and the inclined cracking load. Consequently, Equation 16 requires a smaller number of stirrups. However, if the change in length of the shear span results in inversely proportional changes of all ordinates in a diagram similar to Figure 37, the amount of web reinforcement needed to obtain a flexural failure would be independent of the shear span. This is possible only if the inclined crack develops as a flexure-shear crack and if the first term in Equation 10 is predominant. A beam with such properties will have a relatively small difference between flexural capacity and inclined cracking load. Since this is the condition for which Equation 16 is most conservative, the discrepancy between the shear-compression theory and the design approach seems unimportant.

On the other hand, if the difference between V_f and V_c is large, an increase in the length of the shear span will only cause minor changes in the inclined cracking load and in the additional capacity available after yielding of the stirrups. Only the flexural capacity and the slope of the line in Figure 37 corresponding to ultimate will be affected appreciably. The necessary amount of web reinforcement determined from a diagram similar to Figure 37 will thus decrease providing at least some justification for the reduction found from Equation 16. Figure 37 illustrates this argument. It is seen that despite the change in the length of the shear span, Equation 16 provides in both cases slightly more web reinforcement than needed to develop the flexural strength. It should be noted that the line in Figure 37b corresponding to ultimate is obscured by different failure modes.

The amount of web reinforcement determined by Equation 16 thus seems adequate as far as development of the load capacity is concerned. In fact, in cases where the difference between the flexural capacity and the inclined cracking load is relatively small, the design criterion appears to be rather conservative, although a long shear span may reduce the degree of conservatism.

The shear-compression theory also attracts attention to the fact that a beam may fail at a load very close to its flexural capacity but without developing its full ductility. This may happen in beams with low reinforcement ratios where the steel strain at ultimate is well beyond the elastic range. However, such beams generally have a rather high inclined cracking load compared with the flexural capacity, the condition for which Equation 16 with respect to strength is most conservative. On the other hand, a large difference between V_f and V_c usually corresponds to a beam with a high reinforcement ratio. The ultimate steel strain for a flexural failure in such beams is relatively low. Consequently, the beam will not be able to develop its flexural capacity without simultaneously developing its maximum ductility.

It may be concluded that the design criterion presented in Equation 16 provides a reasonably good compromise between a theoretical and a practical solution to the problem of design of web reinforcement in a prestressed concrete beam.

Since the effect of the web reinforcement is based on its ability to restrain the opening of inclined cracks, it is obvious that not only the amount but also the distribution of the web reinforcement is important. If an inclined crack can develop without crossing at least one stirrup, the beam can

behave as if no web reinforcement at all was provided. The restraining effect of the web reinforcement is largest if the stirrup crosses an inclined crack close to the main tension reinforcement where the crack openings is largest. Ideally, it would be desirable to have the stirrup spacing equal to a very small fraction of the beam depth. However, it has been observed that there is no appreciable decrease in the efficiency of the stirrups at spacings equal to half the effective depth.

5.5 COMPARISON OF CAPACITIES BASED ON EQUATION 16 WITH TEST RESULTS

As mentioned earlier, Equation 16 should not be expected to predict the failure load for a beam with any given amount of web reinforcement. This is brought out clearly by the test results shown in Figure 37. However, the preceding discussion implies that Equation 16 ought to represent a lower bound to the capacity of a beam failing in shear. Table 6 gives a listing of the measured ultimate shear and the capacity computed by Equation 16. A total of 106 beams with web reinforcement were tested. The majority of the beams were provided with approximately the amount of stirrups required by Equation 16 to obtain a flexural failure. As a result, 53 beams failed in flexure without showing any sign of shear distress. Thirteen beams developed their flexural capacity but the failure modes contained elements of both shear and flexural failures. Most of these 13 beams had rather high reinforcement ratios so that even a bona-fide flexural failure would take place without any appreciable ductility. In such cases, it is extremely difficult to determine the correct mode of failure. Of the remaining 40 beams, 38 developed shear failures while two failed in bond.

Most of the beams failing in shear developed at least the load capacity indicated by Equation 16. Six beams did not. One of these beams had a stirrup spacing which was too large (10 inches) and another beam failed at a load slightly higher than its flexural capacity. The remaining four beams had unbonded stirrups with little or no prestress. The unbonded stirrups had a length about 20 per cent larger than the unbonded stirrups. The elongation of the unbonded stirrup at a certain stress in the stirrup was therefore larger and failure could occur at a smaller load.

As described in Chapter IV, the shear cracking load is increased by prestressing the stirrups. After the inclined crack has developed, a certain opening of this crack must take place in order to reach failure. This increases the stress in the stirrups and thus the load. However, the higher the prestress in the stirrups, the smaller is the possible increase in stress after inclined cracking. This was taken into account in a very crude manner in the application of Equation 16. The yield stress of the stirrups entering into Equation 16 was reduced by an amount equal to the effective prestress in the stirrups. This procedure is by no means correct but it seems to give conservative results.

Three beams with inclined stirrups were tested. All three beams developed at least 95 per cent of the calculated flexural capacity and the failures were characterized as flexural or transitional failures. Thus a conclusion with respect to the efficiency of inclined stirrups is not justified on the basis of these tests.

● ● ●

VI. A DESIGN PROCEDURE FOR WEB REINFORCEMENT

This chapter is devoted to the description and discussion of a design procedure for web reinforcement in prestressed concrete beams. The design procedure is based on an interpretation of the experimental work described in this report.

Although references are made to other chapters in order to support statements made, this chapter is written so that it can be studied independently of the rest of the report. It should provide sufficient information so that the basis of the design procedure can be understood with enough depth to enable the reader to use the procedure with confidence in problems out of the ordinary realm of design.

The chapter is concluded with a numerical example.

6.1 BASIC DESIGN EQUATION

The design procedure is based on the assumption that the total ultimate shear on a beam can be assigned to the concrete and the vertical stirrups in accordance with the following equation:

$$V_u = V_c + rf_y bd \qquad (16)$$

The form of Equation 16 does not reflect faithfully the mechanism of the action of web reinforcement as described in Chapter V. However, it is shown in the same chapter that the use of this equation in design is conservative and a more elaborate form would not be justified in view of the small increase in hypothetical accuracy versus the large increase in effort involved in application.

The terms involved in Equation 16 are discussed in the following sections.

6.2 ULTIMATE SHEAR, V_u

Ideally, web reinforcement should always be designed to ensure that a given member will fail in flexure for a given type of loading since flexural failures are generally more ductile than failures in shear. Furthermore, at the cost of adding a small amount of web reinforcement the strength of relatively larger amounts of longitudinal reinforcement, which would otherwise have been wasted, can be utilized.

Accordingly, V_u ought to be taken as the maximum shear corresponding to the loading which produces a flexural failure. Prestressed concrete members, however, may have a factor of safety against flexural failure larger than the actual design requirement because the section properties are governed by limitations pertaining to serviceability criteria rather than to safety. If the ductility of such a member is unimportant, it may suffice to ensure that the shear capacity of the member satisfies the factor of safety given in the design specification provided it is fully understood that failure will be in shear.

6.3 THE SHEAR ASSIGNED TO CONCRETE, V_c

The form of Equation 16 implies that part of the shear is resisted by the concrete and the rest by the web reinforcement. This is not correct. In fact, all the shear is resisted by the concrete as would be indicated by any free body diagram bounded by a section perpendicular to the axis of a beam with vertical stirrups.

A correct interpretation of the action of web reinforcement is that the web reinforcement enhances the shear capacity of the concrete section. This effect is analogous to that of transverse reinforcement in a "spiral" column. The spiral reinforcement contributes indirectly to the strength of the column by confining the concrete and thus increasing its compressive strength. Similarly, web reinforcement in a beam contributes to shear strength ultimately by restraining the inclined cracks and thereby alleviating strain concentrations in the concrete at the top of such cracks.

Up to inclined cracking, the web reinforcement is inert and unnecessary. Above inclined cracking, the web reinforcement is active and essential. Consequently, the amount of web reinforcement required to develop the flexural capacity is related to the shear beyond inclined cracking. Furthermore, the shear at inclined cracking can safely be considered as the useful shear capacity of a beam without web reinforcement. This quantity is important in all calculations relating to shear in reinforced concrete beams.

Depending on the section properties and the loading conditions, the inclined crack may develop either as a shear crack originating in the web while the adjacent portion of the tension flange is still uncracked or as a flexure-shear crack initiated by a flexure crack at some critical section. The inclined cracking shear V_c entering into Equation 16 is the smaller of the shears V_{cs} and V_{cf} corresponding to a shear crack and a flexure-shear crack, respectively.

6.4 THE SHEAR CRACK, V_{cs}

A shear crack is assumed to occur when the principal tensile stress in the web exceeds the tensile strength of the concrete. For a noncomposite section symmetrical about an axis in the plane of the load and with the centroidal axis in the web, the total shear at inclined cracking can be found from Equation 7:

$$V_{cs} = \frac{Ib'}{Q} f_t \sqrt{1 + \frac{F_{se}}{A_c f_t}}$$

In a composite section consisting of a cast-in-place slab on top of a precast and prestressed beam, the prestress and the dead load is resisted only by the precast section. With the centroid in the web, the total shear at inclined cracking becomes (Equation 8):

$$V_{cs} = \frac{I_t b'}{Q_t} \left[f_t \sqrt{1 - \frac{\sigma_x}{f_t}} - V_D \frac{Q}{Ib'} \right] + V_D$$

where $$\sigma_x = - \frac{F_{se}}{A_c} - \frac{F_{se}\, e\, y}{I} + \frac{M_D\, y}{I}$$

If the centroid of a section is in the flange, the maximum principal tensile stress will not occur at the centroid but at the junction between the flange and the web. The normal stress at such a point varies along the span since it depends on the external moment. The maximum principal tensile stress is usually found at the intersection between the web and the flange at a distance from the load point in direction of decreasing moment equal to the distance from the top of the total section to the top of the web. Equating the principal tensile stress at this point

to the tensile strength of the concrete gives the following equations for the shear V_{cs} at inclined cracking.

$$\sigma_\theta = \frac{\sigma_s + \sigma_y}{2} + \sqrt{\tau^2 + \left(\frac{\sigma_x - \sigma_y}{2}\right)^2} = f_t \quad (3)$$

$$\sigma_x = -\frac{F_{se}}{A_c} - \frac{F_{se}\, ey}{I} + \frac{M_D\, y}{I} + \frac{(V_{cs} - V_D)\frac{M}{V} y_t}{I_t} \quad (4)$$

σ_y = normal stress perpendicular to the longitudinal axis (positive as tension)

$$\tau = \frac{V_D Q}{Ib'} + \frac{(V_{cs} - V_D)Q_t}{I_t b'} \quad (5)$$

$\frac{M}{V}$ = ratio of applied moment to shear at point considered.

In the case of a shear crack, the effect of draped reinforcement can be taken into account by adding the vertical component of the prestressing force and V_{cs} found from Equations 3 through 8 to give the total shear at inclined cracking.

The tensile strength of concrete can be taken as

$$f_t = 5\sqrt{f'_c} \quad (2)$$

in all calculations pertaining to a shear crack.

6.5 THE FLEXURE-SHEAR CRACK, V_{cf}

The total shear at flexure-shear cracking is given by Equation 11.

$$V_{cf} = \frac{M'_{cr}}{\frac{M}{V} - \frac{d}{2}} + V_D + b'd\sqrt{f'_c} \quad (11)$$

The first two terms on the right-hand side of this equation express the total shear at which a flexure crack is initiated in the shear span at a distance from the point considered equal to half the depth of the beam. The last term derives from test results. It was obtained from a study of the additional shear which was observed before a flexure-shear crack developed following the initiating crack.

Draping of the reinforcement decreases the cracking moment M'_{cr} and reduces the effective depth d of the beam. Consequently, the shear strength of a beam with draped reinforcement is less than for a similar beam with straight tendons, provided that the inclined crack develops as a flexure-shear crack.

In calculations of the cracking moment, the modulus of rupture of concrete can be taken as

$$f_r = 6\sqrt{f'_c} \quad (1)$$

6.6 CONTRIBUTION OF WEB REINFORCEMENT, $rf_y bd$

The term $rf_y bd$ in Equation 16 may be interpreted as the additional shear which can be resisted by the concrete as a result of the action of the web reinforcement. The web reinforcement ratio r is determined on the basis of the width of the flange of the prestressed section and f_y is the yield stress of the stirrup steel (see also Section 6.9).

As shown in Chapter V, Equation 16 is a lower bound to the strength of beams failing in shear. However, a design procedure must take into account not only strength but also ductility. As discussed in Chapter V, both these requirements seem to be satisfied if Equation 16 is used to determine the amount of web reinforcement required to develop the flexural strength of the member.

6.7 SPACING, DISTRIBUTION, AND ORIENTATION OF WEB REINFORCEMENT

The effect of a stirrup stems from its ability to restrain the opening of an inclined

crack. The restraint is most effective when the inclined crack crosses the stirrup close to the longitudinal reinforcement. Consequently, the spacing between stirrups should not exceed half the effective depth of the beam.

Usually, Equation 16 requires different amounts of web reinforcement at different locations along the span. Wherever it is economically feasible to do so, the spacing or the diameter of the stirrups may be changed according to Equation 16.

In the determination of the required amount of web reinforcement at a section, it is implied that an inclined crack may form and extend a distance beyond the section considered equal to at least half the effective depth of the beam. The amount of web reinforcement required at the section considered should therefore be extended the same distance beyond that section.

Close to a support, part of the shear force is transferred directly to the support. Between the face of the support and a section a distance d away, this effect may be utilized by using the same amount of web reinforcement in the whole region as is required a distance d from the support.

Inclined stirrups may be used as web reinforcement. Test results given in this report are hardly conclusive with respect to the efficiency of inclined stirrups. They indicate, however, that compared on the basis of volume of stirrup steel, the efficiency of the web reinforcement is nearly the same for stirrups with inclination of 45° and 90°.

6.8 MANNER OF LOAD APPLICATION

All the beams tested in this investigation were loaded with concentrated loads applied on the top of the beam. A number of these beams were subjected to a simulated moving load, while the remaining beams were loaded with stationary loads. In either case the strength could be predicted reasonably well by Equations 1 through 16. Therefore, the application of these expressions seems realistic for any load condition, provided that the load is applied on the top of the beam.

Only limited information is available on the shear strength of members loaded indirectly, e.g., beams framing into another beam. It is recommended to provide enough transverse reinforcement at the load point that the total load applied can be transferred to the compression zone through the reinforcement. The remaining part of the beam may be treated as if the load was applied at the top of the beam.

6.9 PROPERTIES OF WEB REINFORCEMENT

The primary effect of an inclined crack is a concentration of strains in the concrete at the top of the crack. As long as the opening of the inclined crack is small, the strain concentration is small and unimportant. In order for the web reinforcement to restrain the opening of the crack, a stress must be developed in the stirrups. This in turn results in an elongation of the stirrup and an opening of the inclined crack. Consequently, the opening of the inclined crack, which must be tolerated in order to develop the yield stress in the stirrups, increases with increasing yield stress. The maximum stress in the stirrups that can be utilized thus depends on how large the opening of the inclined crack can be before the strain concentration in the concrete results in a noticeable reduction in strength or ductility.

Test results discussed in Chapter V indicate that the effect of an inclined crack is negligible as long as the opening of the crack results in an average strain over the height of the stirrup less than 0.0015. This

indicates that the yield stress of intermediate grade steel can be definitely utilized. It is also likely that higher strength steels can be used. In fact, steel with a yield stress of about 80 ksi was used successfully as web reinforcement in some of the tests described in this report.

In all the tests described in this report, stirrups made of plain bars were used. The rather poor bond characteristics of these stirrups resulted in an almost uniform strain along the entire length of the stirrup at the time when an average strain of 0.0015 was reached. The stirrup force restraining the opening of the inclined crack could, therefore, be determined from the average strain. This may not be the case if deformed bars are used as web reinforcement. The better bond characteristics of these bars may result in strain peaks in the stirrups and thus a smaller elongation of the stirrup at a certain stirrup force. On the other hand, the improved bond results in a larger number of inclined cracks with a smaller width, which tends to even out strain peaks along the stirrup. When the opening of inclined cracks is distributed between a larger number of cracks, the strain concentration in the concrete will be reduced and distributed over a larger length. Consequently, the effect of a certain average strain along the stirrup on the concentration of strains in the concrete compression zone becomes less severe as the bond characteristics of the stirrup steel is improved. Thus a higher maximum steel stress can be utilized if deformed rather than plain bars are used as web reinforcement. The same considerations imply that no stirrup is efficient unless it is adequately anchored.

6.10 PRESTRESSED STIRRUPS

The stress condition leading to the formation of a shear crack is described by Equation 3, which shows that the presence of a compressive stress perpendicular to the longitudinal axis of the beam will increase the shear corresponding to shear cracking. The shear at flexure-shear cracking, however, is not directly affected by the vertical prestress. The influence of prestress in the stirrups on the inclined cracking load depends on the properties of the beam.

After the inclined crack has developed, the strain in the stirrups must increase before shear failure can occur. The magnitude of the increase is essentially independent of the level of prestress in the stirrups. The possible stirrup stress increase after inclined cracking thus decreases as the prestress is increased and, consequently, the load carried after inclined cracking decreases. The contribution of the web reinforcement to shear capacity in a beam developing flexure-shear cracks may decrease by as much as the ratio of the prestress to the yield stress. The effect of prestress on the ultimate load of a beam developing a shear crack depends on the relative magnitude of the increase in inclined cracking load and the decreased effect of the stirrups.

If the steel used as stirrups has a yield stress too high to be developed without prestressing, prestressing will make it possible to use the steel more efficiently.

6.11 MINIMUM AMOUNT OF WEB REINFORCEMENT

According to a strict application of the design procedure outlined in this chapter, there is no justification for a requirement of a minimum amount of web reinforcement in a prestressed concrete beam. Such requirements, however, are contained in most design specifications and it is pertinent to consider the background and the implications of these

requirements.

A common motivation for the minimum requirement seems to be that the tensile strength of concrete may be reduced because of imperfections in the erection of a structure or for other similar reasons. This would decrease the inclined cracking load and make web reinforcement necessary. The amount needed to replace part of the concrete strength may be expressed as

$$rf_y bd \geq K_1 b'd \qquad (17)$$

where K_1 is a measure of the reduction in the tensile strength of the concrete. Since Equation 17 requires a larger number of stirrups in a rectangular beam than in an I-beam, it is not reasonable since imperfections are less likely in rectangular beams. Furthermore, the inclined cracking load is used in the design procedure only as a convenient and conservative measure of the ultimate load for a beam without web reinforcement. A decrease in the tensile strength of the concrete because of imperfections may have negligible influence on this capacity. Finally, it seems unreasonable that Equation 17 requires the same minimum amount of web reinforcement for two beams with the same overall dimensions but with different amounts of longitudinal reinforcement.

This objection was the starting point for another proposal according to which the required minimum amount of web reinforcement is related to the amount of longitudinal reinforcement in the following manner.

$$rf_y bd \geq \frac{A_s f'_s}{K_2} \sqrt{\frac{d}{b'}} \qquad (18)$$

This formula requires an increase in minimum amount of web reinforcement as the web thickness is decreased.

6.12 MAXIMUM AMOUNT OF WEB REINFORCEMENT

In beams with very small web thickness, it is possible that the compressive stress in the web can exceed the compressive strength of the concrete. Hence, failure may occur before the full effect of the web reinforcement has been developed and before the strain concentrations in the concrete at the top of the inclined crack become serious. The compressive stress in the web is related to the shear. Consequently, the web-crushing failure could be avoided through a limitation of the nominal shear stress at ultimate. However, none of the beams described in this report showed any sign of web crushing although nominal shear stresses as high as $15\sqrt{f'_c}$ were observed in several cases. Because of this, the test results do not provide the basis for limiting the nominal shear stress nor do they demonstrate any great need for such a limitation.

6.13 NUMERICAL EXAMPLE

In order to illustrate the application of the design principles described in this chapter, the web reinforcement requirements for an AASHO Type III composite girder (Figure 38) will be determined. The basic data are assumed as follows.

Prestressed girder alone:

I	$= 125{,}000$ in^4	A_s	$= 3.7$ in^2
A_c	$= 560$ in^2	F_{se}	$= 515{,}000$ lb
c	$= 20.3$ in	e	$= 12.0$ in
Q	$= 3440$ in^3	f'_s	$= 265{,}000$ psi
w	$= 583$ lb/ft	f'_c	$= 5000$ psi

Composite girder:

I_t	$= 282{,}000$ in^4*	d	$= 41.7$ in
c_t	$= 30.6$ in	Q_t	$= 7380$ in^3
w_t	$= 1020$ lb/ft	f'_c	$= 3000$ psi

---

* Slab concrete "transformed" on the assumption that $E_{slab}/E_{girder} = 0.85$

Span: L = 70 ft (simple supports)
Loading: AASHO standard truck H20-S16-44

6.13.1 Maximum Shear Diagram

The flexural strength of the composite girder may be found from AASHO Bridge Specifications (8), Section 1.13.10

$$p = \frac{A_s}{bd} = \frac{3.7}{72 \times 41.7} = 0.00123$$

$$pf'_s/f'_c = 0.00123 \times 265{,}000/3{,}000 = 0.109$$

$$f_{su} = f'_s\,(1-0.5pf'_s/f'_c) = 265{,}000(1-0.5 \times 0.109) = 251{,}000 \text{ psi}$$

$$M_u = A_s f_{su}\, d(1-0.6\, pf_{su}/f'_c)$$

$$= 3.7 \times 251 \times 41.7(1-0.6 \times 0.00123 \times 251/3)$$

$$= 36{,}300 \text{ k - in.} = 3030 \text{ k - ft}$$

The dead load moment at midspan is

$$M_D = w_t L^2/8 = 1.02 \times 70^2/8 = 630 \text{ k - ft}$$

(Note: No load factor)
The moment available to resist live load is then

$$M_{net} = M_u - M_D = 3030\text{-}630 = 2400 \text{ k-ft}$$

AASHO Bridge Specifications give maximum moment corresponding to a system of loads 8 - 32 - 32 kips as 985.6 k - ft (p. 273). Load factor corresponding to flexural failure is then 2400/985.6 = 2.45 which gives the ultimate wheel loads as 19.6 - 78.4 - 78.4 kips.

Maximum shear occurs under trailing wheel. The extreme conditions are:

(a) Trailing wheel placed at midspan
(b) Trailing wheel placed adjacent to support (with the other wheels on the span)

Condition (a) gives the ultimate shear at midspan:

$$V_u = (78.4 \times 35 + 78.4 \times 21 + 19.6 \times 7)/70 = 64.7 \text{ kips}$$

Condition (b) gives the shear at the support:

$$V_u = 78.4 \times 70 + 78.4 \times 56 + 19.6 \times 42)/70 = 152.9 \text{ kips}$$

Between these points, the maximum shear varies linearly along the span. The maximum shear is shown in Figure 39.

6.13.2 Evaluation of V_{cs}

The normal stress at the centroid of the composite section caused by the prestress is:

$$\sigma = \frac{F_{se}}{A_c} - \frac{F_{se}\, e(c - c_t)}{I}$$

$$= -\frac{515{,}000}{560} + \frac{515{,}000 \times 12.0 \times 10.3}{125{,}000} = -413 \text{ psi}$$

The normal stress caused by the dead load varies along the span:

$$\sigma_D = M_D\,(c - c_t)/I = -M_D \times 8.23 \times 10^{-5}$$

Shear and moment from dead load:

$$V_D = w_t \frac{L}{2}\left(1 - \frac{2x}{L}\right)$$

$$M_D = 1/2\, w_t\, (L - x) \times$$

where x is distance from support. The tensile strength of concrete f_t is found from Equation 2:

$$f_t = 5\sqrt{f'_c} = 353 \text{ psi}$$

The evaluation of Equation 8 at different points along the span is given in the following table:

Distance from support	σ_D	$\sigma_x=\sigma_D-413$	$f_t\sqrt{1-\frac{\sigma_x}{f_t}}$	$V_D\frac{Q}{Ib'}$	$V_{cs}-V_D$
ft	psi	psi	psi	psi	kips
2.5	- 85	-498	548	131	112
5.0	-164	-577	573	120	121
7.5	-236	-649	595	110	130
10.0	-302	-715	615	100	138

6.13.3 Evaluation of V_{cf}

The cracking moment available to resist live load is:

$$M'_{cr} = f_{net}\, I_t/c_t$$

f_{net} = modulus of rupture of concrete ($6\sqrt{f'_c}$ = 423 psi)

+ stress caused by prestress

- stress caused by dead load

The stress caused by prestress:

$$\sigma = \frac{F_{se}}{A_c} + \frac{F_{se}\, ec}{I}$$

$$= -\frac{515{,}000}{560} - \frac{515{,}000 \times 12.0 \times 20.3}{125{,}000} = -1920 \text{ psi}$$

The stress caused by dead load:

$\sigma = M_D\, c/I$ (Note: precast section only)

$= M_D \times 1.62 \times 10^{-4}$

The evaluation of Equation 11 at different points along the span is given in the following table:

Distance from support	Dead load stress	f_{net}	M'_{cr}	$\frac{M}{V}-\frac{d}{2}$	$\frac{M'_{cr}}{\frac{M}{V}-\frac{d}{2}}$	$V_{cf}-V_D$
ft	psi	psi	k-ft	ft	kips	kips
5	321	2022	1560	3.26	479	----
10	593	1750	1350	8.26	163	184
15	815	1528	1180	13.26	89	110
20	988	1355	1040	18.26	57	77.6
25	1110	1233	944	23.26	40.6	61.2
30	1185	1158	893	28.26	31.6	52.2
35	1210	1133	873	33.26	26.2	46.8

6.13.4 Selection of Web Reinforcement

The variation of the maximum shear and the capacity of the beam without stirrups (the lesser of V_{cs} and V_{cf}) are shown in Figure 39. Close to midspan, the largest difference between the maximum shear and V_{cf} is 29 kips and close to the support $V_u - V_{cs}$ = 39 kips. The web reinforcement must be designed to resist the difference. If No. 4 bars with a yield stress of 40,000 psi are to be used, the required web reinforcement percentages may be found from Equation 16:

At support:

$$r = \frac{V_u - V_{cs}}{bdfy} = \frac{39}{16 \times 41.7 \times 40} = 0.00146$$

Close to midspan:

$$r = \frac{V_u - V_{cf}}{bdfy} = \frac{29}{16 \times 41.7 \times 40} = 0.00109$$

The spacing between single stirrups is then:

At support:

$$s = \frac{A_v}{br} = \frac{0.196}{16 \times 0.00146} = 8.5 \text{ in.}$$

Close to midspan:

$$s = \frac{0.196}{16 \times 0.00109} = 11.5 \text{ in.}$$

The minimum amount of web reinforcement required by

AASHO, Reference 8:

$$r = \frac{A_v}{bs} \geq \frac{0.0025b'}{b} = 0.0011$$

ACI (318-63)(Reference 9):

$$r = \frac{A_v}{bs} \geq \frac{A_s f'_s}{80\ bdfy} \sqrt{\frac{d}{b'}}$$

$$= \frac{3.7 \times 265}{80 \times 16 \times 41.7 \times 40} \sqrt{\frac{41.7}{7}} = 0.0011$$

VII. SUMMARY

7.1 OUTLINE OF INVESTIGATION

The objective of this report is to present the information on shear strength of prestressed concrete beams with web reinforcement, obtained during the second phase of an investigation of prestressed reinforced concrete for highway bridges which has been in progress since 1952.

A total of 129 tests on simply supported beams are reported. The overall cross-sectional dimensions were 6 inches by 12 inches. Five beams were rectangular while 114 were I-beams with 1 3/4-inch or 3-inch web thickness. The remaining ten beams had a 2- by 24-inch composite slab. The beams were prestressed with 0.0467 to 0.713 per cent longitudinal reinforcement which was straight in 110 beams and draped under the load points in the remaining beams. The concrete strengths ranged from 2,500 to 7,600 psi and the prestress from 0 to 127 ksi. Vertical or inclined stirrups, with or without prestress, were used. The web reinforcement ratio, based on the flange width, ranged from 0 to 0.67 per cent. The stirrup spacing varied from 1 7/8 inches to 10 1/2 inches. All beams were tested under one or two concentrated loads with shear spans varying from 28 to 78 inches. Seven beams were subjected to a single load applied successively at eleven points along the span to simulate a moving load.

7.2 BEHAVIOR OF TEST BEAMS

Of the 129 beams tested, 54 failed in flexure, 60 failed in shear, and 13 failures were characterized as transition failures. Finally, two beams with draped wires developed secondary anchorage bond failures.

For beams without web reinforcement it was found that the formation of an inclined crack changed the behavior of the beam drastically. For beams with web reinforcement, this change was much more gradual and appeared to be related to yielding in the stirrups rather than to the formation of the inclined crack.

Depending on the amount of web reinforcement, failure occurred either in flexure by crushing of the concrete or fracture of the steel or in shear. Shear failures were classified into two categories: shear-compression and web-distress. Shear-compression failures were similar to flexural compressive failures, except that the concrete crushed at the upper end of the inclined crack where there was a high strain concentration caused by the inclined crack. This mode of failure was observed in both rectangular and I-beams. The term web-distress covers a variety of failures which might be different in appearance although all of them were caused by instability of the arch-like structure to which the beam was transformed by the inclined crack. These failures were observed in beams

with thin webs and small amounts of web reinforcement.

7.3 ANALYSIS OF TEST RESULTS

The inclined cracking load was analyzed by dividing inclined cracks into two categories: shear cracks and flexure-shear cracks. The load corresponding to the shear crack, an inclined crack forming in a previously uncracked portion of the beam, could be determined by calculating the principal tensile stress in the web on the basis of an uncracked section. The load corresponding to the formation of a flexure-shear crack, an inclined crack initiated by flexural cracking, was found to be closely related to the flexural cracking moment.

The test results were compared with the predictions of Equation 16

$$V_u = V_c + rf_y bd \qquad (16)$$

where V_u is the ultimate shear, V_c is the computed inclined cracking load, and the last term represents the contribution of vertical stirrups. This equation does not reflect the true action of web reinforcement. The computed capacities may be very conservative, especially in beams with small amounts of web reinforcement. It was concluded, however, that Equation 16 can be used to determine the amount of web reinforcement necessary to insure a flexural failure.

• • •

VIII. REFERENCES

1. Sozen, M. A., Zwoyer, E. M., and Siess, C. P. Investigation of Prestressed Concrete for Highway Bridges, Part I: Strength in Shear of Beams Without Web Reinforcement. (Engineering Experiment Station Bulletin No. 452). Urbana, Ill.: College of Engineering, University of Illinois, 1959.

2. Hernandez, G. Strength of Prestressed Concrete Beams with Web Reinforcement. Ph.D. thesis, University of Illinois, June, 1958; also (Civil Engineering Studies, Structural Research Series No. 153). Urbana, Ill.: Department of Civil Engineering, University of Illinois, 1958.

3. MacGregor, J. G., Sozen, M. A., and Siess, C. P., "Effect of Draped Reinforcement on Behavior of Prestressed Concrete Beams," ACI Journal, Proceedings, Vol. 57, No. 6 (December, 1960), pp. 649-699.

4. MacGregor, J. G. Strength and Behavior of Prestressed Concrete Beams with Web Reinforcement. Ph.D. thesis, University of Illinois, August, 1960; also (Civil Engineering Studies, Structural Research Series No. 201). Urbana, Ill.: Department of Civil Engineering, University of Illinois, 1960.

5. MacGregor, J. G., Sozen, M. A., and Siess, C. P. "Strength of Prestressed Concrete Beams with Web Reinforcement," Journal of the American Concrete Institute, Proceedings, Vol. 62, No. 12, (December, 1965), pp. 1503-1519.

6. Bruce, R. N. An Experimental Study of the Action of Web Reinforcement in Prestressed Concrete Beams. Ph.D. thesis, University of Illinois, September, 1962.

7. Hawkins, N. M. Strength and Behavior of Two-Span Continuous Prestressed Concrete Beams. Ph.D. thesis, University of Illinois, October, 1961; also (Civil Engineering Studies, Structural Research Series No. 225). Urbana, Ill.: Department of Civil Engineering, University of Illinois, 1961.

8. The American Association of State Highway Officials, "Standard Specifications for Highway Bridges," Washington, D. C., 1961.

9. American Concrete Institute, "Building Code Requirements for Reinforced Concrete, ACI 318-63," Detroit, 1963.

PUBLICATIONS OF THE COLLEGE OF ENGINEERING

Bulletins from the University of Illinois College of Engineering are detailed reports of research results, seminar proceedings, and literature searches. They are carefully reviewed before publication by authorities in the field to which the material pertains, and they are distributed to major engineering libraries throughout the world. They are available at a charge approximately equal to the cost of production.

The annual *Summary of Engineering Research* is available in the fall of each year. It contains a short report on every research project conducted in the College during the past fiscal year, including the names of the researchers and the publications that have resulted from their work. It is available for $5.00.

Engineering Outlook, the College's monthly newsletter, contains short articles about current happenings, new research results, recent technical publications, and educational practices in the College of Engineering. Free subscriptions are available upon request.

The Seminar and Discussion Calendar, which is published and distributed weekly, lists current meetings, lectures, and other events on the engineering campus that are open to the public. Free subscriptions are available upon request.

Requests for a catalog of available technical bulletins or for any of the above publications should be addressed to the Engineering Publications Office, College of Engineering, University of Illinois, Urbana, Illinois 61801.

OTHER PUBLICATIONS IN RELATED FIELDS BY THE ENGINEERING EXPERIMENT STATION

Bulletin 452. *Investigation of Prestressed Concrete for Highway Bridges, Part I: Strength in Shear of Beams Without Web Reinforcement,* by M. A. Sozen, E. M. Zwoyer, and C. P. Siess. 1959. *One Dollar.*

Bulletin 463. *Investigation of Prestressed Concrete for Highway Bridges, Part II: Analytical Studies of Relations Among Various Design Criteria for Prestressed Concrete,* by N. Khachaturian, I. Ali, and L. T. Thorpe. 1962. *One Dollar.*

Bulletin 464. *Investigation of Prestressed Concrete for Highway Bridges, Part III: Strength and Behavior in Flexure of Prestressed Concrete Beams,* by J. Warwaruk, M. A. Sozen, and C. P. Siess. 1962. *Two Dollars.*

These publications are available from:
Engineering Publications Office
112 Engineering Hall
University of Illinois
Urbana, Illinois 61801